



**HAL**  
open science

# Wireless body area networks : co-channel interference mitigation & avoidance

Mohamad Jaafar Ali

► **To cite this version:**

Mohamad Jaafar Ali. Wireless body area networks : co-channel interference mitigation & avoidance. Networking and Internet Architecture [cs.NI]. Université Sorbonne Paris Cité, 2017. English. NNT : 2017USPCB252 . tel-02109264

**HAL Id: tel-02109264**

**<https://theses.hal.science/tel-02109264>**

Submitted on 24 Apr 2019

**HAL** is a multi-disciplinary open access archive for the deposit and dissemination of scientific research documents, whether they are published or not. The documents may come from teaching and research institutions in France or abroad, or from public or private research centers.

L'archive ouverte pluridisciplinaire **HAL**, est destinée au dépôt et à la diffusion de documents scientifiques de niveau recherche, publiés ou non, émanant des établissements d'enseignement et de recherche français ou étrangers, des laboratoires publics ou privés.



UNIVERSITÉ  
PARIS  
DESCARTES

U<sup>S</sup>PC  
Université Sorbonne  
Paris Cité



UNIVERSITY PARIS DESCARTES  
DOCTORAL SCHOOL EDITE

PHD THESIS

**Wireless Body Area Networks:  
Co-channel Interference Mitigation & Avoidance**

submitted in fulfillment of the requirements  
for the Ph.D. degree of Université Paris Descartes

**Specialty : Computer Science & Networking**

Defended by

Mohamad Jaafar ALI

**Jury :**

<i>Reviewers :</i>	Hossam AFIFI	- Télécom SudParis
	Abderrezak RACHEDI	- Université de Paris-Est
<i>Supervisors:</i>	Ahmed MEHAOUA	- Université Paris Descartes
	Hassine MOUNGLA	- Université Paris Descartes
<i>Examinators :</i>	Véronique VEQUE	- Université de Paris-Sud 11
	Marcelo DIAS AMORIM	- Université de Pierre et Marie Curie



# Acknowledgements

A Ph.D. is a life, through which you acquire deep knowledge in your domain of science, makes you understanding the details of the reality. Being realistic, then you are sure there are some problems there. Being a creator, organizing your thoughts, dedicate your power and invest your intelligence to place them in the world of existence.

First of all, I would like to thank my advisor, Professor Ahmed MEHAOUA and Dr. Hassine MOUNGLA, who illuminate my way to science. Thanks to their open-door policy, I can always discuss any problem with them and obtain valuable and pertinent suggestions. Thanks to their consistent support and encouragement, I manage to overcome many obstacles in the long journey of my Ph.D. They are not just advisors to my research, mentors from whom I learnt, but also friends. I feel extremely lucky and want to sincerely say thank you from the deeps of my heart.

My special thanks then go to Dr. Mohamed Younis from university of Maryland, Baltimore County in the United States for his constructive discussion and helpful advice on my research work for more than a year.

I would also like to give my gratitude to all of my friends and colleagues in the LI-PADE laboratory from whom I have benefited enormously and shared many wonderful moments with me and made my life in Paris rich and colorful. Particularly, I would thank Dr. Emira Meharouech, Dr. Rongrong Zhang, Dr. Oula El Ali and Dr. Stansilas Morbieu.

Last but not least, I devote the most deep gratitude to my father Jaafar and my mother Alieh, brothers; Moussa, Ahmad, Ali, Abbass, Hassan and Hussein and sisters Fatima and Khadije for their unconditional love, support and encouragement.



# Abstract

A Wireless Body Area Network (*WBAN*) is a short-range network that consists of a coordinator (*Crd*) and a collection of low-power sensors that can be implanted in or attached to the human body. Basically, *WBANs* can provide real-time patient monitoring and serve in various applications such as ubiquitous health-care, consumer electronics, military, sports, etc. [1].

As the license-free 2.4 GHz *ISM* band is widely used among *WBANs* and across other wireless technologies, the fundamental problem is to mitigate the resulting co-channel interference. Other serious problems are to extend the network lifetime and to ensure reliable transmission within *WBANs*, which is an urgent requirement for health-care applications. Therefore, in this thesis, we conduct a systematic research on a few number of research problems related to radio co-channel interference, energy consumption, and network reliability. Specifically, we address the following problems ranging from theoretical modeling and analysis to practical protocol design:

- Intra-*WBAN* interference mitigation and avoidance
- Cooperative inter-*WBAN* interference mitigation and avoidance
- Non-cooperative inter-*WBAN* interference mitigation and avoidance
- Interference mitigation and avoidance in *WBANs* with IoT

Firstly, to mitigate the intra-*WBAN* interference, we present two mechanisms for a *WBAN*. The first is called *CSMA to Flexible TDMA combination for Interference Mitigation*, namely, *CFTIM*, that dynamically allocates time-slots and stable channels to lower the intra-*WBAN* interference. The second is called *Interference Avoidance Algorithm*, namely, *IAA*, that dynamically adjusts the superframe length and limits the number of channels to 2 to lower the intra-*WBAN* interference and save energy. Theoretically, we derive a probabilistic model that proves the *SINR* outage probability is lowered. Simulation results demonstrate the effectiveness and the efficiency of *CFTIM* and *IAA* in terms of lowering the probability of interference, extending network lifetime, improving throughput and reliability.

Secondly, we address the problem of interference among cooperative WBANs through using orthogonal codes. Motivated by distributed time provisioning supported in IEEE 802.15.6 standard [2], we propose two schemes. The first is called *Distributed Time Correlation Reference*, namely, *DTRC*, that provides each WBAN with the knowledge about which superframes overlap with each other. The second is called *Orthogonal Code Allocation Algorithm for Interference Mitigation*, namely, *OCAIM*, that allocates orthogonal codes to interfering sensors belonging to *sensor interference lists (SILs)*, which are generated based on the exchange of power-based information among WBANs. Mathematically, we derive the successful and collision probabilities of frames transmissions. Extensive simulations are conducted and the results demonstrate that *OCAIM* can diminish the interference, improve the throughput and save the power resource.

Thirdly, we address the problem of co-channel interference among non-cooperative WBANs through time-slot and channel hopping. Specifically, we propose two schemes that are based on Latin rectangles. The first is called *Distributed Algorithm for Interference mitigation using Latin rectangles*, namely, *DAIL*, that allocates a single channel to a time-slot combination to each sensor to diminish inter-WBAN interference and to yield better schedules of the medium access within each WBAN. The second is called *Channel Hopping for Interference Mitigation*, namely, *CHIM*, that generates a predictable interference-free transmission schedule for all sensors within a WBAN. *CHIM* applies the channel switching only when a sensor experiences interference to save the power resource. Furthermore, we present an analytical model that derives bounds on collision probability and throughput for sensors transmissions. We evaluate the performance of *DAIL* and *CHIM* by extensive simulations, and results demonstrate the effectiveness and efficiency of our approach in terms of lowering the probability of interference, transmission delay, network lifetime, throughput and reliability.

Finally, motivated by the emergence of the Bluetooth Low Energy (*BLE*), we develop a protocol called *Channel Selection approach for Interference Mitigation*, namely, *CSIM*, to enable WBAN operation within an *IoT* and facilitate the interference detection and mitigation. We integrate a *BLE* transceiver and a Cognitive Radio (*CR*) module within each WBAN's *Crd* that selects an Interference Mitigation Channel (*IMC*) for the WBAN. *CSIM* enables WBAN sensors that experience interference to switch to *IMC* that will be used later for data transmission within the flexible backup frame of the superframe. Extensive simulations are conducted, and results demonstrate that *CSIM* can reduce the interference, improve the spectrum utilization and the power consumption among *IoT* devices.

# Résumé

L'amélioration de la qualité et de l'efficacité en santé est un réel enjeu sociétal. Elle implique la surveillance continue des paramètres vitaux ou de l'état mental du sujet. Les champs d'applications sont vastes : l'application la plus importante est la surveillance des patients à distance.

Les avancées en micro-électronique, capteurs et réseaux sans-fil permettent aujourd'hui le développement de systèmes ambulatoires performants pour le monitoring de paramètres physiologiques, capables de prendre en compte d'importantes contraintes techniques: forte intégration pour la réduction de la taille et faible consommation pour une plus grande autonomie [1]. Cependant, la conception de ce type de réseaux de capteurs médicaux WBANs (Wireles Body Area Networks) se heurte à un certain nombre de difficultés techniques, provenant des contraintes imposées par les capacités réduites des capteurs individuels : basse puissance, énergie limitée et faible capacité de stockage. Ces difficultés requièrent des solutions différentes, encore très embryonnaires, selon l'application visée (monitoring à but médical).

La forte mobilité et le changement rapide de la topologie du réseau dévoilent un verrou scientifique et social. En outre, l'interférence de différents capteurs constituant le WBAN augmente la difficulté de la mise en place de ce type de réseaux. De nombreuses solutions dans la littérature ont été étudiées, comme nous allons illustrer dans ce manuscrit, néanmoins elles restent limitées. Nous nous intéresserons tout particulièrement à la gestion des interférences Intra- et Inter-WBAN, leur impacte sur la fiabilité des transmissions (des liens) et la durée de vie de ce type de réseaux. Plus précisément, nous abordons ces problématiques en se basant sur des modélisations théoriques et analytiques et avec une conception pratique des solutions proposées. Afin d'atteindre les objectifs cités ci-dessous, nous abordons quatre solutions :

- Une gestion des interférences intra-WBAN
- Une gestion coopérative des interférences Inter-WBAN
- Une gestion non coopérative des interférences, Inter-WBAN

- Une gestion des interférences WBAN dans un contexte IoT

Dans la première partie de cette thèse et afin de répondre en partie aux problèmes de gestion des interférences Intra-WBAN. Nous présentons deux mécanismes pour le WBAN : (a) CFTIM qui alloue dynamiquement des slots et des canaux dit- stables (avec un taux d'interférences le bas possible dans le temps) pour réduire les interférences intra-WBAN. (b) IAA ajuste dynamiquement la taille du superframe et limite le nombre de canaux à 2 pour abaisser les interférences Intra-WBAN et ainsi économiser l'énergie. Une validation avec un model probabiliste est proposé afin de valider théoriquement l'efficacité de notre solution. Les résultats de la simulation démontrent l'efficacité du CFTIM et de l'IAA en termes de réduction de la probabilité d'interférence, l'extension de la durée de vie du réseau et l'amélioration du débit et de la fiabilité des transmissions.

Notre seconde contribution, propose une gestion coopératives des interférences Inter-WBAN en utilisant des codes orthogonaux. Motivé par un approvisionnement temporel distribué basé sur la norme [2] IEEE 802.15.6, nous proposons deux solutions. (a) DTRC qui fournit à chaque WBAN les connaissances sur les superframes qui se chevauchent. Le second, (b) OCAIM qui attribue des codes orthogonaux aux capteurs appartenant à deux listes de groupe de capteur en interférences de deux WBAN différents (SIL). Les résultats démontrent qu'OCAIM diminue les interférences, améliore le débit et préserve la ressources énergétiques.

La troisième partie nous a permis d'aborder la gestion des interférences, mais cette fois ci d'une manière non-coopérative en se basant sur l'affectation couple Slot/Canal. Plus précisément, nous proposons deux schémas basés sur les carrés latins. Le premier DAIL qui alloue un canal unique à une combinaison de Slots/capteur afin de diminuer les interférences entre WBAN. Le second CHIM basé sur une transmission conditionnelle concernant le niveau d'interférences à travers différents canaux. Des résultats démontrent l'efficacité de notre approche en termes d'interférence, délai de transmission, durée de vie du réseau ainsi que le débit.

Enfin, motivé par l'émergence du Bluetooth Low Energy (BLE), nous proposons CSIM une proposition permettant de réduire et détecter les interférences pour les WBAN dans un environnement IoT. Nous intégrons un émetteur-récepteur BLE et un module Cognitive Radio (CR) au niveau du coordinateur WBAN qui adapte le canal de transmission en se basant sur l'état de ce dernier.

# Publications

1. Mohamad Jaafar Ali, H. Moun gla, M. Younis, A. Mehaoua: IoT-enabled Channel Selection Approach for WBANs. 2017 IEEE International Wireless Communications and Mobile Computing Conference (IWCMC'17), Valencia, Spain [3].
2. Mohamad Jaafar Ali, H. Moun gla, M. Younis, A. Mehaoua: Distributed Scheme for Interference Mitigation of Coexisting WBANs Using Latin Rectangles. The 14th Annual 2017 IEEE Consumer Communications and Networking Conference (CCNC'17), Las Vegas, United States [4].
3. Mohamad Jaafar Ali, H. Moun gla, Younis M, A. Mehaoua: Distributed scheme for interference mitigation of coexisting WBANs using predictable channel hopping. In the Proceedings of 2016 IEEE 18th International Conference on E-health Networking, Applications and Services (Healthcom'16), Munich, Germany [5].
4. Mohamad Jaafar Ali, H. Moun gla, M. Younis, A. Mehaoua: Inter-WBANs interference mitigation using orthogonal Walsh Hadamard codes. 2016 IEEE 27 International Symposium on Personal, Indoor and Mobile Radio Communications (PIMRC'16), Valencia, Spain [6].
5. Mohamad Jaafar Ali, H. Moun gla, A. Mehaoua: Interference avoidance algorithm (IAA) for multi-hop wireless body area network communication. In the Proceedings of 2015 IEEE 17th International Conference on E-health Networking, Applications and Services (Healthcom'15), Boston, United States [7].
6. Mohamad Jaafar Ali, H. Moun gla, A. Mehaoua: Dynamic channel access scheme for interference mitigation in relay-assisted intra-WBANs. In the Proceedings of 2015 IEEE in Protocol Engineering (ICPE'15) and International Conference on New Technologies of Distributed Systems (NTDS'15), Paris, France [8].
7. Mohamad Jaafar Ali, H. Moun gla, A. Mehaoua, Y. Xu : Dynamic channel allocation for interference mitigation in relay-assisted wireless body networks. In the

Proceedings of 2015 IEEE In Future Information and Communication Technologies for Ubiquitous HealthCare (UbiHealthTech), Beijing, China [9].

8. Mohamad Jaafar Ali, H. Moun gla, M. Younis, A. Mehaoua: Efficient Medium Access Arbitration Among Interfering WBANs Using Latin Rectangle. Elsevier Ad Hoc Networks Journal [10].
9. Mohamad Jaafar Ali, H. Moun gla, M. Younis, A. Mehaoua: Interference Mitigation Techniques in Wireless Body Area Networks. Book Chapter (2017) [11].
10. Mohamad Jaafar Ali, H. Moun gla, A. Mehaoua: Energy Aware Competitiveness Power Control in Relay-assisted Interference Wireless Body Area Networks. 2017 5th International Workshop on ADVANCEs in ICT Infrastructures and Services (ADVANCE'17), Evry Val d'Essonne, France [12].

# Contents

<b>1</b>	<b>Introduction</b>	<b>1</b>
1.1	Wireless Body Area Networks Overview . . . . .	1
1.1.1	Classification of <i>WBANs</i> . . . . .	2
1.1.2	Intra- <i>WBAN</i> Communication . . . . .	3
1.2	Challenges of Interference Mitigation between <i>WBANs</i> and Other Networks	6
1.3	Challenges of Interference Mitigation among <i>WBANs</i> . . . . .	7
1.3.1	Network Lifetime . . . . .	9
1.3.2	QoS and Reliability . . . . .	9
1.3.3	MAC Design . . . . .	10
1.3.4	PHY Layer Design . . . . .	10
1.3.5	Antenna Design . . . . .	10
1.4	Problem Statement and Motivation . . . . .	10
1.5	Thesis Outline and Main Contributions . . . . .	12
<b>2</b>	<b>Related Works</b>	<b>17</b>
2.1	Resource Allocation . . . . .	18
2.1.1	Channel Assignment . . . . .	19
2.1.2	Transmission Scheduling . . . . .	20
2.1.3	Combined Channel and Time Allocation . . . . .	20
2.1.4	Summary . . . . .	21
2.2	Power Control . . . . .	22
2.2.1	Link-state based Power Control . . . . .	22
2.2.2	Game Theory . . . . .	23
2.2.3	Summary . . . . .	25
2.3	Multiple Access . . . . .	26
2.3.1	Superframe Modification . . . . .	27
2.3.2	Superframe Interleaving . . . . .	27

2.3.3	Hybrid Solutions . . . . .	28
2.3.4	Summary . . . . .	29
2.4	Link Adaptation . . . . .	30
2.4.1	Data Rate Adjustment . . . . .	30
2.4.2	Two-hop Communication . . . . .	30
2.4.3	Summary . . . . .	32
2.5	Conclusions . . . . .	33
<b>3</b>	<b>Interference Mitigation in Multi-Hop WBANs</b>	<b>35</b>
3.1	Introduction . . . . .	36
3.2	Related Work . . . . .	37
3.3	Resource Allocation for Intra-WBAN Interference Mitigation . . . . .	39
3.3.1	System Model . . . . .	39
3.3.2	Superframe Structure - <i>FTDMA</i> . . . . .	40
3.3.3	<i>CFTIM</i> Resource Allocation . . . . .	41
3.3.4	<i>CFTIM</i> Analysis . . . . .	42
3.3.5	Outage Probability . . . . .	42
3.3.6	Stability Condition . . . . .	45
3.3.7	<i>CFTIM</i> Performance Evaluation . . . . .	45
3.4	Improved Resource Allocation for Intra-WBAN Interference Mitigation . . . . .	47
3.4.1	System Model . . . . .	47
3.4.2	<i>IAA</i> Improved Resource Allocation . . . . .	47
3.4.3	<i>IAA</i> Superframe Structure . . . . .	50
3.4.4	<i>IAA</i> Analysis . . . . .	51
3.4.5	<i>IAA</i> Performance Evaluation . . . . .	52
3.5	Conclusions . . . . .	54
<b>4</b>	<b>Cooperative Inter-WBAN Interference Mitigation Using Walsh-Hadamard Codes</b>	<b>55</b>
4.1	Introduction . . . . .	55
4.2	System Model and Preliminaries . . . . .	57
4.2.1	Model Assumptions . . . . .	57
4.2.2	Interference Lists - <i>I</i> . . . . .	57
4.2.3	Interference Sets - <i>IS</i> . . . . .	58
4.2.4	Channel Model . . . . .	58

4.2.5	Cyclic Orthogonal Walsh Hadamard Codes Overview . . . . .	58
4.3	Distributed Time Reference Correlation - <i>DTRC</i> . . . . .	59
4.4	Orthogonal Codes Allocation - <i>OCAIM</i> . . . . .	61
4.5	<i>OCAIM</i> Analysis . . . . .	65
4.5.1	Successful Beacon Transmission Probability . . . . .	65
4.5.2	Successful Data Transmission Probability . . . . .	66
4.6	<i>OCAIM</i> Performance Evaluation . . . . .	68
4.7	Conclusions . . . . .	70
<b>5</b>	<b>Non-Cooperative Inter-WBAN Interference Mitigation Using Latin Rectangles</b>	<b>73</b>
5.1	Introduction . . . . .	74
5.2	System Model . . . . .	75
5.2.1	Model Assumptions and Preliminaries . . . . .	75
5.2.2	Latin Squares Overview . . . . .	76
5.3	Interference Mitigation Using Latin Rectangles - <i>DAIL</i> . . . . .	77
5.3.1	<i>DAIL</i> Algorithm . . . . .	78
5.3.2	<i>DAIL</i> Superframe . . . . .	79
5.3.3	<i>DAIL</i> Analysis . . . . .	80
5.3.4	<i>DAIL</i> Performance Evaluation . . . . .	85
5.4	Interference Mitigation Using Predictable Channel Hopping - <i>CHIM</i> . . . . .	88
5.4.1	<i>CHIM</i> Superframe . . . . .	88
5.4.2	<i>CHIM</i> Algorithm . . . . .	89
5.4.3	<i>CHIM</i> Analysis . . . . .	90
5.4.4	<i>CHIM</i> Performance Evaluation . . . . .	93
5.5	Performance Evaluation . . . . .	96
5.5.1	Comparing <i>DAIL</i> & <i>CHIM</i> . . . . .	96
5.5.2	Comparing <i>CHIM</i> & <i>DAIL</i> & <i>SMS</i> . . . . .	97
<b>6</b>	<b>Interference Mitigation in WBANs with IoT</b>	<b>99</b>
6.1	Introduction . . . . .	99
6.1.1	<i>IoT</i> Communication Technologies . . . . .	100
6.1.2	Problem Statement . . . . .	101
6.1.3	Contribution . . . . .	102
6.2	Related Work . . . . .	103
6.3	System Model and Preliminaries . . . . .	104

---

6.3.1	Bluetooth Low Energy . . . . .	104
6.3.2	System Model and Assumptions . . . . .	104
6.4	Channel Selection Approach for Interference Mitigation - ( <i>CSIM</i> ) . . . . .	105
6.4.1	<i>CSIM</i> Algorithm . . . . .	105
6.4.2	Channel Selection . . . . .	107
6.4.3	Channel Stability . . . . .	107
6.4.4	Superframe Structure . . . . .	109
6.5	Performance Evaluation . . . . .	110
6.6	Conclusions . . . . .	113
<b>7</b>	<b>Conclusions</b>	<b>115</b>
7.1	Thesis Summary . . . . .	115
7.2	Future Works and Research directions . . . . .	117
7.2.1	Mobility . . . . .	117
7.2.2	Putting Human Bodies Into the Internet of Things . . . . .	117
7.2.3	Extension to cloud computing . . . . .	118
	<b>Bibliography</b>	<b>119</b>
	<b>Nomenclature</b>	<b>133</b>

# List of Tables

1.1	SI units . . . . .	2
2.1	Notations & meanings . . . . .	21
2.2	Comparison of published resource allocation interference mitigation proposals for <i>WBANs</i> . A star topology is deployed in the following proposals	21
2.3	Comparison of published link-state based power control interference mitigation proposals for <i>WBANs</i> . . . . .	23
2.4	Comparison of game-based power control interference mitigation proposals for <i>WBANs</i> . . . . .	26
2.5	Comparison of published multiple access interference mitigation proposals for <i>WBANs</i> . . . . .	29
2.6	Comparison of published data rate adjustment interference mitigation proposals for <i>WBANs</i> . . . . .	30
2.7	Comparison of published two-hop based interference mitigation proposals for <i>WBANs</i> . . . . .	32
3.1	Simulation parameters - <i>CFTIM</i> . . . . .	45
4.1	Notation & meaning . . . . .	65
4.2	Simulation parameters - <i>OCAIM</i> . . . . .	69
5.1	Notation & meaning . . . . .	76
5.2	Simulation parameters - <i>DAIL</i> . . . . .	86
5.3	Simulation parameters - <i>CHIM</i> . . . . .	94
5.4	Simulation parameters - <i>DAIL &amp; CHIM</i> . . . . .	96
6.1	Notation meaning . . . . .	106
6.2	Simulation parameters . . . . .	111



# List of Figures

1.1	Radio co-channel interference between a <i>WBAN</i> and a <i>WiFi</i> wireless network	6
1.2	Radio co-channel interference among <i>WBANs</i>	7
1.3	<i>IEEE 802.15.6</i> superframe structure illustrating active and inactive periods [2]	8
2.1	One-hop and two-hop communication schemes	31
3.1	A collision takes place at a receiving node	36
3.2	<i>FTDMA</i> superframe structure	40
3.3	Average <i>SINR</i> vs. time for <i>CFTIM</i> and <i>OR</i>	46
3.4	<i>WEC</i> versus time for <i>CFTIM</i> , <i>OR</i> and <i>TDMA</i>	46
3.5	Throughput ( <i>TP</i> ) vs. time for <i>CFTIM</i> and <i>OR</i>	46
3.6	Source node actions	48
3.7	<i>IAA</i> superframe structure	51
3.8	Minimum <i>SINR</i> vs. time for <i>IAA</i> , <i>PC</i> and <i>OR</i>	53
3.9	Average <i>SINR</i> versus time for <i>IAA</i> and <i>OR</i>	53
3.10	<i>ER</i> vs. time for <i>IAA</i> , <i>PC</i> and <i>OR</i>	53
4.1	Superframe structure proposed for <i>OCAIM</i> scheme	59
4.2	A network of three coexisting <i>WBANs</i>	62
4.3	Overlapping superframes scheme	62
4.4	Average <i>SINR</i> vs. time for <i>OCAIM</i> and orthogonal <i>TDMA</i>	69
4.5	Minimum <i>SINR</i> vs. interference threshold for <i>OCAIM</i> , <i>SMS</i> & <i>OS</i>	69
4.6	<i>WBAN</i> power consumption vs. time for <i>OCAIM</i> , <i>SMS</i> & <i>OS</i>	69
4.7	Data frames delivery ratio versus <i>WBANs</i> count	70
4.8	Probability of successful beacon transmission versus <i>WBANs</i> count	71
5.1	Superframe structure for <i>DAIL</i>	79

5.2	Collision scenarios at sensor- and coordinator-levels . . . . .	79
5.3	A $4 \times 4$ channel to time-slot assignment Latin square . . . . .	80
5.4	$McP$ versus the number of coexisting WBANs ( $\Omega$ ) . . . . .	86
5.5	$McP$ versus the number of time-slots per superframe . . . . .	86
5.6	Mean successful packets received ( $MsPR$ ) versus $\Omega$ . . . . .	86
5.7	Mean power consumption ( $mPC$ ) versus $\Omega$ . . . . .	87
5.8	Superframe structure for <i>CHIM</i> . . . . .	89
5.9	Mean collision probability versus number (#) of colliding sensors . . . . .	93
5.10	Mean collision probability ( $McP$ ) versus $\Omega$ for <i>CHIM</i> & <i>ZIGBEE</i> . . . . .	94
5.11	Mean power consumption ( $mPC$ ) versus $\Omega$ for <i>CHIM</i> & <i>ZIGBEE</i> . . . . .	94
5.12	$DPS$ versus # of TX superframes for <i>CHIM</i> & <i>ZIGBEE</i> . . . . .	94
5.13	$McP$ versus $\Omega$ for <i>DAIL</i> and <i>CHIM</i> . . . . .	96
5.14	$mPC$ versus $\Omega$ for <i>DAIL</i> and <i>CHIM</i> . . . . .	96
5.15	Mean $TP$ versus $\Omega$ for <i>DAIL</i> and <i>CHIM</i> . . . . .	96
5.16	$CFP$ versus $\Omega$ for <i>CHIM</i> & <i>DAIL</i> . . . . .	98
5.17	$McP$ versus $\Omega$ for <i>CHIM</i> & <i>DAIL</i> & <i>SMS</i> . . . . .	98
5.18	$mPC$ versus $\Omega$ for <i>CHIM</i> & <i>DAIL</i> & <i>SMS</i> . . . . .	98
6.1	The overall picture of <i>IoT</i> [13] . . . . .	100
6.2	Collision scenarios at sensor- and coordinator-levels . . . . .	106
6.3	superframe structure . . . . .	109
6.4	$Pr_{AvChs}$ versus cluster size ( $\Omega$ ) . . . . .	111
6.5	$Pr_{AvChs}$ versus $SNR$ threshold ( $SNR_{Thr}$ ) . . . . .	111
6.6	$Pr_{AvChs}$ versus # sensors/WBAN ( $\delta$ ) . . . . .	111
6.7	Average reuse factor ( $avgRF$ ) versus interference threshold ( $\rho$ ) . . . . .	113
6.8	Coordinator's average energy consumption ( $avgEC$ ) versus interference threshold ( $\rho$ ) . . . . .	114

# Chapter 1

## Introduction

### Contents

---

<b>1.1 Wireless Body Area Networks Overview</b> . . . . .	<b>1</b>
1.1.1 Classification of <i>WBANs</i> . . . . .	2
1.1.2 Intra- <i>WBAN</i> Communication . . . . .	3
<b>1.2 Challenges of Interference Mitigation between <i>WBANs</i> and Other Networks</b> . . . . .	<b>6</b>
<b>1.3 Challenges of Interference Mitigation among <i>WBANs</i></b> . . . . .	<b>7</b>
1.3.1 Network Lifetime . . . . .	9
1.3.2 QoS and Reliability . . . . .	9
1.3.3 MAC Design . . . . .	10
1.3.4 PHY Layer Design . . . . .	10
1.3.5 Antenna Design . . . . .	10
<b>1.4 Problem Statement and Motivation</b> . . . . .	<b>10</b>
<b>1.5 Thesis Outline and Main Contributions</b> . . . . .	<b>12</b>

---

### 1.1 Wireless Body Area Networks Overview

The recent technological advances in wireless communication and microelectronics have enabled the development of low-power, intelligent devices that can be implanted in or attached to the human body. Inter-networking these devices is referred to as a *WBAN*, which enables continual monitoring of the physiological state of the body in stationary or mobility scenarios. The coordinator collects the measurements of the individual sensors and sends them to a gateway that in turn delivers the received data to a remote monitoring station for storage, processing, and analysis, using the Internet

**Table 1.1:** SI units

Notation	Meaning	Notation	Meaning
W	Watt	g	Gram
dB	Decibel	Hz	Hertz
m	Meter	mm	Millimeter
Kw	Kilowatt	Kg	Killogram
KHz	Kilohertz	MHz	Megahertz
GHz	Gigahertz	mAh	Milliamp hour
dBm	Decibel-milliwatts	mW	Milliwatt
Kbp/s	Killobit per second	Mb/s	Megabit per second

or the cellular telecommunication infrastructure [14, 15]. Basically, *WBAN* sensors monitor vital signs like blood pressure, sugar level, body temperature,  $CO_2$  concentration, electromyography and observe the heart (electrocardiography) and the brain (electroencephalograph) electrical activities as well as providing real-time feedback to the medical personnel.

The *IEEE 802.15.6* standard [2] classifies *WBAN* applications into medical and non-medical [1]. The non-medical include Entertainment, Real-time streaming, and Emergency. Whilst, the medical are further categorized into three different groups, 1) Remote Control (e.g., Patient monitoring, Telemedicine systems, Ambient assisted living), 2) Implant (e.g., Cancer detection, Cardiovascular diseases) and 3) Wearable (e.g., Wearable health monitoring, Asthma, Sleep staging, etc.). The health-care is the most widely used application, and which may send vital information to the caregiver centers. Thus, a *WBAN* is being unable to send such information, or receiving it with long delays, could be very detrimental to the quality of patient's life. Several factors like the interference, latency, network lifetime, mobility, etc., may negatively affect the performance of *WBANs*, and hence the desired requirements of the underlying applications may not be met thoroughly. Thus, the main goal for the health-care applications is to maintain reliable and timely data transfer, i.e., with a minimal delay, between each sensor and the coordinator as these *WBANs* mainly deal with vital information. In essence, *WBANs* provide to the patients more independence, a lower need of periodic medical supervision, a reduced frequency of their visits to the doctor and offer them more freedom to practice their daily routines. Due to the social nature of *WBANs*, most of the people coexist in highly populated areas such as shopping malls, public places, hospitals, offices and residential communities, these people wearing *WBANs* expose to ever-changing interference.

**Table 1.1** shows the list of SI units that we used throughout this thesis.

### 1.1.1 Classification of *WBANs*

In this section, we provide a brief overview of the various *WBAN* characteristics that affect its design and operation. As per *IEEE 802.15.6* standard, the number of nodes in a

typical WBAN network may range from 6 up to 256. A single WBAN may involve a single coordinator and up to 64 nodes. Since 2 to 4 WBANs may coexist on the same person (per  $1m^2$ ), a maximum of 256 nodes may exist per person. The *IEEE 802.15.6* working group has considered WBANs to operate in either a one-hop or two-hop topology. In one-hop, two possible transmissions may exist; a transmission may initiate from the device to the coordinator and the other way around. Whilst, in two-hop, nodes are connected to the coordinator through intermediate nodes called relays. The latest version of the *IEEE 802.15.6* standard proposed for WBANs [2] supports only two-hop in WBAN standards compliant communication [16]. In addition, two modes of communication may exist in the star topology, namely, beacon mode and non-beacon mode. In beacon mode, the coordinator transmits beacons periodically to define the boundaries of its superframe and enables its nodes to synchronize. In non-beacon mode, a WBAN node can transmit data to the coordinator using CSMA/CA and can poll the coordinator to receive data.

### 1.1.2 Intra-WBAN Communication

In this section, we highlight the primary requirements and design considerations of wireless communication technologies that can be applied in WBANs as follows:

- **Data rates:** data rates should support various WBAN applications and be ranging from 10 kbit/s to 10 Mbit/s. The BER determines the reliability of the data transmission and depends on the criticality of the data. Reliability of WBANs depends upon transmission delay of packets and packets loss probability.
- **Transmission power:** WBAN sensors may transmit at up to 1 mW (0 dBm) which complies with the specific absorption rate (SAR) 1.6 W/Kg in 1g of the human body tissue [17]. The battery lifetime of WBAN nodes should span several months or even years, particularly, for those implanted nodes underneath the skin.
- **Communication range:** WBANs allow the sensors in, on and around the same body to communicate with each other, so 2-5 m operating communication range is enough in a WBAN.
- **Latency:** the main goal of the monitoring applications is to collect information in the real-time, so the tight delay requirement is necessary. As specified in *IEEE 802.15.6* standard, the latency should be less than 125ms in medical applications and less than 250ms in non-medical applications.
- **Mobility:** due to the postural body movements, the WBAN may experience the signal shadowing and fading which could be detrimental to the reliability and QoS metrics such as packet delivery ratio, delay, etc. Such reliability is necessary to

protect the patient's life when a life threatening event has not been detected. Thus, a highly reliable and energy-efficient data transfer with low delay is required to guarantee a successful data transmission.

- **Configuraion:** *WBANs* should be configurable by allowing an individual node to be capable of joining the *WBAN* system without any external intervention.
- **Coexistence:** *WBANs* may interact and coexist with each other as well as with other wireless technologies like Bluetooth, ZigBee, WSN, WLAN, etc. The coexistence algorithm should guarantee a proper functionality of *WBANs* in dynamic and heterogeneous environment where networks of different standards and technologies cooperate amongst each other to communicate information.

These requirements may differ while considering the different operational environments and characteristics of each *WBAN* application. In order to satisfy the requirements of *WBANs*, many wireless technologies are involved in communication among sensor nodes and between the coordinator and sensor nodes.

**Bluetooth:** the *IEEE 802.15.1* standard (Bluetooth) [18, 19] was employed in many e-health applications. Its properties, e.g., high bandwidth requirement, lack of support of multi-hop, long start-up time, make it unsuitable for high-power consuming *WBAN* applications. Bluetooth devices operating in the 2.4 GHz *ISM* band utilize frequency hopping among 791 MHz channels at a nominal rate of 1600 hops/seconds to reduce interference. The standard specifies three classes of devices with different transmission powers and corresponding coverage ranging from 1 to 100m. The maximum data rate is 3 Mbps.

**Bluetooth Low Energy (BLE) :** *BLE* [20, 21] has been introduced as an amendment of the original Bluetooth and as a better choice for *WBAN* applications, where lower power consumption can be achieved by using low duty cycling. However, this exaggerated low duty cycle mechanism makes *BLE* unsuitable for health monitoring applications as they need the high frequency of data transmissions. *BLE* supports bit rate up to 1 Mbps and operates in the 2.45 GHz *ISM* band, where 40 channels, each is 2 MHz wide, are defined. Using fewer channels for pairing devices, synchronization can be done in a few milliseconds compared to Bluetooth. This benefits latency-critical *WBAN* applications, like alarm generation and emergency response, and enhances power saving. Its nominal data rate, low latency, and low energy consumption make *BLE* suitable for communication between the wearable sensor nodes and the access point. The main drawbacks of *BLE* are the lack of multi-hop communication, limited scalability and the support for

star topology only.

**ZigBee:** is a standard [22] defined by *ZigBee* specification as one of the wireless network technologies which are widely employed and adopted by applications that require a low data rate and long battery life. *ZigBee* technology is separated into two parts. First, *ZigBee* alliance designates the application layers, defining the network, security and application software layers. Second, *IEEE 802.15.4* standard [23, 24] defines the physical and medium access control layers, where access to wireless channel is through employing slotted/un-slotted *CSMA/CA* mechanism for channel access and handling *GTS* allocation and management.

**IEEE 802.15.4:** The *IEEE 802.15.4* [23, 24] is a short-range (up to 100 m) communication system intended to enable applications with relaxed throughput and latency requirements in *WBANs*. The key features of *IEEE 802.15.4* are low complexity, low cost, low power consumption, low bit rate transmission, to be supported by cheap either fixed or moving devices. The main field of application of this technology is the implementation of *WSNs*. The network topologies supported are the star, tree, and mesh. *IEEE 802.15.4* specifies a total of 27 half-duplex channels across three frequency bands; the 868 MHz band with just a single channel with the bit rate of 20 kbps, the 915 MHz band where 10 channels with a bit rate of 40 kbps are available and the 2.45 GHz *ISM* band with 16 channels with the bit rate equal to 250 kbps.

A major disadvantage of *ZigBee* for *WBAN* applications is due to interference with *WLAN* transmission, especially in 2.45 GHz band, where numerous wireless systems operate. Another disadvantage is related to its low data rate, which makes it inappropriate for real-time *WBAN* applications, particularly health-care.

**IEEE 802.15.6:** In April 2010, the *IEEE 802.15.6* working group established the first draft of the communication standard of *WBANs* that is optimized for low-power on/in-body nodes for various medical and non-medical applications. The latest standardization of *WBANs*, *IEEE 802.15.6* standard [2], aims to provide an international standard for low power, short range and extremely reliable wireless communication within the surrounding area of the human body, and support a vast range of data rates from 75.9 Kbps up to 15.6 Mbps. Moreover, the standard utilizes different frequency bands; the narrowband (*NB*) uses 400, 800, 900 MHz and 2.3 and 2.4 GHz, the ultra wideband (*UWB*) utilizes 3.1-11.2 GHz and the human body communication (*HBC*) utilizes the frequencies within the range of 10-50 MHz that cannot support high data rate transmissions, e.g., video or audio streaming.

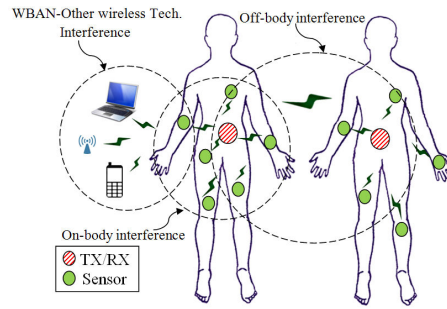


**Figure 1.1:** Radio co-channel interference between a *WBAN* and a *WiFi* wireless network

The  $2.4\text{ GHz}$  band is deemed by practitioners as the best option for the use by medical applications because of its ability against adjacent channel interference. In fact, this standard is a step forward in wearable sensor networks as it is designed specifically for use with a wide range of data rates, less energy consumption, low range, number of nodes (256) per body area network and different node priorities according to the application requirements.

## 1.2 Challenges of Interference Mitigation between *WBANs* and Other Networks

The co-channel interference may occur due to the coexistence of *WBANs* with other wireless networks such as *IEEE 802.11 (WiFi)*, *IEEE 802.15.4 (ZigBee)*, *WSNs*, *IEEE 802.15.1 (Bluetooth)*, *MANETs*, cellular and other appliances that may simultaneously share the same international license-free  $2.4\text{ GHz ISM}$  band with *WBANs*.

An example of co-channel interference that can be experienced between a single *WBAN* represented by a single person, and other wireless networks, denoted by *WBAN-Other wireless Tech.*, is illustrated in **Figure 1.1** [17]. In this figure, the transmissions of the individual nodes collocated within the *WBAN-Other wireless Tech.*, e.g., laptop, mobile phone, may impose the interference on the transmissions of nodes collocated within the neighboring *WBAN*, e.g., sensors, and the other way around.

Dealing with the co-channel interference problem within the same network is easier than across wireless networks due to many reasons. First, the use of the different MAC protocols across wireless networks may increase the frequency of collisions. In other words, the specifics of *PHY* and *MAC* parameters like *CCA*, backoff period, number of retransmission attempts, transmission power, *RSSI* measurements and periodicity, etc., employed in each *MAC* protocol are distinct. As an example, a *WiFi* node may have a higher number of retransmission attempts than a *WBAN* node, which decreases the chances of successful data transmission at the *WBAN* node. Second, some wireless net-

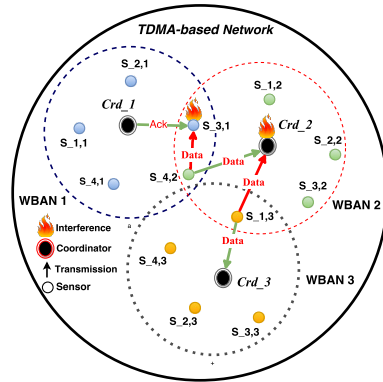


**Figure 1.2:** Radio co-channel interference among WBANs

works like *WiFi* may use larger bandwidth and packet size than those used by *WBANs*, which will reserve the medium for the longer period of time that leads to unfair usage of the medium. Third, some networks like *WiFi* may use higher transmission power level (20 dBm) than *WBAN* (0 dBm), and consequently the *WiFi* transmission dominates the medium and hinders intra-*WBAN* communication.

On the other hand, *WBANs* could be subject to more frequent topology changes due to the human body mobility and move faster than that conventional *WSNs*. Also, *WBANs* may move in a group-based rather than node-based manner as *MANETs*. Their nodes are deployed more densely in a very small area, whilst, the locations of mobile stations in the cellular networks are spread over a wide area. Therefore, the interference mitigation protocols proposed for *WSNs*, *MANETs*, and cellular networks are not only unsuitable but also can not be directly applied to *WBANs*, as these protocols do not consider the special properties of *WBANs* in their design.

### 1.3 Challenges of Interference Mitigation among WBANs

*WBANs* are becoming increasingly pervasive, their coexistence will become a serious issue in the upcoming years. In 2009, eleven million sensors were estimated in use; such a number is predicted to reach 485 million by 2018 [17, 25, 26]. As defined in the *IEEE 802.15.6* standard [2], the *WBAN* system should be capable to support up to 60 sensors in a  $6m^3$  space (256 sensors in a  $3m^3$ ). Though, the standard requires the system to function properly within the transmission range of up to 3 meters when up to 10 *WBANs* are collocated within a space of  $3m^3$ . Nonetheless, when a large number of sensors of different *WBANs* coexisting in the close proximity of each other, access the same channel at the same time, the co-channel interference may still happen, and hence their transmissions face interference (collisions) as illustrated in **Figure 1.2**. As per *IEEE 802.15.6* standard, the superframe is delimited by two beacons and composed

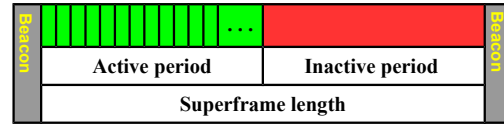


**Figure 1.3:** IEEE 802.15.6 superframe structure illustrating active and inactive periods [2]

of two successive frames: (i) active, that is dedicated for sensors, and (ii) inactive, that is designated for coordinators as illustrated in **Figure 1.3**.

Due to the social interaction of people, *WBANs* may move towards each other in crowded areas such as a hospital's lobby, and due to the absence of coordination amongst them, these *WBANs* could operate on similar channels, i.e., the same international license-free 2.4 GHz ISM band, and hence their corresponding radio communication ranges and the individual active periods of their corresponding superframes, i.e., TDMA- or CSMA/CA-based, may overlap with each other [27, 28]. Although *WBANs* may search for available channels, the interference occurs because of the smaller number of channels in IEEE 802.15.6 [2, 23] than the number of *WBANs*. Even when few number of *WBANs* coexist, such interference may affect the communication links by decreasing the *SINR* of the received signal resulting in more packet losses and performance degradation.

On the other hand, the resource constrained nature of *WBAN* nodes in terms of limited power supply, i.e., small battery capacity, size, transmission range, and cost make the application of advanced antenna and power control techniques used in other wireless networks unsuitable for *WBANs*. These techniques do not consider the special characteristics of *WBANs* [29, 30, 31, 32, 33, 34]. For instance, power control mechanisms which proved their efficiency in cellular systems are unsuitable for *WBANs* since they require high transmission power, which requires larger sensors batteries. The simple design and shape of sensor's antenna make signal processing very hard in *WBANs* because of the inhomogeneous nature of the human body which is characterized by high signal attenuation and distortion. Due to their highly mobile nature, different *WBANs* may change their position relative to each other; in addition to the body posture, the individual sensors in the same *WBAN* may change their location relative to each other. Such dynamic nature and the absence of coordination make the allocation of a centralized entity to manage *WBANs* coexistence and mitigate the interference unsuitable for *WBANs* [14, 15, 25, 35, 36].

Although, there exists lots of work are still going on addressing the detrimental effects of the co-channel interference on the performance of *WBANs*, nonetheless, there

are still many open issues and challenges need to be addressed.

### 1.3.1 Network Lifetime

*WBAN* nodes may operate on non-rechargeable batteries of small size and low-power capacity for several months or even few years, in particular, for those nodes planted underneath the skin. Extending the lifetime of these batteries becomes one of the important issues to increase the span of network lifetime. Hence, the power resource management and the power consumption minimization become a necessity in *WBANs*. Among all the hardware components in the sensor node, the radio transceiver is the most energy-consuming one. Thus, it is necessary to keep its activity in a low-power or sleeping mode as much as possible rather than keeping it active for long periods of time to save the power. However, due to the interference, collisions may happen at the receiving nodes, the packet retransmissions may increase, in consequence, the energy consumption of *WBAN* sensors grows. Also, *WBANs* exposing to interference from other wireless networks may require to transmit at higher levels of power to compete for better *SINR* and overcome the interference, which results in more power consumption. While mitigating the interference, the power consumption may also increase because of the high frequency of switching the radio transceiver between on and off, channel hopping or clear channel assessment, etc.

### 1.3.2 QoS and Reliability

*WBANs* may have specific *QoS* requirements which depend on the *BER* or the priority of the traffic. When there is adverse interference, *WBANs* with high *QoS* constraints must have a higher priority to access the channel as they may report vital data, e.g., heart disease data. Generally, reliability is related to packet delay and the probability of packet loss. The long-term high-level co-channel interference may increase the period of the convergence time, which is defined as the time needed for the interference mitigation algorithm to enable a *WBAN* to operate normally. Consequently, in such severe conditions, the convergence time becomes larger, which negatively impacts the reliability, and provides longer delays than typical. Thus, the faster the interference mitigation converges, the more effective it is. In addition, the probability of packet loss specifies the range to which the packet drop rate impacts the reliability in terms of *BER* or *PER* of the *WBAN*.

### 1.3.3 MAC Design

The design of the *MAC* protocol may play a crucial role in performance degradation of a *WBAN*. Due to the interference, any non-elaborate and non-efficient *MAC* protocol may significantly increase the power consumption due to packets collision, overhearing and idle listening overhead resulting from data and control packets as well as the synchronization costs. Also, a non-elaborate *MAC* protocol may utilize the bandwidth in a non-efficient way and unfairly control the medium access, which negatively impacts the *QoS* by delaying the high-priority traffic, e.g., a sensor carries vital information. Moreover, the design of these protocols should consider the mobility of the person to provide better energy-efficient and reliable communication of *WBANs*.

### 1.3.4 PHY Layer Design

The distribution of implanted/attached sensors in *WBANs*, respectively, in/to the different parts of the human body makes the channel model challenging due to the nature of the human tissue, which creates different communication channels and links among them. Due to the complex nature of the human tissue, a channel modeling plays a crucial role in the design of physical layer technologies. Though lots of works have already proposed few channel models for physical layer in *WBANs*, nevertheless, none of them have taken the movements of the body into account, although the body mobility and posture changes may have severe impacts on the received signal strength, consequently, on the *WBAN* performance.

### 1.3.5 Antenna Design

The antenna design for *WBAN* applications is a challenging problem due to restrictions on the size, material, and shape of the antenna. The dimensions of an implanted antenna depend on its location inside the body, which further limits the freedom of its designer, i.e., only those platinum- or titanium-made antenna can be implanted underneath the skin. Moreover, the human tissue absorption of the energy dissipation and the heating due to the radiation and magnetic properties of the antenna should be taken as a primary concern by antenna designer. Therefore, interference mitigation techniques with minimal adverse radiation are desirable to ensure the short- and long-term safety of the human body.

## 1.4 Problem Statement and Motivation

Because the wireless networks are characterized by their wireless broadcast nature, one of the major issues arises, which is, *radio co-channel interference*. The radio co-channel

interference is caused by the nodes of different overlapping wireless networks that share the same radio spectrum at the same time. In fact, we differentiate between two scenarios: (i) the first, in which, two or more wireless networks employing the same communication protocol impose interference on each other, e.g., *WBAN-WBAN* interference, i.e., the co-channel interference is imposed by nodes of other nearby *WBANs* on the nodes of the desired *WBAN*, and the other way around, (ii) the second, in which, two or more different wireless networks employing different communication protocols and technologies impose interference on each other, e.g., *WBAN-WiFi*, i.e., the co-channel interference is imposed by nodes of any other-than-*WBAN*, e.g., *WiFi*, on the nodes of the desired *WBAN*, and vice versa. In both scenarios, the co-channel interference certainly occurs between two wireless networks if and only if nodes of these networks are simultaneously using the same channel, and the distance between them is smaller than the distance of their corresponding radio transceivers' ranges. In *WBANs*, data may be lost due to the co-channel interference, and hence acknowledgments are required to assure the transmitters the successful reception. Time-outs are used to detect reception failure at the corresponding receivers. We note that collisions may take place at sensor-level and coordinator-levels. An example of interference that can be experienced amongst three *WBANs* is shown in **Figure 1.2**. The sensor-level collision occurs when a sensor  $S_{3,1}$  of *WBAN*<sub>1</sub> is receiving an *Ack* packet from its corresponding *Crd*<sub>1</sub>, while at the same time, another sensor  $S_{4,2}$  of *WBAN*<sub>2</sub> is transmitting a data packet to its corresponding *Crd*<sub>2</sub>, the reception taking place at  $S_{3,1}$  collides with the data transmission initiated by  $S_{4,2}$ . This requires that the receiving sensor  $S_{3,1}$  and the interfering sensor  $S_{4,2}$  are in the transmission range of each other and simultaneously share the same channel. Similarly for the coordinator-level collision. Therefore, dealing with the interference among *WBANs* and their coexistence with other wireless networks is an important problem that warrants special attention [17].

Avoidance and mitigation of co-channel interference have been extensively researched in the wireless networks such as *WSNs*, *MANETs*, *WiFi*, *Cellular*, etc. However, due to the typical and unprecedented features of *WBANs*, such as limited energy resource, short-range low-power communication capabilities, dynamic channel, and mobility; the existing protocols proposed for large-scale wireless communication networks are not only inappropriate but also can not be directly applied to *WBANs*. Basically, when a large number of patients carrying *WBANs* coexist, talk and move towards each other in public places like a hospital's corridor or a health-care center, the radio co-

channel interference may arise accordingly. In fact, this fundamental problem is due to three main reasons. Firstly, no common centralized entity is responsible for the coexistence and interference management among the different *WBANs*. Secondly, though the *WBANs* are essentially designed to operate in distributed manner, nevertheless, due to their particular characteristics, design and nature, they are incapable of negotiating with each other or even coordinating their operation time. Thirdly, the existing protocols and technology standards, designed for *WBANs* so far, do not consider in their design the mobility of *WBAN* sensors relative to each other as well as the *WBANs* towards each other. As motivated by the aforementioned challenges, it is quite necessary to design and establish protocols for efficient and effective communication within a single *WBAN* or among different *WBANs* coexisting with other wireless networks. These new protocols must consider the special characteristics of *WBANs* in their design, ensure their proper and stable operation even in a populated area, under high mobility conditions, and in situations of the high level of interference.

## 1.5 Thesis Outline and Main Contributions

Motivated by the aforementioned challenges and the research problem, we conduct an intensive and systematic research aiming to design energy-efficient and reliable communication protocols for *WBANs*. In this thesis, we focus on research problems of fundamental and practical importance. Specifically, we address the following problems ranging from theoretical modeling and analysis to practical protocol design.

- Intra-*WBAN* interference mitigation and avoidance
- Cooperative Inter-*WBAN* interference mitigation and avoidance
- Non-cooperative Inter-*WBAN* interference mitigation and avoidance
- Interference mitigation and avoidance in *WBANs* with *IoT*

We provide the main contributions of our thesis in Chapter 3, 4, 5, and 6. The thesis is structured as follows:

- **Chapter 2 – Background:** in this chapter, we provide a brief survey of related prior work and conduct a comparative study of different interference mitigation and avoidance protocols for *WBANs* [11].
- **Chapter 3 – Interference Mitigation in Multi-Hop *WBANs*:** in this chapter, we address the problem of interference within a *WBAN* through dynamic time and spectrum allocation. Motivated by the benefits of two-hop communication, we firstly propose a time-based channel allocation mechanism, namely, *CFTIM*, that lowers the probability of interference within a *WBAN*. However, *CFTIM* incurs

additional energy consumption due to frequent channel hopping. Secondly, we propose another mechanism called *IAA* that dynamically adjusts the superframe length to lower the probability of interference and provides better scheduling of the medium access. *IAA* limits the number of channels to 2 to reduce the frequency of channel hopping and reduce the power consumption. We further analyze *CFTIM* and *IAA* and present a probabilistic model that proves the *SINR* outage probability is reduced. Meantime, simulation results demonstrate the effectiveness and efficiency of *CFTIM* and *IAA* in terms of reducing the probability of interference, extending the network lifetime and improving the throughput [8, 7, 9, 12].

- **Chapter 4 – Cooperative Inter-WBAN Interference Mitigation Using Walsh-Hadamard Codes:** in this chapter, we address the problem of sensor-level co-channel interference among cooperative *WBANs* through orthogonal code allocation. Motivated by the distributed time provisioning supported in the *IEEE 802.15.6* standard [2], we firstly propose a distributed time correlation reference scheme, namely, *DTRC*, that generates virtual time-based patterns to determine which superframes and which time-slots within those superframes interfere with each other. Secondly, we propose a cooperative code allocation scheme, namely, *OCAIM*, where each *WBAN* generates *sensor interference lists* and then all sensors belonging to these lists are allocated orthogonal codes to avoid the interference. Mathematically, we further analyze *OCAIM* and present a model that derives the success and collision probability for frames transmissions. Extensive simulations are conducted and results demonstrate that *OCAIM* can significantly diminish the inter-*WBAN* interference, improves the throughput and saves the power resource of the *WBANs* [6].
- **Chapter 5 - Non-Cooperative Inter-WBAN Interference Mitigation Using Latin Rectangles:** in this chapter, we address the problem of sensor-level co-channel interference among non-cooperative *WBANs* through time-slot and channel hopping. Motivated by the availability of multiple channels in the license-free 2.4 GHz *ISM* band of the *IEEE 802.15.6 standard*, we firstly propose a distributed time-based channel hopping mechanism, namely, *DAIL*, for sensor-level interference avoidance among *WBANs* based on Latin rectangles. *DAIL* allocates channel-and-time-slot combination to sensors to lower the probability of inter-*WBAN* interference while enabling autonomous scheduling of the medium access within each *WBAN*. However, *DAIL* incurs additional energy consumption and delay due to

frequent channel hopping. To resolve the problem, we propose another scheme, namely, *CHIM*, that allocates a random channel to each *WBAN* and provisions backup time-slots for failed transmission. Like *DAIL*, *CHIM* generates a predictable interference-free transmission schedule for all sensors within a *WBAN* based on Latin rectangles. Basically, *CHIM* enables only a sensor that experiences interference to hop to an alternative backup channel in its allocated backup time-slot. Furthermore, we develop an analytical model that derives bounds on the collision probability and throughput for sensors transmissions. Extensive and intensive simulation results demonstrate the effectiveness and efficiency of *DAIL* and *CHIM* in terms of collision probability, network energy lifetime, network throughput, transmission delay, and reliability [4, 5, 10].

- **Chapter 6 – Interference Mitigation in WBANs with IoT:** Motivated by the emergence of Bluetooth Low Energy (*BLE*) technology, we propose a distributed protocol, namely, *CSIM*, to facilitate the interference detection and mitigation and enable *WBAN* operation and interaction within an existing *IoT*. We integrate a *BLE* transceiver and a Cognitive Radio (*CR*) module within each *WBAN's Crd* for selecting an Interference Mitigation Channel (*IMC*) for its *WBAN*. To mitigate the interference, *CSIM* opts to extend the active period of the superframe to involve not only a *TDMA* frame, but also a Flexible Channel Selection (*FCS*) and a Flexible Backup *TDMA* (*FBTDMA*) frames. Basically, *CSIM* enables each *WBAN's* sensor that experiences interference on default channel within the *TDMA* frame to eventually switch to an *IMC* for successful data transmission. In essence, all interfering sensor nodes within the same *WBAN* will use the same *IMC*, each in its allocated backup time-slot within *FBTDMA* frame. The simulation results show that *CSIM* mitigates the interference, saves the power resource at both the *sensor-* and *coordinator-*levels [3].
- **Chapter 7 – Conclusions:** finally, we complete our thesis with conclusions that summarize the main contributions of our thesis and provide different directions for future research.

-



# Chapter 2

## Related Works

### Contents

---

<b>2.1 Resource Allocation</b> . . . . .	<b>18</b>
2.1.1 Channel Assignment . . . . .	19
2.1.2 Transmission Scheduling . . . . .	20
2.1.3 Combined Channel and Time Allocation . . . . .	20
2.1.4 Summary . . . . .	21
<b>2.2 Power Control</b> . . . . .	<b>22</b>
2.2.1 Link-state based Power Control . . . . .	22
2.2.2 Game Theory . . . . .	23
2.2.3 Summary . . . . .	25
<b>2.3 Multiple Access</b> . . . . .	<b>26</b>
2.3.1 Superframe Modification . . . . .	27
2.3.2 Superframe Interleaving . . . . .	27
2.3.3 Hybrid Solutions . . . . .	28
2.3.4 Summary . . . . .	29
<b>2.4 Link Adaptation</b> . . . . .	<b>30</b>
2.4.1 Data Rate Adjustment . . . . .	30
2.4.2 Two-hop Communication . . . . .	30
2.4.3 Summary . . . . .	32
<b>2.5 Conclusions</b> . . . . .	<b>33</b>

---

A *WBAN* co-channel interference mitigation and coexistence algorithm should ensure a proper functionality of co-located *WBANs*, and carry out, either independently

or cooperatively, their communications without severe performance degradation. Several *WBAN* coexistence protocols have been proposed in the literature, as well as by the *IEEE 802.15.6* standard, including the beacon shifting, channel hopping, and interleaving mechanisms. Basically, the standard was mainly designed to enable efficient intra-*WBAN* and beyond-*WBAN* communications, whereas, inter-*WBAN* communication is not supported efficiently. It is worth noting that the majority of these protocols are non-cooperative. The design of efficient *WBAN* systems for life and safety critical applications will require the support of cooperative coexistence mechanisms between co-located *WBANs*, where coordinators and/or on-body sensors of different *WBANs* can communicate with each other. Existing cooperative and non-cooperative coexistence approaches could be improved to meet the specific requirements of *WBANs*, especially to enable efficient inter-*WBAN* communications. In this chapter, a comparative review of the co-channel interference mitigation and avoidance techniques in the literature will be provided. Furthermore, we show that existing solutions fall short from achieving satisfactory performance, and outline open problems that warrant more investigation by the research community.

As pointed out, avoidance and mitigation of co-channel interference have been extensively researched in the wireless communication literature, and the published techniques can be categorized as resource allocation, power control, some solutions are also based on incorporation of multiple medium access arbitration mechanisms and link adaptation. An efficient interference mitigation technique should carefully balance between the excessive use of the scarce and limited resources in *WBANs* and the desired requirements of a *WBAN* application.

Although our study qualitatively compares interference mitigation techniques for *WBANs* and provides important insights about them, we arrive at the conclusion that there is no dominating technique that outperforms the others. Moreover, the existing interference mitigation and avoidance protocols do not completely address *QoS* requirements and achieve the desired performance in some health-care applications. We envision that cross-layer based interference mitigation protocols will be a promising solution methodology that is worthy increased attention.

## 2.1 Resource Allocation

Resource allocation, e.g., channels and time, is an effective way for avoiding co-channel interference and medium access collision. Some approaches have pursued this

methodology. We group published work into three categories as we discuss in the balance of this subsection.

### 2.1.1 Channel Assignment

Channel assignment deals with the allocation of channels to individual sensors, coordinators or any combination of them. Once the channels are allocated, *WBAN* coordinators may then allow the individual sensors or another coordinator within the network to communicate via the available channels. The main problem in channel assignment solutions is the limited number of available channels. Yet there is no accurate methodology to determine the level of interference based on *SINR*, *RSSI*, channel quality, etc [37].

Few published protocols pursued the channel assignment. For example, LAH [38] is based on adaptive channel hopping. Such channel hopping is decided according to the combination of a set of interference detection parameters (*RSSI*, etc.). LAH is a non-cooperative algorithm and is shown to improve the network throughput and lifetime. Whilst, DRS [39] is a resource allocation inter-*WBAN* interference mitigation scheme. In DRS, interference-free sensors from different *WBANs* transmit on the same channel, while highly interfering sensors transmit using orthogonal channels to maximize the spatial reuse. In DRS, the coordinators need to exchange *SINR* information with each other. Moreover, the resource allocation performs better for a static than dynamic and mobile *WBAN* network topology. Meantime, AIM is a *flow-based* approach [40] that classifies the sensors transmissions according to the *QoS*, packet length, etc. AIM allocates an orthogonal channel to each sensor that has the highest priority and has not been scheduled yet. Since AIM considers sensor-level interference mitigation, it significantly reduces the number of assigned channels as well as achieves a higher throughput.

On the other hand, some approaches avoided the co-channel interference by assigning conflict free channels. Basically, such approaches do not suit crowded environments where *WBANs* accidentally become in the proximity of each other. Nonetheless, this approach fits scenarios where the number of *WBANs* that coexist in a particular area can be predicted in advance. A common way is to use graph coloring for channel assignment in this case. Some approaches such as RIC [41] assume global control for assigning a channel to each *WBAN* using a lightweight random incomplete coloring algorithm. RIC does not optimally utilize the spectrum as it considers channel assignment at *WBAN*- rather than node-level. Meanwhile, GCS [42] is a graph coloring and cooperative scheduling based scheme for *WBANs*. Basically, GCS uses cooperative scheduling within each clus-

ter to minimize interference and increase the spatial reuse and a graph coloring scheme for channel allocation for *WBANs* rather than for sensors. However, GCS increases the time needed by sensors to complete their transmissions which is undesirable in a *WBAN*.

### 2.1.2 Transmission Scheduling

Intuitively the medium may be shared on a time basis. Basically, the data packet rescheduling is used to mitigate interference by assigning unused time-slots. Some interference mitigation schemes pursued careful scheduling of sensor transmissions so that the medium access collision could be avoided. Yan et al. [43] presented a QoS-driven transmission scheduling approach to limit the duration that a node in a *WBAN* has to be in active mode under time-varying traffic and channel conditions. The approach, which is named QSC, optimally assigns time-slots for each sensor node according to the QoS requirement while minimizing their energy consumption. CWS [44] cluster sensors of different *WBANs* into groups that avoid node-level interference. Then, CWS maps groups to the available time-slots by using the random coloring algorithm. CWS improves the system throughput and the network lifetime. Similarly, CSM [45] is a graph coloring-based scheduling method that avoids the inter-*WBAN* interference by assigning different time-slots to adjacent *WBANs* and by allocating more time-slots to traffic-intensive *WBANs* to increase the overall throughput. In CAG [46], different time-slots are mapped to distinct colors and a color assignment is found for each node in the network. The *WBAN* coordinators exchange messages to achieve a conflict-free coloring in a distributed manner.

### 2.1.3 Combined Channel and Time Allocation

A number of approaches try to mitigate interference by considered channel and time allocation collectively. Basically, variations in channel assignment due to mobility scenarios of sensors positions within each *WBAN* and *WBANs* relative to each other is factored in when allocating time-slots. Accordingly, Movassaghi et al. [47] proposed a distributed prediction-based inter-*WBAN* interference algorithm for channel allocation. The algorithm, which is called CAS, allocates transmission time based on such prediction-based channel allocation in order to reduce the number of interfering sensors, extend *WBAN* lifetime and improve the spatial reuse and throughput. Similarly, ACT [37] is an adaptive scheme to allocate channel and time to improve the probability of successful transmissions in *WBANs*. ACT adaptively allocates channel and time simultaneously by considering the channel conditions and the density of *WBANs*. Unlike CAS

**Table 2.1:** Notations & meanings

Notation	Meaning	Notation	Meaning
Med	medium	Dyna	dynamic
MOB	mobility	TPO	topology
COP	cooperation	DEL	delay
TOF	trade-off	DR	data rate
SPR	spatial reuse	CMX	complexity
NEG	negotiation	CHST	channel status
CHP	channel parameter	REL	reliability
CHUT	channel utilization	THR	throughput
MAC	medium access control	CEX	coexistence
CNV	convergence time	EC	energy consumption
LCR	level crossing rate	OP	outage probability

**Table 2.2:** Comparison of published resource allocation interference mitigation proposals for *WBANs*. A star topology is deployed in the following proposals

	EC	REL	THR	SPR	DEL	QoS	COP	MOB	CEX	CMX	CNV	MAC
JAD [17]	Low	High	High	High	Low	Yes	Yes	Yes	Yes	N/A	N/A	TDMA
ACT [37]	Low	High	High	N/A	N/A	Yes	No	Yes	Yes	N/A	N/A	TDMA
LAH [38]	High	Low	Low	Low	High	No	No	No	Yes	N/A	N/A	CSMA
DRS [39]	Med	Low	Low	High	High	No	Yes	No	Yes	N/A	N/A	TDMA
AIM [40]	Med	Med	High	Med	High	Yes	Yes	No	Yes	N/A	N/A	TDMA
RIC [41]	Low	N/A	High	High	N/A	N/A	No	Yes	Yes	Low	Fast	TDMA
GCS [42]	Low	N/A	High	High	N/A	N/A	No	Yes	Yes	Med	Slow	TDMA
QSC [43]	Low	Med	Med	N/A	Med	Yes	No	No	No	N/A	N/A	TDMA
CWS [44]	Low	N/A	High	High	N/A	N/A	Yes	No	Yes	Med	Slow	TDMA
CSM [45]	N/A	High	N/A	N/A	N/A	N/A	No	No	Yes	Low	Fast	TDMA
CAG [46]	Low	N/A	N/A	N/A	N/A	N/A	No	No	Yes	Med	Fast	TDMA
CAS [47]	Low	High	High	High	N/A	Yes	Yes	Yes	Yes	N/A	N/A	TDMA

and ACT, JAD [17] is an adaptive scheme based on social interaction (JAD). By knowing the mobility pattern of *WBANs*, JAD factors in traffic load, *RSSI*, and the density of sensors in a *WBAN* to efficiently utilize the time of sensor's transmission, diminish the interference and the power consumption as well as to improve the throughput. **Table 2.1** shows the list of symbols and the corresponding notations that we used in the balance of this subsection. **Table 2.2** provides a comparative summary of the different channel, time and hybrid allocation interference mitigation proposals discussed in this subsection.

#### 2.1.4 Summary

Resource allocation protocols, when applied in *WBANs*, must take topology and link changes as well as the dynamic traffic into account. If carefully designed, these protocols may work efficiently under the high level of interference and mobility conditions. Nonetheless, they require a frequent exchange of information among *WBANs* and lead to a cost, e.g., energy, delay, etc., in updating information. Whilst, graph-based resource allocation protocols do not suit the dynamic environment and are unsuitable for a topol-

ogy with high-frequent changes, e.g., *WBANs*, because they introduce additional costs due to update and message exchanges. In highly mobile and densely deployed *WBANs*, a graph-based resource allocation protocol may be not only inefficient but also detrimental for health-care applications. In addition, the convergence time of graph-based algorithms is a concern in the context of *WBANs*. Under high level of interference and highly mobile topology of *WBANs*, such protocols do not even support the minimal accepted requirements of QoS to *WBAN* applications.

## 2.2 Power Control

### 2.2.1 Link-state based Power Control

Saving energy by adjusting the link transmission power is very crucial to extend the lifetime of the *WBAN*. In *WBANs*, different factors such as fading, path loss and shadowing determine the link state quality and hence the transmission power can be adaptively controlled based on its link state. Centralized transmission power control (TPC) solutions proved their efficiency in wireless cellular networks and *WSNs*; however, these solutions are unsuitable for dynamic and highly mobile *WBANs* as each individual *WBAN* operates in a distributed manner [48, 49, 50, 51, 52].

See et al. [53] and Ge et al. [54] conducted different experiments to capture the PRR corresponding to *RSSI* variation measured in static and dynamic body posture scenarios for healthcare applications at 2.48 GHz. A correlation between the path loss and the PRR was made via the probability distribution of the *RSSI* for a given transmit power. In addition, the optimal transmit power at the different locations of sensors was obtained in order to conserve the battery energy. Quwaider et al. [55] developed a dynamic body posture-based power control mechanism (DOI) based on *RSSI*. Though DOI assigns transmission power to links amongst *WBAN* sensors in an optimal way; however, it incorrectly predicts such assignments when the state of these individual links varies rapidly. Whilst, Guan et al. [56] presented a transmission power control scheme, called DTP, which achieves high link reliability in mobile *WBANs*. Basically, DTP calculates the adjustment in transmission power according to the variation of the channel conditions, e.g., SINR, path loss, etc.

In [57], Xiao et al. promote a real-time reactive scheme (RTR) that adjusts the transmission power according to the *RSSI* feedback from the receiver, under different mobility conditions. Similarly, the link state estimation TPC protocol (LSE) [58] adapts the transmission power according to short-term and long-term link-state estimations. The

**Table 2.3:** Comparison of published link-state based power control interference mitigation proposals for WBANs

	THR	EC	REL	MOB	NEG	CHP	TOF
DOI [55]	Med	Med	Med	Yes	No	RSSI	No
DTP [56]	High	Low	High	Yes	No	RSSI	No
RTR [57]	Med	Low	Med	Yes	No	RSSI	Yes
LSE [58]	High	Med	High	Yes	No	RSSI	No
HOS [59]	High	Med	High	No	Yes	SINR	Yes
AGA [60]	Med	Low	Med	No	Yes	SINR	Yes

short-term estimations were generated from several *RSSI* samples and the long-term estimations were generated through adjusting the *RSSI* threshold range according to variations in *RSSI* samples. *RSSI* variations are studied according to stationary and non-stationary movement patterns of a patient carrying a WBAN.

On the other hand, HOS [59] is an opportunistic scheduling algorithm which assumes the interference mitigation at sensor-level and energy harvesting model to extend energy lifetime of WBANs. Interference-free sensors may transmit on the same channel while high interfering sensors may transmit through using orthogonal channels. Basically, sensors harvest energy from the wireless of other nodes in the network. Thus, HOS uses the interference as a source of energy. Meantime, AGA [60] is a power allocation algorithm based on genetic algorithm (GA) to mitigate inter-WBAN interference while ensuring heterogeneous QoS guarantees. An optimization model using GA is utilized to minimize the transmission power of the sensor in a WBAN. However, AGA did not consider the real-world mobility which may lead to a long convergence time. **Table 2.3** provides a comparative summary of the different link-state based power control interference mitigation proposals discussed in this subsection.

### 2.2.2 Game Theory

Game theory has been popular in the context of power control in WBANs. It has been shown in [61, 62] that the non-cooperative games are more appropriate for inter-WBAN interference mitigation since WBANs are independent of each other while pursuing cooperative games increase the energy consumption of WBANs. We review published techniques in the balance of this section.

#### Cooperative Games

Very few research studies have pursued the cooperative game theory approach for controlling transmission power in WBANs. Gengfa et al. [63] proposed an inter-WBAN interference aware proactive power control algorithm (PAU) motivated by the game theory which assumes some limited cooperation and information exchange (e.g., current

transmit power, channel gain, etc.) amongst *WBANs*. Although PAU has fast convergence time and low overhead, it is unsuitable for mobile *WBANs* because it assumes the channel and interference gains stay fixed. Similarly, Wang et al. [62] proposed a distributed cooperative scheduling scheme (CSR) to reduce inter-*WBAN* interference and increase the throughput. CSR formulates single-*WBAN* scheduling as an assignment problem which has been solved by using horse racing scheduling algorithm. The multi-*WBAN* concurrent scheduling is then formulated as a game, and its convergence to NE is shown. Meanwhile, NCL [64] is a low complexity game based power control approach is shown to reach NE based on best response and to determine the adjustment in transmission power for each transmission in a *WBAN* according to the interference level.

### Non-cooperative Games

As pointed out earlier, non-cooperative games theory approach proved to better suits TPC in *WBANs*. In [65], Kazemi et al. propose a non-cooperative power control game (NPG) based approach, which considers inter-network interference amongst nearby *WBANs*. In NPG, the existence and uniqueness of NE have been shown to match the best response solution. Nonetheless, NPG is more efficient than PAU, discussed above, because it assumes an adaptive power price and factors in the power budget. Unlike PAU and NPG, Kazemi et al. [66] proposed a distributed power control game (GRL) employing reinforcement learning (RL). In GRL, each *WBAN* acts as an agent and learns from experience to appropriately control the transmission power level in a dynamic environment without any message exchange. In addition, RL results in a better tradeoff, i.e., between network utilization and the power constraint for each *WBAN*, than PAU or NPG despite its long convergence time. To expedite convergence, the authors proposed a genetic fuzzy (GA) power controller (FPA) approach [67] that do not require any negotiation amongst *WBANs*. FPA requires the *SINR* and the current transmission power as inputs into GA in order to maximize the capacity, minimize the power consumption and the convergence time. Although FPA outperforms PAU, NPG, and GRL, it does not handle dynamic scenarios in which the interference level is unpredictable. On the other hand, NCR [68] considers the problem of joint relay selection and power control in *WBANs*, where each sensor a strategy to select its next hop and its transmission power independently in order to ensure short delay.

## Non-conventional Games

Unlike the game-based solution discussed above, the social nature, which is germane to *WBANs*, has been considered in the interference mitigation process. SIP [69] pursues a power-based game to diminish the interference among *WBANs* and to maximize the power resource. Each individual *WBAN* determines the distance to other interfering *WBANs* and informs other reachable *WBANs* in order for them to optimize its transmission power and avoid interference. Similarly, Dong et al. [70] proposed a non-cooperative social-based game theoretic transmit power control scheme (CPC) to maximize the packet delivery ratio amongst different coexisting *WBANs* so that the average transmission power is minimized.

Some game-theory interference mitigation schemes opt to provide QoS guarantees. PEG [71] pursues a non-cooperative power control game to mitigate the inter-*WBAN* interference. In PEG, the utility function is designed so that the QoS requirement can be met with minimal power consumption for each *WBAN*. To obtain an approximation of the NE point, a non-cooperative interference segmentation estimate algorithm has been proposed, which guarantees zero information exchange among the coordinator of *WBANs*. Similarly, Zhou et al. [72] proposed a game theoretical framework for interference mitigation and time-slots allocation for *WBANs* (SAG). The coordinator of the *WBAN* manages the probability of sensor access in the CAP based on sensors' priority and allocates time-slots with strategies for best payoff based on link states in GTSS. Whilst, BNC [73] employs a Bayesian non-cooperative game for power control. By modeling *WBANs* as players and active links as types of players in the Bayesian model, BNC tries to maximize each player's expected payoff involving both throughput and energy efficiency without any message passing amongst *WBANs*. The uniqueness of Bayesian equilibrium for the game has been derived. **Table 2.4** provides a comparative summary of the different game-based power control interference mitigation proposals discussed in this subsection.

### 2.2.3 Summary

The existing link-state based power control interference mitigation protocols have been qualitatively discussed and compared. Various protocols have shown that power control is suitable for highly mobile and populated environments with *WBANs*. Though link-state based protocols do not require message exchange among *WBANs*, nonetheless, they consume lots of energy and even do not support the accepted level of QoS requirements. These protocols do not suit environments with high-density of *WBANs* as the

**Table 2.4:** Comparison of game-based power control interference mitigation proposals for WBANs

	THR	EC	REL	MOB	COP	CHST	QoS	TOF	CNV
CSR [62]	High	Med	Med	No	Yes	Dyna	No	No	Slow
PAU [63]	Low	High	Low	No	Yes	Static	No	Yes	Slow
NCL [64]	High	Low	High	No	Yes	Dyna	No	No	Fast
NPG [65]	High	Low	High	No	No	Dyna	Yes	Yes	Slow
GRL [66]	High	Low	Med	No	No	Dyna	No	Yes	Slow
FPA [67]	Med	Low	High	No	No	Dyna	No	No	Fast
NCR [68]	Low	Low	Low	Yes	No	Dyna	Yes	Yes	Slow
SIP [69]	High	Low	High	No	Yes	Dyna	Yes	No	Slow
CPC [70]	High	Low	High	No	No	Dyna	No	No	Slow
PEG [71]	High	Low	Med	No	No	Dyna	Yes	No	Fast
SAG [72]	High	Med	High	No	No	Dyna	Yes	No	Fast
BNC [73]	High	High	High	No	No	Dyna	No	Yes	Slow

individual link states vary rapidly due to body movements. On the other hand, game-based power control protocols do not support the mobility of WBANs. Nonetheless, the majority of them are non-cooperative game-based protocols that support dynamic channel conditions, e.g., varying channel gain, interference power, etc., and do not require message and information exchange, which reduces the energy consumption across coexisting WBANs. However, game-based protocols do not support QoS and are characterized by long delays.

## 2.3 Multiple Access

In contention-based MAC, e.g., CSMA/CA, sensors can decide their medium access individually. When the density of WBANs is high, the performance of individual WBANs could be degraded because of the incurred medium access collisions, e.g., time and energy consumption during a backoff. On the other hand, contention-free protocols use time synchronization to provide interference-free transmissions and high communication efficiency. However, a major limitation of such approach is the need for time synchronization which is very costly to achieve in WBANs, particularly those employ non-similar duty cycles. Contention-free MAC is reliable and energy-efficient [74, 75] in low-density WBANs, though extra energy is consumed due to time synchronization and control messages.

The IEEE 802.15.6 [2] MAC protocol does not support all the requirements of WBANs. There are some time parts distributed within the superframe structure which are not occupied most of the time that reduces the channel utilization. Some sensors should wake-up periodically only to receive beacons which increases their energy consumption. Body gestures could lead to deep fading which may span for up to 400 ms [76, 77], which is not taken into account in the IEEE 802.15.6 MAC design as well as the TDMA ordering

is kept fixed in the superframe, which both cause packet losses and reduce the reliability of *WBANs*. Importantly, the standard does not mandate a particular *MAC* layer which assumes heterogeneous traffic and dynamic environments in *WBANs*. Such flexibility motivated for a few studies for interference mitigation among *WBAN* at the *MAC* level as we discussed below.

### 2.3.1 Superframe Modification

Some of the published protocols have pursued superframe modification in order to diminish the probability of medium access collision; they basically modify the internal structures and their ordering as well as the size of the superframe in order to provide energy-efficient and reliable communication for *WBANs*. ASL [78] is an example of these adaptive *MAC* protocols and which opts to reduce the energy consumption and improve the throughput as well. ASL employs *CSMA/CA* to adjust superframe length according to the level of interference. Whereas, in [79], a novel transition matrix method to estimate the channel dynamics has been proposed. Based on channel dynamics estimation, Zhou et al. have revealed the fundamental effect of a proper superframe length in opportunistic scheduling and further designed a simple scheduling scheme, namely, QSM, that dynamically adjusts the superframe length according to the channel condition. Whilst, DIM [80] adjusts the length between superframe's scheduling phase (SP) and contention access phase dynamically according to the different levels of interference. In essence, the length of SP will be reduced when the channel utilization in SP decreases and will be expanded on the contrary. On the other hand, RAP [81] is a *MAC* protocol based on adaptive resource allocation and traffic prioritization for *WBANs*. RAP adaptively modifies the interval of the consecutive transmissions according to the medical status of the *WBAN* user and the channel conditions. Moreover, RAP employs a synchronization method which instructs sensors that do not have pending data to sleep in order to save the power resource. CAC [82] is a *TDMA*-based *MAC* protocol that aims to achieve an accepted level of QoS. CAC dynamically adjusts the sensor's transmission time and order based on mobility-incurred channel status and traffic characteristics in *WBANs*. In addition, the time-slot allocation is further optimized by minimizing energy consumption and synchronization overhead of sensors subject to QoS constraints.

### 2.3.2 Superframe Interleaving

One way to limit the probability of collision is through superframe interleaving. Basically, the coordinators of *WBANs* exchange information in order to prevent the active

periods of their corresponding superframes from overlapping with each other. CST [83] pursues the simplest and most intuitive, yet inefficient solution by creating a common TDMA medium access schedule among multiple coexisting WBANs in order to mitigate the interference and in consequence improve the throughput. CST determines the time for WBANs coordinators to exchange their transmission schedules. DCD [28] is an approach through which WBANs coordinators cooperatively rearrange the individual active periods of their corresponding superframes. DCD efficiently mitigates the interference and improves channel utilization. Meanwhile, FBS [84, 85] is a distributed TDMA-based beacon interval shifting protocol to reduce the packet loss, power consumption, and data delivery latency. FBS employs carrier sensing before any beacon transmission to prevent the wake-up periods of WBANs from overlapping with each other. Grassi et al. [27] used centralized multiple access mechanisms which reschedule beacons to avoid active period overlapping and to reduce the interference amongst WBANs ( $B^2R$ ). Whilst, AIA [61] employs a distributed asynchronous inter-WBAN interference avoidance scheme based on both CSMA/CA and TDMA. AIA includes the timing offset and dynamically adjusts the schedule of the TDMA period to avoid collisions when such period overlaps with those of between nearby WBANs. AIA adapts to the level of interference in multiple mobile WBAN environments as well as improves the coordination time without incurring significant complexity overhead.

### 2.3.3 Hybrid Solutions

Some interference mitigation solutions have pursued a hybrid contention-free and contention-based approach in order to leverage their advantages. 2LM [1] is a two-layer based MAC protocol in which the coordinator of the WBAN schedules transmissions within its WBAN using TDMA, and employs a carrier sensing mechanism to deal with inter-WBAN collisions. 2LM reduces transmission collisions, delay, and energy. However, 2LM is not adaptive to the interference level and does not specify any sleeping mechanism to avoid unnecessary wake-up and the delay due to the long back-off. Whilst, HEH [86] is a hybrid polling MAC protocol leverages harvested energy from the human body. HEH combines polling and probabilistic contention access methods in order to enable prioritized medium access to the sensors. HEH improves the WBAN energy efficiency, throughput, and QoS. QoM [87] is a QoS-based MAC designed for heterogeneous high-traffic WBANs. QoM employs preemptive priority scheduling mechanism among WBANs and a fuzzy inference within a WBAN to avoid interference. QoM does not assume in its design the dynamic movements of the body and the large crowd

**Table 2.5:** Comparison of published multiple access interference mitigation proposals for WBANs.

	EC	CHUT	THR	DEL	REL	QoS	COP	CEX	MOB	MAC
2LM [1]	Med	High	Med	High	Med	Med	No	Yes	No	Hybrid
$B^2R$ [27]	Med	Med	Med	Low	Med	Med	No	Yes	No	CSMA
DCD [28]	High	Low	Low	High	Low	Low	Yes	Yes	No	CSMA
AIA [61]	Med	Med	Med	Low	Low	Low	No	Yes	Yes	Hybrid
ASL [78]	Med	High	Low	Low	Med	Med	No	Yes	No	CSMA
OSM [79]	Low	High	High	High	Med	High	No	No	No	TDMA
DIM [80]	High	Med	Low	High	Low	Low	No	Yes	No	CSMA
RAP [81]	Med	Med	Low	Med	Med	Med	No	No	Yes	Hybrid
CAC [82]	Med	Med	Med	Med	Med	Med	No	Yes	Yes	Hybrid
CST [83]	Low	N/A	Med	High	Low	Low	Yes	Yes	NO	TDMA
FBS [84, 85]	Low	High	High	Low	High	High	No	Yes	No	TDMA
HEH [86]	Low	High	High	Low	High	High	No	No	Yes	TDMA
QoM [87]	Med	Med	Med	High	Low	Med	No	Yes	No	Hybrid
isM [88]	High	Med	Med	Med	Med	Med	No	Yes	Yes	CSMA

of WBANs. Meantime, isM [88] is a multi-channel MAC protocol based on channel hopping for WBANs. isM employs an anti-collision mechanism, a rotation mechanism for coordinators and a power adjustment method to reduce end-to-end delay and save energy resource in WBANs. It is worth noting that a star topology is employed by all multiple access based interference mitigation protocols discussed in this subsection. *Hybrid* denotes a mix of TDMA and CSMA/CA is employed by an interference mitigation protocol, as explained above. **Table 2.5** provides a comparative summary of the different multiple access interference mitigation proposals discussed in this subsection.

### 2.3.4 Summary

The published work on MAC protocols have demonstrated that, due to their flexibility, contention-based protocols cope better with distributed networks, which make them possible solutions for WBAN applications. Whilst, contention-free, e.g., TDMA, could be one possible solution to avoid intra-WBAN interference [89]. Contention-free and contention-based approaches are recommended for environments with small number of WBANs with low-occupancy channels and a small number of sensors [90, 91]. However, these approaches are not recommended for WBANs with high mobility and traffic load as well as characterized by large number of sensors as these approaches impose significant medium access collision problems and long delays, due to the channel condition that changes very quickly, and hence their implementation becomes inefficient. Particularly, time-sharing based solutions in which WBANs interleave their active period through negotiation or contention are ineffective when the load in WBANs is heavy and duty cycle of WBAN is high. The rescheduling may cause significant transmission delay if there are a large number of coexisting WBANs.

**Table 2.6:** Comparison of published data rate adjustment interference mitigation proposals for *WBANs*

	DR	EC	THR	PER	CHP	TPO	MAC	MOB	CEX
MRC [92]	High	Low	High	Low	SINR	Star	TDMA	No	Yes
LAC [93]	Med	Med	Med	Low	SNR	Star	CSMA	No	No
TDM [94]	High	Low	High	Low	SINR	2-hop	TDMA	Yes	No

## 2.4 Link Adaptation

Interference, in essence, affects the individual wireless links. Therefore, one way to mitigate the effect of interference is to adjust the link parameters. For instance, the link data rate, modulation, etc., can be dynamically varied according to the channel conditions, e.g., the path loss, *RSSI*, etc. These protocols invariably require some channel state information at the transmitter. In the balance of this section, we provide an overview of published link adaptation schemes in the realm of *WBANs*.

### 2.4.1 Data Rate Adjustment

The implementation of TPC mechanism is very challenging in dynamic scenarios when the channel conditions vary rapidly as the *WBANs* expose to mobility. On the other hand, data rate adjustment protocols are very simple to implement and can provide an accepted level of the link quality in high interference conditions.

Yang et al. [92] presented a few number of interference mitigation methods (MRC), e.g., data rates, adaptive modulation, etc., in order to provide an acceptable level of link quality. The coordinator picks the suitable scheme for the sensors based on the level of experienced interference. Similarly, LAC [93] is a contention-based link adaptation scheme for interference mitigation within a single *WBAN*. In LAC, the sensors employ link adaptation strategy to pick the suitable adaptive data rate to lower the bit error rate according to the channel conditions. On the other hand, Moun gla et al. [94] presented a tree-based topology design called TDM for a mobile *WBAN* that ensures reliable communication. In TDM, the sensors and relays share, respectively, a small and large number of channels to ameliorate the data flow among different sensors of the *WBAN*. Basically, TDM employs adaptive schemes, e.g., data rate, to diminish the interference among relays **Table 2.6** provides a comparative summary of the different data rate adjustment interference mitigation proposals discussed in this subsection.

### 2.4.2 Two-hop Communication

The nature of human body tissues and its mobility make the deployment of one-hop communication inefficient due to signal attenuation and shadowing. Thus, the *IEEE*

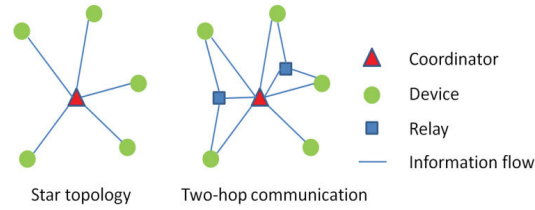


**Figure 2.1:** One-hop and two-hop communication schemes

802.15.6 standard proposes two-hop communication as an alternative solution because it exploits the benefits of spatial diversity to ameliorate the communication efficiency and transmission reliability in WBANs. Moreover, using the two-hop communication allows for better WBAN interference mitigation and coexistence. However, using two-hop may exhaust the energy resource of the relays because of the frequent relaying process through them. In [95], the performance of one-hop and two-hop communications schemes is compared to demonstrate the effectiveness of the relay transmission mechanism in WBANs. **Figure 2.1** shows an example for one-hop and two-hop communication schemes [96].

Several interference mitigation solutions based on two-hop communication have been published for WBANs. Feng et al. [97] presented temporal and spatial correlation models to better characterize the slow fading effect of on-body channels. They proposed a dynamic prediction-based relay transmission scheme (PRT) which uses all the characteristics of on-body channels and provides an enhancement in power savings and reliability in a WBAN. PRT decides the time and the set of nodes that should relay in an optimal way according to channel conditions. PRT needs neither extra signaling procedure nor dedicated channel sensing period. DMT [98] is a decode-with-merge technique (DMT) that maintains the relaying mode by merging frames from the relayed and generated by relay nodes in order to increase the throughput at the WBAN coordinator without increasing the energy consumption. However, DMT does not address the interference occurring at relay nodes. Whilst, Dong et al. [96] proposed a relay-assisted cooperative communications scheme (LRS) for a WBAN. LRS considers two relay nodes and provides a 3-link diversity gain (DG) to the coordinator with selection combining (SC). Similarly, SOR [99] is a two-hop scheme integrated with opportunistic relaying (OR) for mobile WBANs (SOR). By using received SINR at the relay and coordinator nodes, SOR chooses the best relay to decode and forward the data at the same time with the direct link. JNT [100] is a two-hop cooperative scheme integrated with transmit power control (JNT) and based on simple channel prediction for WBANs. In JNT, a transmit power control mechanism is integrated into sensor and relay nodes to prolong

**Table 2.7:** Comparison of published two-hop based interference mitigation proposals for WBANs

	EC	REL	OP	LCR	THR	CHP	MAC	MOB	CEX
DFP [25]	N/A	High	High	N/A	High	SINR	TDMA	Yes	Yes
PRT [97]	Low	High	High	Low	High	SINR	TDMA	Yes	No
DMT [98]	Low	Low	N/A	N/A	High	LQI	CSMA	No	No
LRS [96]	N/A	High	High	Low	High	Gain	CSMA	Yes	Yes
SOR [99]	N/A	High	High	Low	High	SINR	TDMA	Yes	Yes
JNT [100]	Low	High	High	N/A	High	SINR	TDMA	No	Yes

sensor battery lifetime and mitigate the interference at the WBAN coordinator. Mean-time, DFP [25] is a TDMA-based two-hop communication scheme (DFP) among multiple mobile non-coordinated WBANs. The coordinator of designated WBAN employs a decode-and-forward mechanism with two links, two relays and selection combining as well as a TDMA for time-slot allocation for each link transmission. Table 2.7 provides a comparative summary of the different two-hop based interference mitigation proposals discussed in this subsection.

### 2.4.3 Summary

Data rate adjustment protocols are effective and simple to implement and can achieve acceptable link quality. However, they do not suite highly mobile and densely deployed WBANs because of the fast-changing channel conditions, e.g., SINR. On the other hand, using two-hop interference mitigation based protocols improve the channel gain and SINR thresholds at low outage probability which further increases the throughput at WBAN receivers. Moreover, these protocols reduce the level crossing rate (LCR) at low SINR values, e.g., an LCR of 1 Hz, a SINR threshold value increases by 6 dB, and extend the average non-fade duration that both lower the overhead for scheduling transmissions [96]. Level crossing rate (LCR) is a statistic that describes the measure of the rapidity of the fading and quantifies how often the fading crosses some threshold. Whilst, the non-fade duration quantifies how long the signal spends above some threshold, where there exists sufficient signal strength during which the receiver can work reliably and at low bit error rate. Therefore, using two-hop based protocols allow for more packets of large size to be transmitted, i.e., larger data rates, which reduce the transmission delay. However, the two-hop transmission may also introduce some additional latency to the packet delivery that may be unacceptable in time-sensitive health-care applications, e.g., heart vital data.

## 2.5 Conclusions

In this chapter, a comparative review of the co-channel interference mitigation and avoidance techniques in the literature has been provided and analyzed. These techniques are categorized as resource allocation, power control, some solutions which are based on incorporation of multiple medium access arbitration mechanisms and link adaptation. We summarize the advantages and disadvantages of each technique as follows:

- Channel and time resource allocation protocols suit highly mobile and densely deployed WBANs and high interference conditions. These protocols can provide an accepted level of QoS requirements. Graph-based resource allocation protocols do not suit WBAN topologies which are characterized by high-frequent changes. Such topologies add costs in terms of update and message exchanges which make them not only inefficient but also detrimental for health-care applications. Moreover, these protocols do not support QoS requirements to sensors.
- The existing link-state based power control interference mitigation protocols have been qualitatively discussed and compared. Power control protocols suit highly mobile and populated environments with WBANs. Although link-state based protocols do not need message exchange among the different coexisting WBANs, these protocols exhaust the power resource in WBANs and do not support their QoS requirements. In addition, these protocols are unsuitable for densely deployed WBANs because the link state varies very rapidly due to body gestures. On the other hand, game-based power control protocols are not recommended for mobile WBANs. Nonetheless, the majority of them are non-cooperative game-based protocols that support dynamic channel conditions, e.g., varying channel gain, interference power, etc., and do not require message and information exchange, which reduces the energy consumption across coexisting WBANs. However, game-based protocols do not support QoS and are characterized by long delays.
- The published work on MAC protocols have demonstrated that, due to their flexibility, contention-based protocols cope better with WBANs, which make them possible solutions for WBAN applications. Whilst, contention-free, e.g., TDMA, could be one possible solution to avoid intra-WBAN interference. Contention-free and contention-based approaches are suitable for low-density of WBANs with low-occupancy channels and few sensors. However, these approaches are not recommended for mobile and densely deployed WBANs and with the high-traffic load as

these approaches impose significant medium access collision problems and long delays, due to the channel condition that changes very quickly. Particularly, time-sharing based solutions in which *WBANs* interleave their active period are inefficient with a high density of *WBANs* and the duty cycle of the individual *WBAN* is high. The rescheduling could lead to longer delays with densely deployed *WBANs*.

- Data rate adjustment protocols do not suite highly mobile and densely deployed *WBANs* because of the fast-changing channel conditions, e.g., *SINR*. On the other hand, using two-hop based protocols improve the channel gain and *SINR* which further increase the throughput at *WBAN* receivers. Using two-hop based protocols allow for more packets of large size to be transmitted, which reduce the transmission delay. However, the two-hop transmission may also introduce some additional latency to the packet delivery that may be unacceptable in some health-care applications.

We arrived at the conclusion that the majority of proposals published in the literature for *WBANs* so far focused on either mitigating the interference at *WBAN's* coordinator or very few number of these proposals focused on mitigating the interference at sensor-level. However, in our thesis, we go a step further and consider interference mitigation and avoidance not only at sensor-level but also at sensor- and time-slot-levels through using multi-channel hopping with superframe adjustment and multi-code with superframe interleaving. In this chapter, we arrive at the conclusion that there is no dominating technique that outperforms the others. Moreover, the existing interference mitigation techniques do not completely address QoS requirements and achieve the desired performance in some health-care applications. We envision that cross-layer based interference mitigation protocols will be a promising solution methodology that is worthy increased attention.

# Chapter 3

## Interference Mitigation in Multi-Hop WBANs

### Contents

---

<b>3.1 Introduction</b> . . . . .	<b>36</b>
<b>3.2 Related Work</b> . . . . .	<b>37</b>
<b>3.3 Resource Allocation for Intra-WBAN Interference Mitigation</b> . . . . .	<b>39</b>
3.3.1 System Model . . . . .	39
3.3.2 Superframe Structure - <i>FTDMA</i> . . . . .	40
3.3.3 <i>CFTIM</i> Resource Allocation . . . . .	41
3.3.4 <i>CFTIM</i> Analysis . . . . .	42
3.3.5 Outage Probability . . . . .	42
3.3.6 Stability Condition . . . . .	45
3.3.7 <i>CFTIM</i> Performance Evaluation . . . . .	45
<b>3.4 Improved Resource Allocation for Intra-WBAN Interference Mitigation</b> .	<b>47</b>
3.4.1 System Model . . . . .	47
3.4.2 <i>IAA</i> Improved Resource Allocation . . . . .	47
3.4.3 <i>IAA</i> Superframe Structure . . . . .	50
3.4.4 <i>IAA</i> Analysis . . . . .	51
3.4.5 <i>IAA</i> Performance Evaluation . . . . .	52
<b>3.5 Conclusions</b> . . . . .	<b>54</b>

---

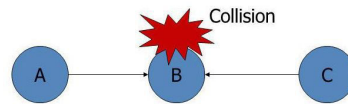


**Figure 3.1:** A collision takes place at a receiving node

### 3.1 Introduction

A viable solution to avoid the interference within a *WBAN* is to use *TDMA*. Due to the different requirements of *WBAN* applications, duty cycles, sampling and data rates, etc., it is hard to predict the number of active nodes in a period of time. According to the level of the interference, a dynamic way of scheduling the medium access within the *WBAN* is promising to efficiently utilize its limited resources, e.g., spectrum, energy, etc.

Recently, the *IEEE 802.15.6* standard [2] has adopted the multi-hop communication which improves the *SINR* values at the receiver nodes. With contention-based MAC, the individual performance of *WBAN* nodes may be degraded because of the incurred long delay and high energy consumption during backoffs, when the density of nodes is high. Though contention-free protocols can achieve collision-free transmissions and high throughput, nonetheless, these protocols need tight time synchronization which is very costly to achieve in *WBANs*. Contention-free is reliable and energy-efficient approach [17, 75] in low-density *WBANs*, though extra energy is consumed for their periodic synchronization and control packets. **Figure 3.1** illustrates the collision problem. A and B are transmitting nodes, while, C is a receiving node (e.g., a coordinator or a relay node).

- A transmits to B
- C senses the channel
- C does not hear A's transmission (i.e., A is not in the range of C)
- C transmits to B
- Transmissions from A and C collide at B

In this chapter, we address the problem of co-channel interference within a *WBAN* through time-based resource allocation. Motivated by the two-hop communication, our approach exploits the 16 channels in the *IEEE 802.15.6* standard [2] and takes advantage of the superframe length adjustment to lower the probability of interference, while enabling autonomous scheduling of the medium access within the *WBAN*. Specifically, we propose two schemes, the first is called CSMA to Flexible TDMA combination for Interference Mitigation (*CFTIM*), assigns time-slots and stable channels to sensors to minimize the intra-*WBAN* interference. Basically, *CFTIM* enables interference-free source

nodes to transmit directly to the relay nodes using the base channel in the first round. Whilst, the high interfering source and relay nodes transmit directly to the WBAN's coordinator through using flexible TDMA and stable channels in the second round. Despite being very effective, CFTIM involves overhead in terms of energy due to the frequent channel switching. The second is called Interference Avoidance Algorithm (IAA), that dynamically adjusts the length of the superframe according to the channel conditions and limits the number of channels to 2 only to minimize the frequency of channel switching and save the power resource. IAA enables the interference-free source nodes to transmit directly to the relay nodes using the base channel. Meanwhile, the high interfering source nodes employing the base channel may extend the contention window or switch to another channel in the first round. Whereas, the relay nodes employ a flexible TDMA to transmit to the coordinator using the base channel in the second round. The main contributions of this chapter are summarized as follows:

- *CFTIM, a scheme which enables dynamic time-based resource allocation based on a flexible TDMA to diminish the probability of the interference and allow for better scheduling of the medium access within a WBAN.*
- *IAA, a scheme that dynamically adjusts the length of the superframe according to the channel conditions and enables time-based resource allocation through using a flexible TDMA and two channels only. IAA opts to lower the impact of intra-WBAN interference significantly and save the energy resource while enabling better scheduling of the medium access within a WBAN.*
- *A probabilistic model analytically proves the SINR outage probability is minimized.*
- *Simulation results show that our approach can significantly reduce the probability of interference, save the energy resource and improve the throughput within a WBAN.*

## 3.2 Related Work

Several studies have focused on the adverse effects of co-channel interference on the performance of a WBAN. Resource allocation, e.g., channels and time, is an effective way for avoiding the interference, either by assigning unused time-slots or sharing the medium on a time basis. Some interference mitigation schemes pursued the medium access scheduling approach so that the collisions could be avoided within the WBAN. Yan et al. [43] pursued this methodology and presented a QoS-driven transmission scheduling approach to limit the duration that a node in a single WBAN has to be in active mode under time-varying traffic and channel conditions. Their approach opti-

mally assigns time-slots for each sensor node according to the QoS requirement while minimizing their energy consumption.

The transmission power can be adaptively controlled based on its link state to improve the reliability and extend the lifetime of the WBAN. Published work pursued this approach include [55, 56, 57, 58]. Quwaider et al. [55] developed a body posture-based power control mechanism which provides optimal power assignments for fixed links amongst sensors of a WBAN to maintain high throughput. Whilst, Guan et al. [56] proposed another algorithm that calculates the adjustment in transmission power according to the variation of the channel conditions to save the energy and achieve high link reliability in a mobile WBAN. In [57], Xiao et al. promote a real-time reactive scheme (RTR) that adjusts the transmission power according to the RSSI feedback from the receiver, under different mobility conditions. Similarly, the link state estimation protocol (LSE) [58] adapts the transmission power according to short-term and long-term link-state estimations. RSSI variations are investigated according to stationary and dynamic states of a patient. LSE achieves low transmission power levels and packet loss.

A number of published works pursued the approach of multiple access include [81, 86, 79]. RAP [81] is a MAC protocol based on adaptive resource allocation and traffic prioritization for a WBAN. RAP adaptively modifies the interval of the consecutive transmissions according to the channel conditions and employs a synchronization method to keep sensors sleeping as long as they do not have data to transmit. Whilst, HEH [86] is a hybrid polling MAC protocol leverages harvested energy from the human body and combines polling and probabilistic contention access methods to enable prioritized medium access to the sensors. Whereas, in [79], a novel transition matrix method to estimate the channel dynamics has been proposed. Zhou et al. have revealed the fundamental effect of a proper superframe length in opportunistic scheduling and further designed a simple scheduling scheme that dynamically adjusts the superframe length according to the channel condition.

Yang et al. [101] proposed several interference mitigation schemes such as adaptive modulation, data rates, and duty cycles to preserve acceptable link quality. The coordinator selects the appropriate scheme for the sensors based on the level of experienced interference. Similarly, LAC [93] is a contention-based link adaption scheme for interference mitigation within a WBAN. In LAC, the sensors employ link adaptation strategy to select the appropriate modulation scheme like adaptive data rate to decrease the PER according to the level of interference. On the other hand, Moun gla et al. [94]

proposed a multi-hop tree-based *WBAN* topology design that assumes the mobility of the *WBAN* while ensuring reliable data delivery. In such a design, which is called TDM, the *WBAN* sensors share a small number of channels, whereas, the relay nodes share the most number of channels to improve the data flow across the *WBAN*.

Meanwhile, Feng et al. [97] presented a relay-based transmission scheme that characterizes the slow fading effect of on-body channels to improve the energy efficiency and reliability in a *WBAN*. When to relay and which node to become a relay, are decided in an optimal way based on the last known channel states. Whilst, Dong et al. [96] proposed a cooperative scheme for a *WBAN*, which considers two relay nodes and provides 3-link diversity gain to the coordinator with selection combining. Similarly, SOR [99] is a two-hop scheme integrated with opportunistic relaying for mobile *WBAN*. By using received *SINR* at the relay and coordinator nodes, SOR chooses the best relay to decode and forward the data with the direct link. Meantime, JNT [100] is a two-hop cooperative scheme (JNT) based on simple channel prediction for a *WBAN*. In JNT, a transmit power control mechanism is integrated into sensor and relay nodes to prolong sensor battery lifetime and mitigate the interference at the coordinator.

### 3.3 Resource Allocation for Intra-*WBAN* Interference Mitigation

As pointed out, a dynamic way of scheduling transmissions is required to avoid the interference and better utilize the limited resources in the *WBAN*.

#### 3.3.1 System Model

We consider a single *WBAN* that consists of  $N$  source nodes,  $R$  relay nodes and a coordinator, denoted by *Crd*. A node can be a source that senses and transmits its data packet to a relay node or to the *Crd*, whilst, the relay node can convey other node's data packet to the *Crd*. We consider the following assumptions on the nodes and network:

- A mobile and dynamic topology of a *WBAN* are considered.
- The number of active nodes within the *WBAN* is unexpected.
- One-hop and two-hop are employed within the *WBAN*.
- CSMA/CA and flexible TDMA are employed within the *WBAN*.
- A node transmits one data packet in a time-slot.
- The number of available stable channels is always larger than the number of nodes demanding for that channels.
- Only one relay node transmits the node's packet to the *Crd*.

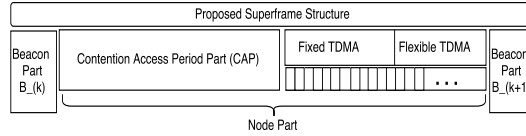


**Figure 3.2:** FTDMA superframe structure

In the balance of this subsection, we propose a flexible *TDMA*-based superframe structure, denoted by *FTDMA*

### 3.3.2 Superframe Structure - *FTDMA*

In the traditional *TDMA*, a superframe is usually delimited by beacons and consists of active and inactive parts. Basically, an active part consists of a fixed number of equal intervals, each called a time-slot. Each time-slot is assigned to a single node through which it transmits its packet to the *Crd*. In our approach, a superframe is divided into two parts. The first part is denoted by *beacon part* and used by the *Crd* to determine the size and the structure of the next superframe as well as for broadcasting beacons and synchronization. The second part is denoted by *node part* and used by the source nodes for transmitting their packets directly or via relay nodes to the *WBAN's Crd* as illustrated in **Figure 3.2**. Moreover, the node part is further composed of two parts, 1) a contention-based part denoted by *CAP* in which a *CSMA/CA* is employed by the interference-free source nodes to transmit their packets to the relay nodes and, 2) a contention-free part in which a *TDMA* is employed by both high interfering source and relay nodes to transmit directly to the *Crd*, each within its allocated time-slot. Basically, a node in the contention-free part verifies whether its *ID* exists in the *nodeSlotlist*, if it finds it, it transmits its packet in one of the  $m$  time-slots. Otherwise, it synchronizes with the *Crd* and then randomly selects one of the  $p-m$  empty time-slots of the flexible *TDMA* through which it transmits its packet. Since these time-slots are free and not yet assigned, there is a chance of collision with the transmission of any other node trying to transmit at the same time. If the packet is successfully sent, the *Crd* will allocate a time-slot for that node in the node part. However, if collision happens, the *Crd* will not include its *ID* in the *nodeSlotlist* of the next superframe. In such cases, a node keeps trying different empty time-slots randomly until a time-slot is assigned to it. In our approach, the size of the contention-free part is made dynamically changing according to the level of the interference. Based on the history and the number of the active sensors currently connected to the *Crd*, this latter collects some information to construct the node part of the next superframe. Basically, a node is considered active if it has received at least one beacon during the last previous  $k=3$  superframes. If there are  $m$  active nodes

connected, the *Crd* allocates  $p$ , where  $p > m$ , time-slots in the contention-free part of the node part. The first  $m$  time-slots are allocated to the active nodes and the rest  $p-m$  time-slots are reserved to the newly incoming nodes. It is worth noting that  $m$  time-slots form the fixed *TDMA* part, and the  $p-m$  time-slots form the flexible *TDMA* part of the contention-free part. In essence, the *nodeSlotList* includes all *IDs* of the nodes that are allocated time-slots in the fixed *TDMA*. The *Crd* reports the new size and structure of the superframe to its *WBAN* through the beacon. **Algorithm 1** shows high level summary of the proposed *FTDMA* construction.

---

**Algorithm 1** *FTDMA* Superframe Structure
 

---

**Require:** *ISBR*, High interfering source or Best relay *RS*, Node identifier *ID*, Beacon *B*

- 1: *Crd* broadcasts  $B^k$ ;
  - 2:  $m = 0$ ;
  - 3: **for**  $i=1$  to  $\text{sizeof}(\text{ISBR})$  **do**
  - 4:   **if** *Crd* acknowledges  $RS_i$  **then**
  - 5:     *Crd* includes  $ID_{RS_i}$  in *nodeSlotList* of  $B^{k+1}$
  - 6:      $m = m + 1$ ;
  - 7:   **end if**
  - 8: **end for**
  - 9: *Crd* forms the interference-free part of  $p$  time-slots;
  - 10: *Crd* forms the fixed *TDMA* part of  $m$  time-slots;
  - 11: *Crd* forms the flexible *TDMA* part of  $p-m$  time-slots;
  - 12: *Crd* forms the *nodeSlotlist* of  $m$  *IDs* of nodes; =0
- 

### 3.3.3 CFTIM Resource Allocation

After the last beacon frame is successfully received, all source nodes compete to access the base channel using a *CSMA/CA*. During this competition, two sets of source nodes are generated, 1) interference-free source nodes that are denoted by **{TS}**, and 2) high interfering source nodes that are denoted by **{IS}**. We denote *SINR* by  $\delta$ , *SINR* threshold by  $\delta_{Thr}$  and define the following:

- **Interference-free source node:** is a *CSMA/CA*-based source node that can successfully transmit its data packet to the relay node, i.e., it does not experience the interference because  $\delta \geq \delta_{Thr}$ , which reports the channel is clear. Such nodes will form **{TS}**.
- **High interfering source node:** is a *CSMA/CA*-based source node that experiences the interference and fails to transmit directly its sensed data packet to the relay node, i.e., it experiences the interference because  $\delta < \delta_{Thr}$ , which reports the channel is unclear. Such node will always communicate with the *Crd* directly using flexible *TDMA*. All high interfering source nodes form **{IS}**.
- **BR:** is a set that consists of all relay nodes that have successfully received data

packets from source nodes in the current superframe.

- **ISBR:** is a set that includes all high interfering source nodes and all relay nodes in the current superframe, where  $\{ISBR\} = \{IS\} \cup \{BR\}$ .

Each interference-free source node included in  $\{TS\}$  transmits its data packet to the relay node in the first round. When the contention-free *TDMA* frame commences, the best relay nodes transmit the data packet they have received from all members in  $\{TS\}$  to the *Crd* in the second round. In essence, a relay node checks the last beacon it has received, if it finds its *ID* in the *nodeSlotlist*, it transmits its packet in the corresponding time-slot within the fixed *TDMA* part to *Crd*. However, if the relay node does not find its *ID*, it randomly selects one time-slot from the flexible *TDMA* part through which it transmits its packet to *Crd*.

Similarly, each member in  $\{IS\}$ , i.e., high interfering source node, checks the last beacon received, if it finds its *ID* in the *nodeSlotList*, it waits until the *TDMA* schedule commences and then transmits its packet in its allocated time-slot directly to *Crd* through a stable channel. However, if that member does not find its *ID* in the *nodeSlotList*, it then randomly selects one time-slot of flexible *TDMA* part through which it transmits the packet to the *Crd*. If the member does not succeed to find a free time-slot, it keeps trying until it finds a one. As a node determines a time-slot in the *TDMA* part of the current superframe, it starts immediately scanning a fixed number of available channels (16). Based on the aforementioned assumptions, the node will find a stable channel through which it transmits its packet directly to *Crd*.

After the contention-free schedule completes, the *Crd* receives all the *IDs* of nodes that have successfully succeeded in their transmissions in the current superframe, i.e.,  $m$  *IDs* and hence the *Crd* forms the *nodeSlotlist* of  $m$  members. Based on that, the *Crd* forms a new superframe formed of  $p$  time-slots, i.e.,  $m$  time-slots for the fixed *TDMA* part and  $p-m$  free time-slots for the flexible *TDMA* part of the next superframe. **Algorithm 2** shows high level summary of the proposed *CFTIM*.

### 3.3.4 CFTIM Analysis

### 3.3.5 Outage Probability

In fading channels, the received signal is characterized by its variable rate of the power which depends on the channel conditions and can be described by probability models. We use the *SINR* ( $\delta$ ), as a parameter to describe the channel quality, and hence the  $\delta$  and the maximum capacity of the channel become random variables in such fading channels. *OP* is defined as the probability of  $\delta$  value being smaller than the *SINR*

**Algorithm 2** CFTIM for Intra-WBAN Interference Mitigation

**Require:** Source nodes  $N$ , Relay nodes  $R$ , Interference-free source nodes  $TS$ , High interfering source nodes  $IS$ , Best relay nodes  $BR$ , Source node  $S$ , Relay node  $R$ , High interfering source or Best relay  $RS$ , Time-slot  $T$

```

1: Begin CAP
2: for  $i = 1$  to  $\text{sizeof}(TS)$  do
3:    $S_i \in TS$  transmits to  $R_i$  on baseChannel in the first round;
4: end for
5: for  $k = 1$  to  $\text{sizeof}(IS)$  do
6:    $S_k \in IS$  defers the transmission and waits until TDMA commences;
7: end for
8: End CAP
9: Begin FTDMA
10: for  $j = 1$  to  $\text{sizeof}(ISBR)$  do
11:   if  $ID_{RS_j} \in \text{nodeSlotList}$  of currentSuperframe then
12:      $RS_j \in ISBR$  transmits to the Crd on stableChannel in  $T_j$  of the fixed TDMA in the second round;
13:     Crd includes  $ID_{RS_j}$  in nodeSlotList of nextSuperframe;
14:   else
15:     counter = 0;
16:     for  $k = 1$  to  $\text{maxRetries}$  do
17:       counter++;
18:        $RS_j \in ISBR$  randomly selects time-slot  $T_k$  from the flexible TDMA;
19:       if  $T_k == \text{freeSlot}$  then
20:          $RS_j \in ISBR$  transmits to Crd on stableChannel in  $T_k$  in the second round;
21:         Crd includes  $ID_{RS_j}$  in nodeSlotList of nextSuperframe;
22:         counter = 0;
23:         break;
24:       end if
25:       if counter ==  $\text{maxRetries}$  then
26:          $RS_j \in ISBR$  waits for the nextSuperframe;
27:         Crd includes  $ID_{RS_j}$  in nodeSlotList of nextSuperframe;
28:         counter = 0;
29:         break;
30:       end if
31:     end for
32:   end if
33: end for
34: End FTDMA =0

```

threshold, denoted by  $\delta_{Thr}$  which is given by **Eq. (3.1)**. We present a simple probabilistic approach which we prove analytically it lowers the *OP*.

$$OP = Pr(\delta < \delta_{Thr}) \quad (3.1)$$

$\delta$  is given by **Eq. (3.2)** below,  $P$  is the desired power received at the receiver,  $I_i$  is the interference power received from interfering node  $i$  at the receiver and  $N_0$  is additive white Gaussian noise.

$$\delta = \frac{P}{\sum_{i=1}^N I_i + N_0} \quad (3.2)$$

As pointed out, any node whose received  $\delta$  is lower than a threshold is added to the interference set of nodes ( $IS$ ). The received  $\delta$  at a node  $j$  in the WBAN is  $\delta_j$ . In this analysis, we denote the probability that the total interference at time instant  $i$  within the WBAN consisting of  $N$  nodes is larger than  $\delta_{Thr}$  by  $P_{outage}$ .  $P_{outage}$  is given by Eq. (3.3).

$$P_{outage} = \left( \sum_{j=1}^N \delta_j > \delta_{Thr} \right) \quad (3.3)$$

If  $\delta_j < \delta_{Thr}$ , an orthogonal channel from the set of available channels within the license-free 2.4 GHz band of the IEEE 802.15.6 standard [2] is assigned to that node with certain probability which equals  $\frac{\delta_j}{\delta_{Thr}}$ . Thus, at time instant  $i$ , we can calculate the average interference level using the proposed probabilistic approach as given by Eq. (3.4).

$$\delta_i = \sum_{j=1}^{IS} \delta_j \left( 1 - \frac{\delta_j}{\delta_{Thr}} \right) \quad (3.4)$$

Based on the probabilistic approach, any node with probability  $\frac{\delta_i}{\delta_{Thr}}$  is assigned an orthogonal channel.

**Lemma 3.1.** *We denote by  $P_{Probabilistic}$  and  $P_{Original}$  the outage probability of probabilistic approach and the outage probability of the original scheme, i.e., without the probabilistic approach, respectively. Then,  $P_{Probabilistic} < P_{Original}$ .*

*Proof.* Based on Eq. (3.3), we have:

$$P_{Probabilistic} = p \left( \left( \sum_{i=1}^{IS} \delta_i \left( 1 - \frac{\delta_i}{\delta_{Thr}} \right) \right) > \delta_{Thr} \right) \quad (3.5)$$

$$= p \left( \left( \sum_{i=1}^{IS} \delta_i - \sum_{i=1}^{IS} \frac{\delta_i^2}{\delta_{Thr}} \right) > \delta_{Thr} \right) \quad (3.6)$$

$$= p \left( \sum_{i=1}^{IS} \delta_i > \delta_{Thr} + \sum_{i=1}^{IS} \frac{\delta_i^2}{\delta_{Thr}} \right) \quad (3.7)$$

$$< p \left( \sum_{j=1}^{IS} \delta_j > \delta_{Thr} \right) = P_{Original} \quad (3.8)$$

Where the last line of  $P_{Probabilistic}$  is based on the fact that the CDF is an increasing function of its argument. Therefore, the lemma is proved.  $\square$

**Table 3.1:** Simulation parameters - *CFTIM*

Parameter name	Value
Simulation time	45 minutes
Source nodes	12
Relay nodes	4
Transmission power	0 dBm
Noise floor	-100 dBm
Data rate	250 kbps
Packet size	12 bytes
Frequency band	2.4 GHz
Pathloss exponent ( $\alpha$ )	4.22
IEEE 802.15.6 channels	16

### 3.3.6 Stability Condition

We determine the stability of a channel as referred to in Chapter 6.4.3 [Channel Stability](#).

### 3.3.7 *CFTIM* Performance Evaluation

This section compares the performance of *CFTIM* to that of competing schemes, opportunistic relaying, namely, *OR*, [99] and original *TDMA* scheme, namely, *TDMA*, which are defined as follows:

- ***Opportunistic Relaying (OR)*** scheme : a *WBAN* uses three branches, one direct link from the source node to the *Crd* and two additional links via two relay nodes. In *OR*, only a single relay node with the best network path towards the *Crd* will be selected to forward a packet per a hop.
- ***TDMA Original (TDMA)*** scheme : a *WBAN* employs one-hop between source nodes and the *WBAN's Crd*. A *TDMA* is also employed, in which each source is assigned a time-slot through which it transmits its packet to the *WBAN's Crd*.

We have performed simulation experiments through Matlab. We have considered a mobile *WBAN* consisting of  $N = 12$  source nodes and a set of relay nodes  $R = 4$  located in an area of  $2 \times 2 \times 2m^3$ . All the nodes operate in a half-duplex mode and their individual locations change to mimic random mobility and consequently, the interference pattern varies. We assume that all the IEEE 802.15.6 channels of the international license-free 2.4 GHz band are available at the source, relay and the *Crd* nodes [2]. The following performance metrics, *SINR*, *WBAN* energy consumption and the throughput are considered. The simulation parameters are provided in **Table 3.1**.

The average *WBAN's SINR* versus time for *CFTIM* and *OR* are compared in **Figure 3.3**. As can be clearly seen in this figure, the *SINR* of *CFTIM* is always larger than that for *OR* all the time. Such distinct performance for *CFTIM* is mainly due to the use of the flexible *TDMA* and stable channels. However, in *OR*, few interference-free nodes can

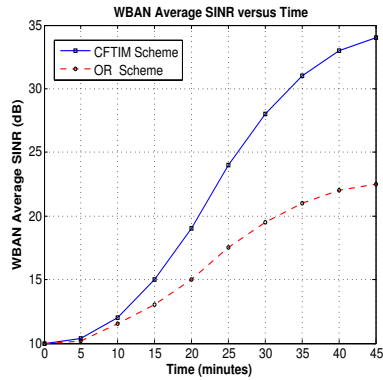


**Figure 3.3:** Average  $SINR$  vs. time for  $CFTIM$  and  $OR$

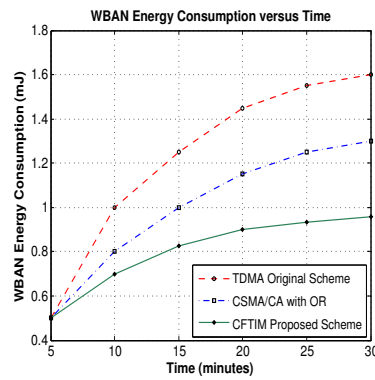


**Figure 3.4:**  $WEC$  versus time for  $CFTIM$ ,  $OR$  and  $TDMA$

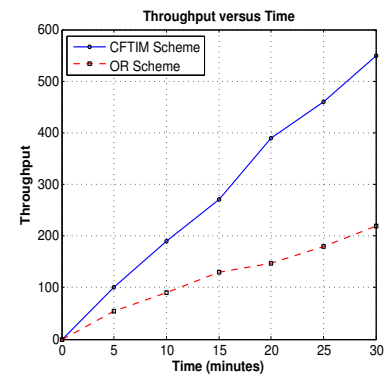


**Figure 3.5:** Throughput ( $TP$ ) vs. time for  $CFTIM$  and  $OR$

now transmit, while at the same time, several nodes will defer the transmission to the next superframe (due to the absence of flexible  $TDMA$ ) which provides lower values of  $SINR$ .

The  $WBAN$  energy consumption, denoted by  $WEC$ , versus time for  $CFTIM$ ,  $OP$  and  $TDMA$  are compared in **Figure 3.4**. This figure shows that the  $WEC$  for  $CFTIM$  is always smaller than that for  $OR$  and  $TDMA$  all the time because of the dynamic time-slot and channel allocation. Such distinct performance for  $CFTIM$  is mainly due to the reduced collisions that lead to fewer retransmissions and consequently lower power consumption. Whilst, the  $WEC$  for  $PC$  is lower than that for  $TDMA$  all the time due to the two-hop employment (spatial diversity), which better lowers the energy consumption than the one-hop.

We define the throughput as the sum of the number of packets successfully delivered per a unit time at the  $WBAN$ 's  $Crd$ . The throughput, denoted by  $TP$ , for  $CFTIM$  and  $OR$  is reported in **Figure 3.5** as a function of the time. As can be seen in this figure,  $CFTIM$  always achieves higher  $TP$  than that for  $OR$  all the time. Such high throughput is mainly because of the reduced collisions and availability of time-slots and channels for high interfering nodes, which boosts the number of data packets that are successfully delivered at the  $WBAN$ 's  $Crd$ . However, the  $TP$  of  $OR$  is low because of the lower number of source nodes transmitting their packets to the relay nodes due to the medium access collisions as well as the collisions that happen at the relay nodes. Such collisions lower the successful delivery of packets at the  $WBAN$ 's  $Crd$ , and hence the throughput.

$CFTIM$  is a medium access scheduling scheme that assigns dynamic time and channels to nodes to diminish the probability of intra- $WBAN$  interference. Nonetheless,  $CFTIM$  drains the power resource of the individual nodes due to the frequent channel switching.

## 3.4 Improved Resource Allocation for Intra-WBAN Interference Mitigation

### 3.4.1 System Model

We consider a single WBAN that consists of  $N$  source nodes,  $R$  relay nodes and a  $Crd$ . Each WBAN's node, i.e., a source or relay node, may operate on a base channel or a reserved channel. When the base channel is engaged, a node may extend its contention window (CW), if it experiences a high level of interference. We consider the following assumptions on the nodes and network:

- A dynamic and mobile topology of a WBAN.
- The number of active nodes within the WBAN is unexpected.
- Two-hop is employed among source nodes  $\rightarrow$  relay nodes  $\rightarrow$   $Crd$ .
- CSMA/CA is employed between source nodes  $\rightarrow$  relay nodes.
- Flexible TDMA is employed between relay nodes  $\rightarrow$   $Crd$ .
- A node transmits one data packet in a time-slot.
- The number of channels is limited to 2, base and reserved.

We define the following sets:

- $\{P\}$ : a set consists of source nodes that have data to transmit in  $CAP$  period of the current superframe.
- $\{BR\}$ : a set that consists of relay nodes that have successfully received data packets from source nodes in the current superframe.

### 3.4.2 IAA Improved Resource Allocation

Initially, all source nodes ( $\{P\}$ ) that have data start the competition to access the base channel, and thus two different sets are formed,  $\{TS\}$  and  $\{IS\}$ . Each source node, denoted by  $s_i$ , measures the SINR ( $\delta$ ), if it finds  $\delta_{s_i} \geq \delta_{Thr}$ , which means, it does not experience the interference, i.e., no medium access collision happens,  $s_i$  transmits the data packet directly to the relay nodes (**Case 1**). Such node will be included in  $\{TS\}$  which is defined in Eq. (3.9)

$$\{TS\} = \{s_i \in \{P\} \mid (\delta_{s_i} \geq \delta_{Thr}), \forall i\} \quad (3.9)$$

If  $s_i$  finds  $\delta_{s_i} < \delta_{Thr}$ , which means, it experiences the interference. In this case,  $s_i$  extends its contention window (CW) by doubling the backoff to avoid the medium access collision. When the CW extension period completes,  $s_i$  immediately senses the base channel by measuring  $\delta_{2s_i}$ , if it finds  $\delta_{2s_i} \geq \delta_{Thr}$ , which means that  $s_i$  does not experience the

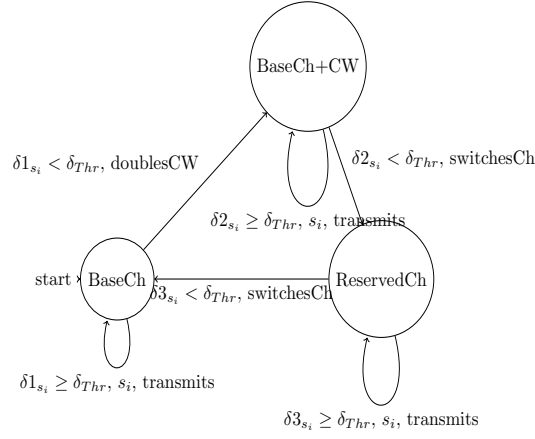


**Figure 3.6:** Source node actions

interference, it immediately transmits its packet to relay nodes using the base channel (**Case 2**). Such node will be included in  $\{IS\}$  which is defined in Eq. (3.10)

$$\{IS\} = \{s_i \in \{IS\} \mid (\delta 2_{s_i} \geq \delta_{Thr}), \forall i\} \quad (3.10)$$

However, if  $s_i$  finds  $\delta 2_{s_i} < \delta_{Thr}$ , which means, it experiences the interference again. In this case,  $s_i$  switches to the reserved channel (**Case 3**). **Figure 3.6** illustrates all possible actions taken by source nodes in CAP period. The different cases are summarized as follows:

- **Case 1** :  $\forall s_i \in \{TS\}$  &  $\delta_{s_i} \geq \delta_{Thr}$ ,  $s_i$  uses the base channel.
- **Case 2** :  $\forall s_i \in \{IS\}$  &  $\delta 2_{s_i} \geq \delta_{Thr}$ ,  $s_i$  uses base channel with CW extension.
- **Case 3** :  $\forall s_i \in IS$  &  $\delta 2_{s_i} < \delta_{Thr}$ ,  $s_i$  uses the reserved channel.

Then,  $s_i$  measures  $\delta 3_{s_i}$  and if it finds  $\delta 3_{s_i} \geq \delta_{Thr}$ , then  $s_i$  accesses the reserved channel and transmits its packet to the relay node, otherwise, it switches to the base channel eventually after few attempts. **Algorithm 3** shows a high level summary of IAA and the actions taken by the source nodes.

### Source to Relay Communication

The communication between source and relay nodes is achieved through three successive periods. During the period CAP-1A, each source node  $s_i$  measures its  $\delta_{s_i}$ , if it finds  $\delta_{s_i} \geq \delta_{Thr}$ , it uses the base channel to transmit its packet to the relay nodes (**Case 1**). If  $s_i$  finds  $\delta_{s_i} < \delta_{Thr}$ , then  $s_i$  will be considered a high interfering node, it extends its CW and waits until CAP-1A finishes. When CAP-1B period commences,  $s_i$  measures  $\delta 2_{s_i}$ , if it finds  $\delta 2_{s_i} \geq \delta_{Thr}$ , it then transmits to the relay nodes using the base channel (**Case 2**). However, if  $s_i$  finds its  $\delta 2_{s_i} < \delta_{Thr}$ , it waits until the CAP-1B finishes and switches to the reserved channel. When CAP-2 commences,  $s_i$  competes to access the reserved

**Algorithm 3** IAA - Source Actions

---

**Require:** Coordinator  $Crd$ , Source Nodes  $P$ , SINR Threshold  $\delta_{Thr}$ , Base Channel  $baseChannel$ , Reserved Channel  $reservedChannel$ , Contention Window  $CW$

```

1: for  $i = 1$  to  $sizeof(P)$  do
2:   if  $(\delta_{s_i} \geq \delta_{Thr})$  then
3:      $s_i$  is an interference-free source node  $\Leftrightarrow s_i \in TS$ ;
4:      $s_i \in TS$  sendsPacketOn  $baseChannel$  in CAP-1A;
5:   else
6:      $s_i$  is a high interfering source node  $\Leftrightarrow s_i \in IS$ ;
7:      $s_i$  doubles  $CW$  & waits until CAP-1A finishes;
8:     if  $CW_{s_i}$  isOver then
9:       if  $\delta_{2s_i} \geq \delta_{Thr}$  then
10:         $s_i$  sendsPacketOn  $baseChannel$  in CAP-1B;
11:       else
12:         $s_i$  switchesTo  $reservedChannel$  & waits until CAP-1B finishes;
13:       if  $\delta_{3s_i} \geq \delta_{Thr}$  then
14:         $s_i$  sendsPacketOn  $reservedChannel$  in CAP-2;
15:       else
16:         $q = 0$ ;
17:        for  $m=1$  to  $maxRetries$  do
18:          if  $\delta_{3s_i} < \delta_{Thr}$  then
19:             $q = q + 1$ ;
20:          end if
21:          if  $q > q_{Thr}$  then
22:             $s_i$  switchesTo  $baseChannel$ ;
23:            break;
24:          end if
25:        end for
26:      end if
27:    end if
28:  end if
29: end if
30: end for

```

---

channel and completes its transmission to the relay nodes (**Case 3**). **Figure 3.6** illustrates all possible actions taken by source nodes during the different CAP periods. **Algorithm 3** shows the different actions taken by the source nodes.

### Relay Actions and Channel Synchronization

Our approach ensures that there are always a set of relay nodes capable to receive from sensor nodes in the CAP. Initially, each relay node denoted by  $r_i$  listens on the base channel and measures periodically  $\delta_{r_i}$  in a specific periods of time within each CAP period. If  $r_i$  finds  $\delta_{r_i} \geq \delta_{Thr}$ , then it can receive from source nodes on the base channel. Such relay node will be included in the set  $\{BR\}$ . However, if  $r_i$  finds  $\delta_{r_i} < \delta_{Thr}$ , i.e, it experiences the interference, it then switches to the reserved channel where it starts listening again. Whenever the relay node encounters a collision, it immediately transmits a jam signal to inform the source nodes to stop the transmission, it waits a short period of time, i.e., by performing a simple backoff, and then it retries [2]. As pointed out, the same process takes place when both the base and reserved channels are

engaged. When all the receptions in the relay nodes are complete and the CAP period finishes, all the source and relay nodes switch to the base channel. **Algorithm 4** shows the different actions taken by the relay node.

---

**Algorithm 4** IAA - Relay Actions
 

---

**Require:** Transmitted Relays  $BR$ , SINR Threshold  $\delta_{Thr}$

```

1: for  $k = 1$  to  $\text{sizeof}(BR)$  do
2:    $r_k$  listensOn baseChannel;
3:   if  $\delta_{r_k} \geq \delta_{Thr}$  then
4:      $r_k$  receivesOn baseChannel;
5:   else
6:      $r_k$  switchesTo & ListensOn reservedChannel;
7:     if  $\delta_{2r_k} \geq \delta_{Thr}$  then
8:        $r_k$  receivesOn reservedChannel;
9:     else
10:       $r_k$  switchesTo baseChannel after maxRetries;
11:    end if
12:  end if
13: end for
  
```

---

### 3.4.3 IAA Superframe Structure

We propose a superframe structure that is composed of two main parts, a CAP part and TDMA part as shown in **Figure 3.7**. The CAP part, in which a slotted CSMA/CA is employed, is divided into CAP-1 in which the base channel is used, and CAP-2 in which the reserved channel is used. Whilst, the TDMA part consists of a fixed and a flexible TDMA parts. CAP-1 is further divided into two parts, CAP-1A which involves **Case 1** and CAP-1B involves **Case 2**. Basically, all the source nodes' transmissions that happen in CAP-1A and CAP-1B, must complete before the end of CAP-1. Also, all source nodes' transmissions take place in CAP-2, in which the reserved channel is used (**Case 3**) must complete before the end of the CAP-2. Basically, all the source nodes' transmissions completed in the CAP period are transmitted to the relay nodes, and no direct communication between the source nodes and the *Crd* is possible. When the CAP period completes, the fixed TDMA frame commences through which relay nodes transmit all data packets they have been received in the CAP period to the *Crd* using the base channel. In essence, each relay node is allocated a fixed number of time-slots within the fixed TDMA frame to complete the transmission of these data packets to the *Crd*.

The fixed number of the time-slots allocated to a relay node within the fixed TDMA is denoted by  $T$ , where  $T = A + B + C$ .  $A$  denotes the number of time-slots that are allocated on the behalf of source nodes completed their transmission successfully in CAP-1A,  $B$  denotes the number of time-slots that are allocated on the behalf of source nodes

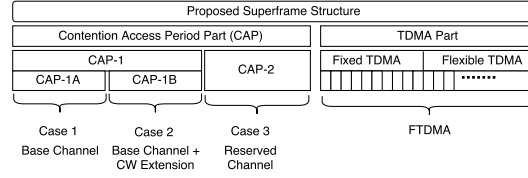


**Figure 3.7:** IAA superframe structure

completed their transmission successfully in CAP-1B, and  $C$  denotes the number of time-slots that are allocated on the behalf of source nodes completed their transmission successfully in CAP-2. With conditions of high level interference, a relay node may require additional time-slots to complete the transmission and hence it may pick some of the available free time-slots within the flexible TDMA part. Similarly, **Algorithm 1** shows high level summary of the actions taken by the coordinator to construct the TDMA part of the next superframe. However, only *ISBR* in the algorithm of *CFTIM* is replaced by *BR* as *IAA* requires the relay nodes only to transmit to the coordinator. Refer to **Section 3.3.2** to see in detail.

### 3.4.4 IAA Analysis

In this section, we opt to analyze our approach based on outage probability, denoted by  $OP$ , and present a simple probabilistic model that analytically proves the  $OP$  has been lowered. The  $OP$  at given  $SINR$  threshold ( $\delta_{Thr}$ ), is defined as the probability of the  $SINR$  ( $\delta$ ), is being smaller than  $\delta_{Thr}$ .  $OP$  is given by **Eq. (3.11)**.

$$OP = Pr(\delta < \delta_{Thr}) \quad (3.11)$$

We denote by  $P_{out}$  the probability that the total interference at time instant  $i$  is being larger than  $\delta_{Thr}$  at a given node  $s$  of the WBAN. We denote by  $\delta_j$  the received  $SINR$  from node  $j$  at node  $s$  in the WBAN. Then, we calculate  $P_{out}$  as follows.

$$P_{out} = \left( \sum_{j=1}^{N-1} \delta_j > \delta_{Thr} \right) \quad (3.12)$$

We present a probabilistic approach which we prove analytically it lowers the outage probability. Any node  $s$  whose received  $\delta$  is lower than a given threshold, it doubles its contention window, i.e., if  $\delta_j < \delta_{Thr}$ , and so, node  $s$  extends its CW with certain probability which equals  $\frac{\delta_j}{\delta_{Thr}}$ . Thus, at time instant  $i$ , we can calculate the average interference level at node  $s$  using the proposed probabilistic approach as follows.

$$\delta_i = \sum_{j=1}^{N-1} \delta_j \left( 1 - \frac{\delta_j}{\delta_{Thr}} \right) \quad (3.13)$$

Based on the probabilistic approach and the proposed scheme, any node with probability  $\frac{\delta_j}{\delta_{Thr}}$  doubles its contention window. If the node is in the contention window case, it may switch to the reserved channel (i.e., depending on  $\delta$ ) with probability of  $\left(\frac{\delta_j}{\delta_{Thr}}\right)^2$ .

**Lemma 3.2.** *We denote by  $P_{prob}$  and  $P_{out}$  the outage probability of probabilistic approach and the outage probability of the original scheme respectively. Then,  $P_{prob} < P_{out}$ , i.e. the probabilistic approach has better  $\delta$  than that of the original scheme.*

*Proof.* Based on the definition given in Eq. (3.12), we have:

$$P_{prob} = p \left( \sum_{i=1}^{N-1} \delta_i \left( 1 - \left( \frac{\delta_i}{\delta_{Thr}} + \left( \frac{\delta_i}{\delta_{Thr}} \right)^2 \right) \right) > \delta_{Thr} \right) \quad (3.14)$$

$$= p \left( \sum_{i=1}^{N-1} \delta_i > \delta_{Thr} + \sum_{i=1}^{N-1} \frac{\delta_i^2}{\delta_{Thr}} + \sum_{i=1}^{N-1} \frac{\delta_i^3}{\delta_{Thr}^2} \right) \quad (3.15)$$

$$< p \left( \sum_{j=1}^{N-1} \delta_j > \delta_{Thr} \right) = P_{out} \quad (3.16)$$

□

Where  $\left(\frac{\delta_j}{\delta_{Thr}} + \left(\frac{\delta_j}{\delta_{Thr}}\right)^2\right)$  denotes the probability of the node is being in **Case 2** or the probability of the node is being in **Case 3**. The last line of  $P_{prob}$  is based on the fact that the CDF is an increasing function of its argument. We define  $P_{prob,L,i}$  as the probabilistic's approach deployment probability that a node of WBAN doubles its contention window is given by Eq. (3.17).

$$P_{prob,L,i} = P(\delta_i < \delta_{Thr}) + P(\delta_i < \delta_{Thr}) \frac{\delta_i}{\delta_{Thr}}, \quad (3.17)$$

which is greater than  $P_i = P(\delta_{avg} > \delta_{Thr})$ .

### 3.4.5 IAA Performance Evaluation

This section compares the performance of IAA to that of competing schemes, cooperative communication integrated with transmit power control, namely, Power Control, [100] and opportunistic relaying, namely, OR, [99], which are defined as follows:

- **Power Control (PC)** scheme : a two-hop scheme integrated with opportunistic relaying for a mobile WBAN. By using the received SINR at the relay and the coordinator nodes, this scheme chooses the best relay node to decode and forward the data at the same time with the direct link.

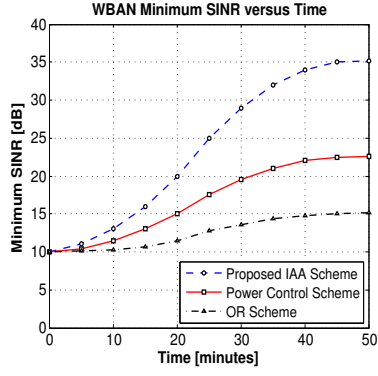


**Figure 3.8:** Minimum  $SINR$  vs. time for IAA, PC and OR

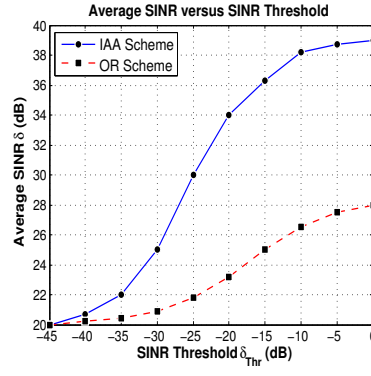


**Figure 3.9:** Average  $SINR$  versus time for IAA and OR

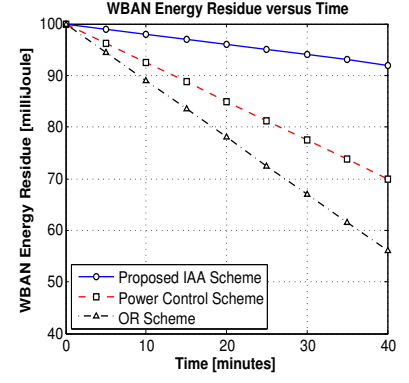


**Figure 3.10:** ER vs. time for IAA, PC and OR

- **Opportunistic Relaying (OR)** scheme : a WBAN uses three branches, one direct link from the sensor node to the coordinator and two additional links via two relay nodes. In OR, only a single relay node with the best network path towards the coordinator will be selected to forward a packet per a hop.

We have performed simulation experiments through Matlab, where the simulation setup and configuration parameters of IAA are set exactly the same as those in CFTIM simulation setup. The following performance metrics, minimum  $SINR$ , outage probability and WBAN energy residue are considered. The simulation parameters are provided in **Table 3.1**, except that the number of channels is limited to 2 only rather than 16 and the simulation time is set to 50 rather than 45 minutes. The minimum  $SINR$ , denoted by  $\delta_{min}$ , versus time for IAA, PC and OR are compared in **Figure 3.8**. As can be seen in this figure,  $\delta_{min}$  for IAA is always larger than that for PC and OR all the time because of CW extension mechanism and channel hopping. However, PC depends on the power control mechanism to mitigate the interference. Though PC exploits the benefits of diversity gain, nonetheless, it does not address the interference happening at the relay nodes as IAA does. Whilst, PC provides a larger  $\delta_{min}$  than that for OR because of the power control mechanism, in which the nodes dynamically adjust the transmission power level, which reduces the interference. The average  $SINR$  ( $\delta$ ) versus the  $SINR$  threshold ( $\delta_{Thr}$ ) for IAA and OR are compared in **Figure 3.9**. It is worth noting that a higher  $SINR$  refers to a lower outage probability. As seen in the figure, the average  $\delta$  for IAA is always larger than that for OR for all  $\delta_{Thr}$  values. As pointed out, this is because of CW extension mechanism and channel hopping to avoid the interference. Increasing the  $\delta_{Thr}$  values means putting more sensor nodes in the interference set, and hence more nodes mitigate the interference, which provides better  $\delta$  values. In OR, only sensor nodes that succeeded to access the channel are allowed to transmit to the relay nodes, whilst, the others that experienced the interference, are not allowed to transmit in the

current period. Such interfering sensor nodes do not mitigate the interference as *IAA* does, and hence they should wait until the next round. In addition, *OR* does not address the problem of interference that may happen at the relay nodes as well, which minimize the *SINR*. The *WBAN*'s energy residue, denoted by *ER*, versus time for *IAA*, *PC* and *OR* are compared in **Figure 3.10**. We define *ER* at time  $t$  as the sum of the amount of the remaining energy in the battery of each node. As can be observed in this figure, the *ER* of *IAA* is always larger than that for *PC* and *OR*, which provides a longer *WBAN*'s energy lifetime. This is due to the use of CW extension and the channel hopping, which lowers the collisions and hence the retransmissions, in consequence, the energy consumption is minimized. In *PC*, the collisions may result from the interference that could happen at the level of sensor and relay nodes due to the contention and the retransmissions, which provides higher energy consumption. However, *OR* provides the highest energy consumption due to the absence of contention window extension mechanism and channel switching as well as the power control mechanism.

### 3.5 Conclusions

In this chapter, we have presented an approach based on time-based channel allocation and dynamic superframe length adjustment to minimize the impact of intra-*WBAN* interference. Specifically, we propose two schemes. The first scheme is called *CFTIM* that enables the interference-free nodes using the default base to transmit to the relay node in the first round. Whilst, *CFTIM* allocates the high interfering source and relay nodes time-slots and stable channels to transmit to the coordinator and avoid the interference through flexible *TDMA* in the second round. Basically, *CFTIM* involves overhead due to frequent channel switching. The second scheme is called *IAA* that dynamically adjusts the superframe length and allocates time-slots to nodes in order to diminish the probability of medium access collision within the *WBAN*. *IAA* lowers the frequency of channel switching and limits the number of channels to only 2 to save the power. We have further presented an analytical model that proves the outage probability is minimized. Simulation results show that *CFTIM* and *IAA* outperform other competing schemes in terms of interference mitigation, saving the power and improving the throughput.

# Chapter 4

## Cooperative Inter-WBAN Interference Mitigation Using Walsh-Hadamard Codes

### Contents

---

<b>4.1 Introduction</b> . . . . .	<b>55</b>
<b>4.2 System Model and Preliminaries</b> . . . . .	<b>57</b>
4.2.1 Model Assumptions . . . . .	57
4.2.2 Interference Lists - <i>I</i> . . . . .	57
4.2.3 Interference Sets - <i>IS</i> . . . . .	58
4.2.4 Channel Model . . . . .	58
4.2.5 Cyclic Orthogonal Walsh Hadamard Codes Overview . . . . .	58
<b>4.3 Distributed Time Reference Correlation - <i>DTRC</i></b> . . . . .	<b>59</b>
<b>4.4 Orthogonal Codes Allocation - <i>OCAIM</i></b> . . . . .	<b>61</b>
<b>4.5 <i>OCAIM</i> Analysis</b> . . . . .	<b>65</b>
4.5.1 Successful Beacon Transmission Probability . . . . .	65
4.5.2 Successful Data Transmission Probability . . . . .	66
<b>4.6 <i>OCAIM</i> Performance Evaluation</b> . . . . .	<b>68</b>
<b>4.7 Conclusions</b> . . . . .	<b>70</b>

---

### 4.1 Introduction

The *IEEE 802.15.6* standard [2] has recently defined three mechanisms for inter-WBAN interference mitigation called beacon shifting, channel hopping, and active su-

perframe interleaving. A number of research works pursued the approach of superframe interleaving including [83, 28, 84, 85, 27, 61]. In this approach, the coordinators of WBANs exchange information to prevent the overlapping of the superframes' active periods with each other.

Spread spectrum is a method by which a signal with a particular bandwidth is deliberately spread in the frequency domain, resulting in a signal with a wider bandwidth. It is worth noting that spread spectrum techniques use the same transmit power levels because they transmit at a much lower spectral power density than that of the narrow band transmitters [2, 23]. Due to the wide use of the orthogonal codes in cellular networks [102, 103, 104, 105], a very few published work has been conducted for interference mitigation in WBANs. Tawfiq et al. [106] have presented a direct sequence code division multiple access (DS-CDMA) based asynchronous WBAN that employs a unique set of Cyclic Orthogonal Walsh-Hadamard Codes (COWHC) to eliminate multiple access interference caused by packet collision in the WBAN's coordinator.

In this chapter, we address the problem of sensor-level co-channel interference among cooperative WBANs through orthogonal code allocation to interfering sensor nodes based on distributed time correlation reference. Motivated by the distributed time provisioning and the clock synchronization supported in the standard [2], we propose two schemes to mitigate the interference. The first is called *Distributed Time Correlation Reference*, namely, *DTRC*, that determines which superframes overlap with each other, and the second is called *Orthogonal Code Allocation Algorithm for Interference Mitigation*, namely, *OCAIM*, that allocates orthogonal codes to interfering sensor nodes within each WBAN. In addition, *OCAIM* adds no complexity to the sensor nodes as WBANs' coordinators are only required to compute and negotiate with each other for code assignment. The main contributions of this chapter are summarized as follows:

- *DTRC*, a distributed scheme for determining which superframes and their corresponding times-slots overlap with each other. *DTRC* is used as the building block of *OCAIM*, and provides each WBAN employing *OCAIM* with the knowledge about, 1) which superframes and, 2) which time-slots within those superframes overlap with the time-slots of its superframe.
- *OCAIM*, a distributed cooperative scheme that allocates orthogonal codes to interfering sensor nodes belonging to *sensor interference lists (SILs)*. In *OCAIM*, each WBAN generates *SILs*, and then all sensor nodes belonging to these lists are allocated orthogonal codes.

- An analysis of the success and collision probability model for data and beacon frames transmissions.
- Extensive simulations and benchmarking are conducted, and the results demonstrate that *OCAIM* can significantly diminish inter-WBAN interference, improves the throughput and saves the power resource at *sensor*- and *WBAN*-levels.

## 4.2 System Model and Preliminaries

### 4.2.1 Model Assumptions

We consider a network composed of  $N$  *WBANs*, each consists of up to  $K$  sensor nodes. Each sensor node transmits its data to the *WBAN*'s coordinator (*Crd*) at a maximum data rate of  $250\text{Kb/s}$  within the  $2.4\text{ GHz}$  international license-free band using the same transmission power at  $-10\text{ dBm}$  and the same modulation scheme. Furthermore, we make the following assumptions about the sensor nodes, *WBANs* and the network.

- Star topology between sensor nodes and the *Crd* is employed within each *WBAN*.
- All *WBAN* sensor nodes and the individual *WBANs* are subject to mobility.
- *TDMA* scheme is employed within each *WBAN*.
- All coordinators are equipped with richer power supply than sensor nodes.
- No coordination is considered among *WBANs*, i.e., the superframes are neither aligned nor synchronized and may overlap with each other.
- Cooperation is considered among *WBANs*.

### 4.2.2 Interference Lists - $I$

When  $k^{\text{th}}$  sensor node in *WBAN* $_i$ , denoted by  $S_{i,k}$ , transmits to its corresponding *Crd* $_i$ , at the same time, all other *WBANs*' coordinators compute the power received from  $S_{i,k}$ 's transmitted signal. Let  $\delta_{i,j,k}$  denotes the power received from  $k^{\text{th}}$  sensor node of *WBAN* $_j$  at *Crd* $_i$  of *WBAN* $_i$ . When all the transmissions complete, each *Crd* $_i$  creates a table that consists of the power values received from all sensor nodes. Furthermore, we denote by  $\rho_i^{\text{min}}$  the minimum power received within a *WBAN* $_i$ , where  $\rho_i^{\text{min}} = \min\{\delta_{i,k=1,\dots,K}\}$ . Thus, we denote by  $I_i$  the *Interference list* of *WBAN* $_i$ , which is defined in **Eq. (4.1)**.

$$I_i = \{S_{l,m} | \delta_{i,l,m} > \rho_i^{\text{min}} - \theta, \forall i \neq l\} \quad (4.1)$$

With  $\theta$  denotes the interference threshold. When the computations are done, each *Crd* $_i$  starts broadcasting its corresponding  $I_i$  to all coordinators in the network.

### 4.2.3 Interference Sets - IS

When a WBAN's coordinator receives the power tables from other WBANs, it updates its own table, and then verifies which of its sensor nodes impose interference on sensor nodes of other WBANs and which sensor nodes of other WBANs impose interference on its WBAN's sensor nodes. It then creates an *Interference Set*, denoted by  $IS_i$ , which is defined in Eq. (4.2).

$$IS_i = I_i \cup \{S_{i,k} | S_{i,k} \in I_l, \forall l \neq i\} \quad (4.2)$$

### 4.2.4 Channel Model

We apply the path loss model, denoted by  $P$ , as defined in Eq. (4.3) to obtain the mean path loss without shadowing between any pair of WBANs. This model uses the path loss exponent  $\alpha = 4$  and is proportional to the distance between WBANs.

$$P(d) = P(d_0) + 10 \times \log_{10} \left( \frac{d}{d_0} \right)^\alpha + 10 \times \log_{10}(h_i^\alpha) + X_\sigma \quad (4.3)$$

Where  $P(d)$  and  $P(d_0)$  is the path loss at distance  $d$  and reference distance  $d_0$ , respectively, from the transmitter,  $X_\sigma$  is a log normal distributed random variable and  $h_i$  is the channel gain between the transmitter and the receiver.

### 4.2.5 Cyclic Orthogonal Walsh Hadamard Codes Overview

In this section, we provide a brief overview of cyclic orthogonal Walsh Hadamard codes that we used in this chapter [106]. The network consists of  $N$  WBANs sharing the same channel, and each WBAN's coordinator is assigned a unique orthogonal spreading code for interference mitigation. In a time-slot  $TS_i$  of sensor node  $r_i$  of a WBAN $_i$ , during the transmission,  $r_i$  multiplies its modulated signal  $s_i$  by the spreading code  $\omega_i$ . We assume the worst case scenario when  $r_i$  is interfering with  $N-1$  sensor nodes in  $TS_i$ . The received signal  $X_r$  at  $Cr d_i$  of WBAN $_i$  is given by Eq. (4.4).

$$X_r = \omega_i \times s_i + \sum_{j=1, j \neq i}^{N-1} \omega_j \times s_j + \mu \quad (4.4)$$

Basically, all the codes generated from the Walsh Hadamard denoted by  $WH$  matrix  $M_{2^n}$  are orthogonal in the zero-phase with  $N = n + 1$ .  $M_{2^n}$  is a special matrix of size  $2^N \times 2^N$ .

$$M_1 = \begin{pmatrix} 1 \\ 1 \end{pmatrix}, M_2 = \begin{pmatrix} 1 & 1 \\ 1 & -1 \end{pmatrix} \quad (4.5)$$

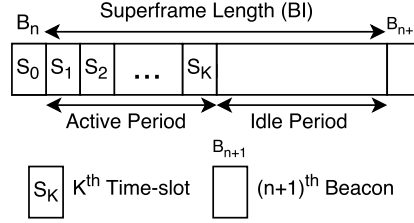


**Figure 4.1:** Superframe structure proposed for OCAIM scheme

are given, one can generate a generic  $WH$  matrix  $M_{2^n}$ ,  $n > 1$ , as follows.

$$M_{2^n} = \begin{pmatrix} M_{2^{n-1}} & M_{2^{n-1}} \\ M_{2^{n-1}} & M_{2^{n-1}} \end{pmatrix} = M_2 \otimes M_{2^{n-1}} \quad (4.6)$$

Where  $\otimes$  denotes the Kronecker product. The rows in each matrix are orthogonal to each other. However, the orthogonality property of  $WH$  codes is lost if the codes are phase shifted. So, to keep the orthogonality property with any phase shift ( $\phi = 0, 1, 2, \dots, 2^k - 1$ ), a special set of codes is required, which can be extracted from the  $WH$  matrix  $M_{2^k}$ . Thus, one can extract  $N = n + 1$  orthogonal codes from  $M_{2^k}$  matrix that have zero cross correlation for all  $\phi = 0, 1, 2, \dots, 2^k - 1$ . This set of  $N$  cyclic orthogonal spreading codes is called Orthogonal Walsh Hadamard Codes and denoted by ( $COWHC$ ). If the  $COWHC$  set is used to spread the transmitted signals, then,  $d_i$  is the decoded signal of sensor node  $r_i$  at  $Crd_i$ , which is also given by Eq. (4.7).

$$d_i = \omega_i \times X_r = \omega_i^2 \times s_i + \sum_{j=1, j \neq i}^{N-1} \omega_i \times \omega_j \times s_j + \omega_i \times \mu \quad (4.7)$$

$\omega_i^2 = 1$  and  $\omega_i \times \omega_j = 0$  due to their orthogonality. Therefore, the decoded signal is  $d_i = s_i + \omega_i \times \mu$ .

### 4.3 Distributed Time Reference Correlation - DTRC

In this section, we develop a Distributed Time Reference Correlation, namely,  $DTRC$ . Motivated by distributed time provisioning,  $DTRC$  determines which superframes, and, which time-slots of those superframes overlap with each other.

Basically, a  $WBAN$ 's superframe is delimited by two beacons and composed of equal length active and inactive periods that are dedicated for the sensor nodes and the coordinators, respectively, as shown in Figure 4.1. Due to the absence of coordination among  $WBANs$ , the transmissions of the individual sensor nodes of different  $WBANs$  may face collisions at the same time-slots, as the individual  $WBANs$  share similar channels.

In this work, we do not aim to add extra time-slots in order to avoid the co-channel

interference, i.e., collisions. Instead, we present *DTRC* to predict which time-slots within each superframe collide with other time-slots within other overlapping superframes. In essence, *DTRC* allows each *WBAN* to relate the start time of other superframes to its local time and hence to predict which sensor nodes within its *WBAN* will be interfering with sensor nodes of other *WBANs*. Thus, all *WBANs*' coordinators generate virtual time-based patterns involving the schedule of the transmission and reception of frames. More precisely, each coordinator according to its local clock calculates the *timeshift* from the *actual start transmission time* of a frame. Basically, the *timeshift* comprises, 1) non-deterministic parameters such as the *synchronization error tolerance*, *the timing uncertainty* and *the clock drift* and, 2) the *difference* between the *non-deterministic parameters* and the *virtual start transmission time* of a frame [2, 23]. We define the following parameters that we used in our proposed *DTRC* scheme:

- ***PHY Timestamp (PTP)***, encodes the time when the last bit of the frame has transmitted to the air
- ***MAC Timestamp (MTP)***, encodes the time when the last bit of a frame has been transmitted at the *MAC*
- ***PHY Receiving Time (PRT)***, a time elapsed from the first to the last bit of a frame at the *PHY*
- ***MAC Receiving Time (MRT)***, a time elapsed from receiving the first bit to the last bit of a frame at the *MAC*
- ***Propagation Delay (L)***, a time elapsed by the bit to travel from the transmitter to the receiver through the air
- ***PHY Processing Time (PPT)***, a time elapsed from receiving the last bit of a frame at *PHY* until the delivery of the first bit to the *MAC*
- ***Frame Reception time (FRT)***, encodes the time when the last bit of a frame has been received at the *MAC*

Whenever a *WBAN's* coordinator has a frame to transmit, the *MAC* service (resp. the *PHY* service) adds a *MAC*-level timestamp denoted by *MTP* (resp. *PHY*-level timestamp denoted by *PTP*) that encodes the time when the last bit of the frame is transmitted to the *PHY* layer (resp. to the air). Such addition with other *PHY*- and *MAC*-level parameters enable the receiving coordinator to calculate the *timeshift*. Furthermore, when the coordinator receives a frame at the *MAC*, it timestamps the reception of the last bit of that frame through *FRT* according to its local clock. Thus, as the frame bits pass through the *PHY* and *MAC* layers, the receiving services at each layer calculates the following

parameters:

- The time spent by the *MAC* service to receive the frame (*MRT*).
- The time spent by the *PHY* service to process the frame (*PPT*).
- The time spent by the *PHY* service to receive the frame (*PRT*).
- The time spent by the first bit of the frame to be received at the *PHY* from the air.

Subsequently, each coordinator relates the calculated parameters and timestamps as well as the frame reception times to compute the *timeshift* as shown in **Algorithm 5**. Afterward, it generates a pattern which consists of differently computed *timeshifts* of the different superframes. Based on a *timeshift* of a particular superframe, the coordinator aligns the start transmission time of its superframe to the superframe of that *timeshift* to predict which time-slots within its superframe are interfering with the time-slots of that superframe. To summarize, *DTRC* provides each coordinator with two fundamental functionalities, 1) it determines which superframes may overlap, and more precisely, 2) which time-slots within those superframes may collide with each other as shown in **Figure 4.3**. **Algorithm 5** provides high level summary of *DTRC*. Where, *Diff*, *timeshift*,

---

#### Algorithm 5 *DTRC* Algorithm

---

**Require:** *N* WBANs, *K* Sensors/WBAN, *K* Time-slots/Superframe

```

1: for i = 1 to N do
2:   for l = 1 to N - 1 & i ≠ l do
3:     Crdi receives Bl at FRTi,l & Crdi computes;
4:     Diffl = PTPl - MTPl = PPTl + PRTl;
5:     timeshifti,l = FRTi - [MRTi + PPTi + PRTi + L + Diffl]
6:     IntrfrnSlotsi,l = timeshifti,l/TS;
7:     ID = ⌈ | IntrfrnSlotsi,l | ⌋;
8:     switch (timeshifti,l)
9:     case timeshifti,l < 0 & (| timeshifti,l | < TS):
10:      ∀ z ≥ ID & ∀ t ≥ ID, Ti,z ⊗ Tl,t;
11:     case timeshifti,l < 0 & (TS < | timeshifti,l | < BI/2):
12:      (∀ z > (K - ID) & ∀ t ≤ ID), Ti,z ⊗ Tl,t;
13:     case timeshifti,l = 0:
14:      Complete interference of Crdl & Crdi active periods;
15:     end switch
16:   end for
17: end for=0

```

---

*IntrfrnSlots*, *BI*, *B*, respectively, denote the difference, time shift, interfering time-slots, superframe length and beacon.

## 4.4 Orthogonal Codes Allocation - OCAIM

In this section, we develop a distributed cooperative algorithm to lower the probability of inter-WBAN interference, namely, *OCAIM*, through code allocation to interfering sensor nodes based on *DTRC*. Furthermore, we present an analytical model that de-

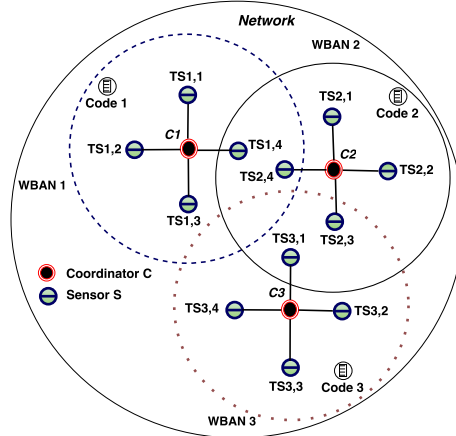


Figure 4.2: A network of three coexisting WBANs

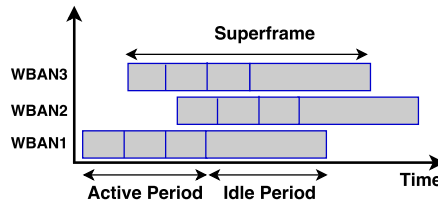


Figure 4.3: Overlapping superframes scheme

gives the success and collision probability for data and beacon frames transmissions. Subsequently, we evaluate the performance of *OCAIM* in terms of the minimum *SINR*, network lifetime, throughput, and compare with two other schemes, smart spectrum allocation and orthogonal *TDMA*.

As pointed out, when different sensor nodes of *WBANs* in the close proximity of each other simultaneously share the same channel, a co-channel interference may arise due to the absence of coordination among them, as shown in **Figure 4.2**. Hence, the superframes of different *WBANs* may overlap as illustrated in **Figure 4.3**. In *OCAIM*, each *WBAN* is allocated a unique cyclic orthogonal code from the set *COWHC* to be used by its interfering sensor nodes. Based on the interference that a particular sensor experiences in one or more time-slots it has been assigned, the coordinator instructs that sensor to immediately use the code in that time-slots for spreading its signal. Accordingly, each sensor multiplies its signal by the spreading code to increase its bandwidth and make it more interference resistant.

We denote  $k^{th}$  *Sensor Interference List* of sensor node  $S_{i,k}$  of *WBAN<sub>i</sub>* by  $SIL_{i,k}$ .  $SIL_{i,k}$  comprises all sensor nodes of other *WBANs* which impose interference on  $S_{i,k}$ . Hence,  $Crd_i$  adds all sensor nodes  $S_{l,m}$  to  $SIL_{i,k}$  that

- interfere with  $S_{i,k}$  in its assigned time-slot  $T_{i,k}$ , denoted by  $S_{l,m} \bowtie S_{i,k}$ , (*DTRC* determines the time-slot level interference) and,
- whose binary bitwise OR with that of  $S_{i,k}$  equals to 1, denoted by  $F_{i,k} \otimes F_{l,m} = 1$ .

Where  $F_{i,k}$  and  $F_{l,m}$  are indicator functions, respectively, defined as follows:

$$F_{i,k} = \begin{cases} 1 & \text{if } S_{i,k} \in IN_{i,l} \\ 0 & \text{if } S_{i,k} \notin IN_{i,l} \end{cases}$$

$$F_{l,m} = \begin{cases} 1 & \text{if } S_{l,m} \in IN_{i,l} \\ 0 & \text{if } S_{l,m} \notin IN_{i,l} \end{cases}$$

Which means that  $WBAN_l$  is an interfering to  $WBAN_i$  and  $IN_{i,l} = IS_i \cap IS_l$ . Then, we define  $SIL_i$  in **Eq. (4.8)**.

$$SIL_{i,k} = \{S_{l,m} | T_{l,m} \bowtie T_{i,k} \& F_{i,k} \otimes F_{l,m} = 1\} \quad (4.8)$$

Therefore,  $Crd_i$  assigns a code to  $S_{i,k}$  within its  $WBAN$  and each sensor belongs to  $SIL_{i,k}$  is also assigned a code within its  $WBAN$  to avoid the interference. In other words, all interfering sensor nodes of the same  $WBAN$  use the same code, each in its assigned time-slot. Furthermore, each coordinator updates its code assignment pattern with every new beacon broadcast, i.e., at the beginning of every new superframe. **Algorithm 6** provides high level summary of *OCAIM*.

We illustrate *OCAIM* through an example of three coexisting *TDMA*-based  $WBANs$  scenario as shown in **Figure 4.2**. However, we denote  $j^{th}$  sensor of  $WBAN_i$  is transmitting to its coordinator  $Crd_i$  by  $S_{i,j}$ . Assuming sensor nodes of same index are simultaneously transmitting. Then, the interference lists are as follows:

- $I_1 = \{S_{2,4}\}$ .
- $I_2 = \{S_{1,4}, S_{3,1}\}$ .
- $I_3 = \{S_{2,3}\}$ .

Whilst, the interference sets are:

- $IS_1 = \{S_{1,4}, S_{2,4}\}$ .
- $IS_2 = \{S_{2,3}, S_{2,4}, S_{1,4}, S_{3,1}\}$ .
- $IS_3 = \{S_{3,1}, S_{2,3}\}$ .

Thus, for  $WBAN_2$ , the *sensor interference sets* are defined as follows:

- $SIL_{2,1} = \{S_{3,1}\}$ .
- $SIL_{2,2} = \Phi$ .
- $SIL_{2,3} = \{S_{3,3}\}$ .
- $SIL_{2,4} = \{S_{1,4}\}$ .

Whereas, the code assignment is as follows:

- $Crd_1$  assigns  $Code_1$  to  $S_{1,4}$ , each in its time-slot.
- $Crd_2$  assigns  $Code_2$  to  $S_{2,1}$ ,  $S_{2,3}$  and  $S_{2,4}$ .
- $Crd_3$  assigns  $Code_3$  to  $S_{3,1}$  and  $S_{3,3}$ .

---

### Algorithm 6 OCAIM Scheme

---

**Require:**  $N$  WBANs,  $K$  Sensors/WBAN

```

1: Phase 1: TDMA Orthogonal Transmissions
2: for  $i = 1$  to  $N$  do
3:    $Crd_i$  broadcasts Beacon  $B^i$ ;
4:   for  $k=1$  to  $K$  do
5:      $S_{i,k}$  is transmitting in time-slot  $T_{i,k}$  to  $Crd_i$ ;
6:      $Crd_l \forall l \neq i$  calculates  $\delta_{i,l,k}$ ;
7:   end for
8:    $Crd_i$  finds  $\rho_i^{min} = \min\{\delta_{i,k}\}_{\forall k=1\dots K}$ ;
9: end for
10: Phase 2: Interference Lists (I) and Sets (IS) Formation
11: for  $i = 1$  to  $N$  do
12:   for  $l = 1$  to  $N$ ,  $l \neq i$  do
13:     for  $M = 1$  to  $K$  do
14:       if  $\delta_{i,l,m} > \rho_i^{min} - \theta$  then
15:         Add  $S_{l,m}$  to set  $I_i$ ;
16:       end if
17:     end for
18:   end for
19:    $Crd_i$  broadcasts  $I_i$  & sets  $IS_i = I_i \cup \{S_{i,k} \mid S_{i,k} \in I_l, \forall l \neq i\}$ ;
20: end for
21: Phase 3: Distributed Time Reference Correlation Formation (DTRC)
22: for  $i = 1$  to  $N$  do
23:    $Crd_i$  executes Algorithm 5;
24: end for
25: Phase 4: Sensor Interference List (SIL) Formation
26: for  $i = 1$  to  $N$  do
27:   for  $l = 1$  to  $N$ ,  $i \neq l$  do
28:      $IN_{i,l} = \{IS_i \cap IS_l\}$ ;
29:     for  $k = 1$  to  $K$  do
30:        $SIL_{i,k} = \{(S_{l,m} \mid S_{l,m} \bowtie S_{i,k}) \& (F_k \otimes F_m = 1)\}$ ;
31:     end for
32:   end for
33: end for
34: Phase 5: Orthogonal Codes Assignments
35: for  $i = 1$  to  $N$  do
36:   for  $k = 1$  to  $K$  do
37:     for  $l = 1$  to  $N$ ,  $i \neq l$  do
38:       if  $S_{l,m} \in SIL_{i,k}$  then
39:          $Crd_i$  assigns  $Code_i$  to  $S_{i,k}$ 
40:          $Crd_l$  assigns  $Code_l$  to  $S_{l,m}$ 
41:       end if
42:     end for
43:   end for
44: end for
45:  $Crd_i$  updates  $code - to - timeslot - assignment - pattern_i, \forall i; = 0$ 

```

---

**Table 4.1:** Notation & meaning

Notation	Meaning
B	beacon
Crd	coordinator
TS	time-slot length
BI	superframe length
$S_i$	$i^{th}$ sensor
SIFS	short inter-frame spacing
$TD_i$	time duration $S_i$ occupies the channel
$T_B$	time required by Crd to transmit a beacon
G	all data frames generated during an active period
$Pr_{Bcoll}$	collision beacon transmission probability
$Pr_{Bsucc}$	successful beacon transmission probability
$T_{fr}$	time required by $S_i$ to transmit a data frame
$W_{succ}$	number of WBANs succeed in beacon transmissions
$Pr_{wbansucc}^i$	successful transmission probability of $WBAN_i$
H	all data frames successfully transmitted during an active period
$Pr_{FRsucc}^i$	successful data frame transmission probability of $S_i$
$Nfrs_i$	expected number of data frames transmitted by $S_i$ in an active period
$D_{coll}$	time duration in which $S_i$ 's transmission collide with other transmissions
$T_{Bcoll}$	time durations in which a beacon transmission collide with other active periods
$D_{succ}$	time duration in which $S_i$ 's transmission does not collide with other transmissions

## 4.5 OCAIM Analysis

In this section, we model and analyze the successful and collision probabilities of the beacons and data frames transmissions to validate our approach. For the simplicity of the analysis, we consider all WBANs in the network have similar superframe and time-slot lengths, respectively, denoted by  $BI$  and  $TS$ . Basically, a sensor  $S_i$  transmits multiple data frames separated by short inter-frame spacing ( $SIFS$ ), where each data frame and beacon require transmission time  $T_{fr}$  and  $T_B$ , respectively. **Table 4.1** provides the notations and their corresponding meanings that we used in the analysis of OCAIM.

### 4.5.1 Successful Beacon Transmission Probability

We say a superframe does not interfere when its active period is not commencing at the same time when other WBANs are transmitting. If we assume a coordinator succeeds in beacon transmission with a probability  $Pr_{succ}$ , then a beacon may be lost with probability, denoted by  $Pr_{lost}$ , where  $Pr_{lost} = 1 - Pr_{succ}$ . We denote the expected number of data frames transmitted by  $S_i$  during the active period by  $Nfrs_i$ . However, a sensor  $S_i$  may occupy the channel for the time duration denoted by  $TD_i$  or for the whole time-slot, then,  $TD_i$  per a superframe is calculated in **Eq. (4.9)**.

$$TD_i = \text{Min}(TS_i, Nfrs_i \times T_{fr} + (Nfrs_i - 1) \times SIFS) \quad (4.9)$$

The transmission of a beacon may interfere with the transmissions that take place in the active periods of other *WBANs*, assuming two *WBANs* coexist, then, the sum of these periods is the duration of possible beacon interference (collision) calculated in Eq. (4.10).

$$T_{Bcoll} = 2 \times T_B + \sum_{i=1}^K (TD_i + T_B) \quad (4.10)$$

Then, the beacon collision probability is calculated in Eq. (4.11).

$$Pr_{Bcoll} = T_{Bcoll} / BI \quad (4.11)$$

Whilst in the case of  $N$  coexisting *WBANs* are collocated, a coordinator may succeed in beacon transmission that does not interfere with the transmission of  $N - 1$  *WBANs*. The probability of successful beacon transmission  $Pr_{Bsucc}$  is calculated in Eq. (4.12) which implies that there will be an expected number  $W_{succ}$  *WBANs* out of  $N - 1$  *WBANs* where their beacons and data frames transmissions are successful.  $W_{succ}$  is calculated in Eq. (4.13).

$$Pr_{Bsucc} = \prod_{i=1}^{N-1} (1 - Pr_{Bcoll}) = (1 - Pr_{Bcoll})^{N-1} \quad (4.12)$$

$$W_{succ} = (N - 1) \times Pr_{Bsucc} \quad (4.13)$$

Doing so, Eq. (4.13) becomes as follows:

$$Pr_{Bsucc} = (1 - Pr_{Bcoll})^{(N-1) \times Pr_{Bsucc}} \quad (4.14)$$

## 4.5.2 Successful Data Transmission Probability

It is interesting to analyze the successful data transmission probability, i.e., the probability of transmitting a data frame successfully without colliding with transmissions of other  $N-1$  *WBANs*. However, the duration of successful data transmission of each *WBAN* counted on specific periods of the superframe where no collisions take place. This time duration is calculated as in Eq. (4.15).

$$D_{succ} = BI \times (1 - Pr_{Bcoll})^{W_{succ}} \quad (4.15)$$

Similar to (4.10), the time duration a data frame may collide with the transmission of another WBAN will be calculated in Eq. (4.16).

$$D_{coll} = \sum_{i=1}^K (TD_i + T_{fr}) \quad (4.16)$$

To present the probability of successful transmission of WBAN<sub>1</sub> coexisting with another WBAN<sub>2</sub>, the transmitted data frames of WBAN<sub>1</sub> do not experience collision with the transmitted data frames of WBAN<sub>2</sub> during a time period of  $D_{succ} - 2 \times D_{coll}$  and during the period of  $2 \times D_{coll}$ , half of the frames collide on average. The successful probability of WBAN<sub>1</sub> transmission denoted by  $Pr_{wbansucc}^1$  coexisting with WBAN<sub>2</sub> is calculated as in Eq. (4.17).

$$Pr_{wbansucc}^1 = \frac{D_{succ} - 2 \times D_{coll}}{D_{succ}} \times 1 + \frac{2 \times D_{coll}}{D_{succ}} \times 1/2 \quad (4.17)$$

$$= (D_{succ} - D_{coll})/D_{succ} \quad (4.18)$$

Moreover, to derive the successful data transmission probability, it is required to know all the data frames generated (G) and the number of data frames successfully transmitted (H) in a superframe. As we mentioned earlier, whenever a beacon is successfully received,  $Nfrs_i$  frames are expected to be buffered. But, it may or may not be the case that a sensor  $S_i$  succeed in transmitting all data frames in its assigned time-slot  $T_i$  and so the number of frames will be actually transmitted is bounded by the length of its time-slot  $TS$ . It is calculated in Eq. (4.19).

$$Ntxfrs_i = \text{Min}(TS/(T_{fr} + SIFS), Nfrs_i) \quad (4.19)$$

However, a data frame will be successfully transmitted if the beacon has been received without any collision with other coexisting transmissions. Now, let us calculate the successful data frame transmission probability for sensor  $S_i$  as in Eq. (4.20).

$$Pr_{FRsucc}^i = \frac{H}{G} = \frac{Pr_{Bsucc} \times Ntxfrs_i \times (Pr_{wbansucc}^1)^{W_{succ}}}{P_i} \quad (4.20)$$

By assuming all the beacons are received successfully, this puts an upper bound on the probability of successful data frame transmission. Doing so, the occupancy time of the channel by sensor  $S_i$  is calculated as follows in Eq. (4.21).

$$TD_i = P_{FRsucc}^i \times T_{fr} + (1 - P_{FRsucc}^i) \times SIFS \quad (4.21)$$

Similar to (4.10), the time duration a data frame may collide with the data frames of a coexisting WBAN is given by Eq. (4.22).

$$D_{coll} = \sum_{i=1}^K (TD_i + T_{fr}) \quad (4.22)$$

Moreover, the probability that data frames of WBAN<sub>1</sub> does not collide with the data frames transmissions of WBAN<sub>2</sub> is calculated in Eq. (4.23).

$$Pr_{FRsucc}^1 = (BI - D_{coll}) / BI \quad (4.23)$$

Whilst this probability is modified to Eq. (4.24) when WBAN<sub>1</sub> coexist with  $N - 1$  WBANs, i.e., the data frames transmissions of WBAN<sub>1</sub> do not interfere (collide) with the transmissions of  $N - 1$  coexisting WBANs.

$$Pr_{FRsucc} = (Pr_{FRsucc}^1)^{N-1} \quad (4.24)$$

## 4.6 OCAIM Performance Evaluation

This section compares the performance of OCAIM to that of competing approaches, smart spectrum allocation [39] and orthogonal TDMA, which are defined as follows:

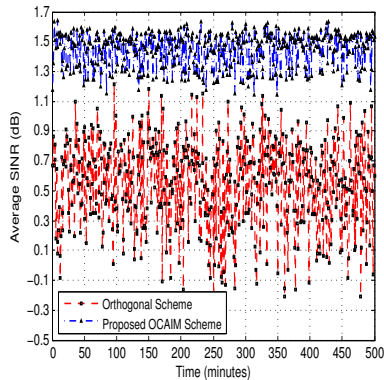
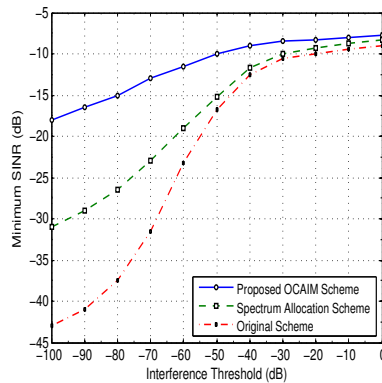
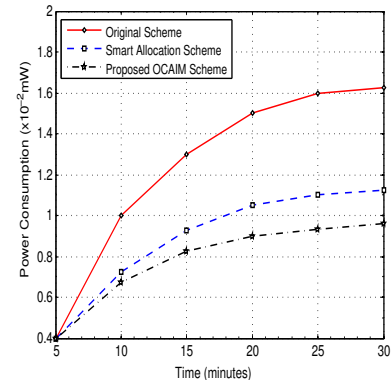
- **Smart spectrum allocation** : is a distributed scheme that assigns orthogonal channels to interfering sensor nodes belonging to each pair of coexisting WBANs.
- **orthogonal TDMA** : a WBAN employs one-hop between sensor nodes and the WBAN's Crd. A TDMA is employed, in which each sensor node is assigned a time-slot through which it transmits its packet to the WBAN's Crd.

In addition, the analytical results derived the data and beacon frames transmission probability and network throughput are validated by simulations. We have performed simulation experiments through Matlab, where the density of WBANs is varied. The locations of the individual WBANs change to mimic random mobility in a space of  $5 \times 5 \times 3m^3$  and consequently, the interference pattern varies. Each WBAN consists of  $K = 10$  sensor nodes and a single WBAN's coordinator, and all sensor nodes use the same transmission power at -10 dBm. Each WBAN is assigned an orthogonal code from the set COWHC. The simulation parameters are provided in Table 4.2.

The average SINR versus time for OCAIM and orthogonal TDMA, denoted by OS are compared. As can be clearly seen in Figure 4.4, OCAIM achieves more than two times higher SINR than OS and the channel seems to be more stable because of the code

**Table 4.2:** Simulation parameters - *OCAIM*

Parameter name	Description/Value
Codes/WBAN	1
Sensors/WBAN	10
Coordinator/WBAN	1
WBANs/Network	up to 30
Sensor TxPower	-10dBm
SINR threshold range	[-100, 0] dB
Simulation time	30 minutes
Simulation space	$5 \times 5 \times 3m^3$
Mobility pattern	random
Medium access scheme	TDMA

**Figure 4.4:** Average *SINR* vs. time for *OCAIM* and orthogonal *TDMA***Figure 4.5:** Minimum *SINR* vs. interference threshold for *OCAIM*, *SMS* & *OS***Figure 4.6:** *WBAN* power consumption vs. time for *OCAIM*, *SMS* & *OS*

assignment.

The average *SINR* versus the interference threshold for *OCAIM*, smart spectrum allocation, denoted by *SMS*, and *OS* are compared. As can be seen in **Figure 4.5**, *OCAIM* achieves higher *SINR* than that for *SMS* and *OS* for all interference thresholds. However, *OS*, where no coordination is considered, achieves higher probability of superframes overlapping because neither channels nor codes are assigned to interfering sensor nodes, which lowers the *SINR* values. Unlike *SMS* where orthogonal channels are cooperatively assigned based on sensor-level interference only, *OCAIM* assigns codes based on sensor- and time-slot-level interference, which explains *SINR* improvement that *OCAIM* has compared to *SMS*. Furthermore, a higher *SINR* is achieved when the interference threshold is increased, which implies that more sensor nodes are probably assigned codes leading to higher *SINR*.

The power consumption versus time for *OCAIM*, *SMS* and *OS* are compared in **Figure 4.6**. In this figure, *OCAIM* achieves lower power consumption than *SMS* and *OS* all the time. In *OS*, due to the absence of coordination and the overlapping of superframes results in more collisions, which leads to higher retransmissions and hence higher power consumption. In *SMS*, the *WBAN* coordinators cooperatively negotiate to assign orthogonal channels which explains the reduction in power consumption com-

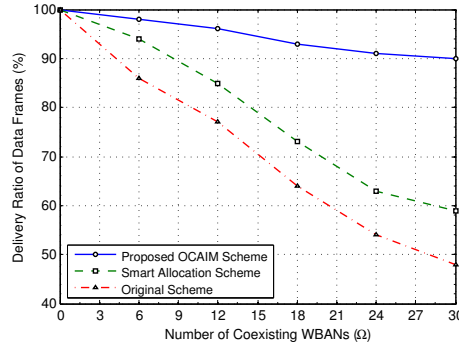


Figure 4.7: Data frames delivery ratio versus WBANs count

pared to *OS*. Whilst, in *OCAIM*, the coordinators assign codes rather than channels, which justifies the increase in power consumption in *SMS*. This increase is only because of the switching among channels consumes more energy than code assignments which has been confirmed by the simulation results shown in **Figure 4.6**.

The data frames delivery ratio, denoted by *FDR*, versus the number of *WBANs*, denoted by  $\Omega$  for *OCAIM*, *SMS* and *OS* are compared in **Figure 4.7**. This figure shows that *OCAIM* always achieves higher *FDR* than that of *SMS* and *OS* for all  $\Omega$  values. Due to the absence of coordination among *WBANs* and channel/code assignments in *OS*, the overlapping of the individual superframes among each other results in more collisions, which eventually lowers *FDR* values. Though, *SMS* limits the number of channels to 16, nonetheless, the *WBAN* coordinators cooperatively negotiate to assign channels to sensor-level interference only, which justifies the increase in *FDR* compared to *OS*. However, in *OCAIM*, codes are assigned to sensor- and time-slot-levels, which explains the improvement in *FDR* on *SMS* and *OS* schemes.

On the other hand, **Figure 4.8** compares the simulated successful beacon transmission probability, denoted by  $Pr_{Bsucc}^{simulated}$ , and the theoretical successful beacon transmission probability, denoted by  $Pr_{Bsucc}^{theoretical}$ , with varying the number of *WBANs* ( $\Omega$ ). As can be observed in the figure, the simulated and theoretical probabilities significantly approach each other for all values of  $\Omega$ , which confirms the correctness of our theoretical results.

## 4.7 Conclusions

In this chapter, we presented a cooperative approach to reducing the probability of inter-*WBAN* co-channel interference through code allocation based on distributed time correlation reference. To the best of our knowledge, we are the first that consider the interference at sensor- and time-slot-levels. Furthermore, our approach lowers the power consumption at both *sensor*- and *WBAN*-levels and improves the network throughput.

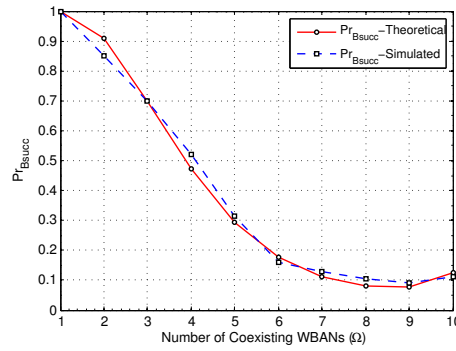


**Figure 4.8:** Probability of successful beacon transmission versus WBANs count

Specifically, we propose two schemes, *DTRC* that determines which superframes overlap with each other, and *OCAIM* that allocates orthogonal codes to high interfering sensor nodes within each WBAN. We further presented an analytical model that derives the success and collision probabilities of frames' transmissions. In addition, extensive simulations and benchmarking have been conducted, and the results show that our approach minimizes the interference, improves the power savings and the network throughput.



# Chapter 5

## Non-Cooperative Inter-WBAN Interference Mitigation Using Latin Rectangles

### Contents

---

<b>5.1 Introduction</b> . . . . .	<b>74</b>
<b>5.2 System Model</b> . . . . .	<b>75</b>
5.2.1 Model Assumptions and Preliminaries . . . . .	75
5.2.2 Latin Squares Overview . . . . .	76
<b>5.3 Interference Mitigation Using Latin Rectangles - <i>DAIL</i></b> . . . . .	<b>77</b>
5.3.1 <i>DAIL</i> Algorithm . . . . .	78
5.3.2 <i>DAIL</i> Superframe . . . . .	79
5.3.3 <i>DAIL</i> Analysis . . . . .	80
5.3.4 <i>DAIL</i> Performance Evaluation . . . . .	85
<b>5.4 Interference Mitigation Using Predictable Channel Hopping - <i>CHIM</i></b> . .	<b>88</b>
5.4.1 <i>CHIM</i> Superframe . . . . .	88
5.4.2 <i>CHIM</i> Algorithm . . . . .	89
5.4.3 <i>CHIM</i> Analysis . . . . .	90
5.4.4 <i>CHIM</i> Performance Evaluation . . . . .	93
<b>5.5 Performance Evaluation</b> . . . . .	<b>96</b>
5.5.1 Comparing <i>DAIL</i> & <i>CHIM</i> . . . . .	96
5.5.2 Comparing <i>CHIM</i> & <i>DAIL</i> & <i>SMS</i> . . . . .	97

---

## 5.1 Introduction

Spectrum allocation approaches have proved their efficiency in interference avoidance and mitigation in low-density wireless networks. Recently, the co-channel interference avoidance and mitigation has been subject to extensive research in [39, 40, 47, 17, 46, 41, 45]. In such approaches, individual nodes are allocated orthogonal channels to avoid the interference. However, the main problems in these approaches are not only the limited number of channels but also different wireless cross-technology networks may simultaneously share the same international license-free 2.4 GHz ISM band. On the other hand, the problem of medium access scheduling has been researched in the multi-hop packet radio and cellular networks using *Latin squares* and *Galois field theory* [107, 108, 109]. For a single-channel networks, using the *Latin square design* can obtain much smaller *frame length* when compared with the *modified Galois field design* [108].

Compared to the related work covered in this section, our approach combines two solution strategies, multi-channel, and time-slot adjustment. Thus, we exploit the international license-free spectrum available in the *IEEE 802.15.6* standard and pursue the approach of spectrum allocation to resolve the problem of co-channel interference among non-cooperative *WBANs* not only through the channel but also the channel to time-slot hopping.

In this chapter, we propose a distributed approach that adapts to the size of the network in terms of the number of *WBANs* and to the density of sensors within each *WBAN* to lower the impact of co-channel interference through dynamic channel hopping based on Latin rectangles. Thus, we employ Latin rectangles for channel and time-slot allocation to sensors, while enabling autonomous scheduling of the medium access within each *WBAN*. To mitigate interference, our approach exploits the availability of multiple channels and leverages the properties of Latin rectangles to reduce the co-channel interference among non-cooperative *WBANs*, the overhead resulting from channel hopping, the transmission delay and save the power resource at both *sensor-* and *WBAN-*levels. Specifically, we propose two schemes, the first is called *Distributed Algorithm for Interference mitigation using Latin rectangles*, namely, *DAIL*, that suits the high-density of *WBANs*. In *DAIL*, sensors within each *WBAN* are allocated a single channel to time-slot combination and this simplifies inter-*WBAN* coordination and time synchronization. *DAIL* yields better schedules of the medium access and significantly diminishes the inter-*WBAN* interference. Like *DAIL*, the second is called *Channel Hopping algorithm for Interference Mitigation*, namely, *CHIM*, which also leverages the properties

of Latin rectangles to generate a predictable interference-free transmission schedule for all sensors within a WBAN. Unlike *DAIL*, *CHIM* suits the low-density of WBANs and minimizes the frequency of channel switching significantly, i.e., *CHIM* applies channel switching only when a sensor experiences interference to save the power resource at both sensor- and WBAN-levels. Moreover, *DAIL* and *CHIM* do not require any mutual coordination among the individual WBANs. The main contributions of this chapter are summarized as follows:

- *DAIL*, a distributed scheme that enables time-based channel hopping using Latin rectangles to avoid the co-channel interference among non-cooperative WBANs and to minimize the medium access collision.
- *CHIM*, a distributed scheme that allocates a random channel to each WBAN, and provisions backup time-slots for failed transmission. The backup time-slots are scheduled in a way that is similar to *DAIL*. *CHIM* enables only a sensor that experiences collisions to hop to an alternative backup channel in its allocated backup time-slot.
- An analytical model that derives bounds on the collision probability and throughput for sensors transmissions.
- we comprehensively conducted extensive simulations to evaluate the performance of *DAIL* and *CHIM*. The results demonstrate the effectiveness and efficiency of our approach in terms of lowering the medium access collision probability, the transmission delay, extending the network lifetime and maximizing the network throughput as well as the network reliability compared with other competing solutions.

## 5.2 System Model

### 5.2.1 Model Assumptions and Preliminaries

We consider  $N$  non-cooperative WBANs coexist in an area, e.g., when a group of patients moving around in a large hall of a hospital. Each WBAN consists of a single coordinator and up to  $K$  sensors, in which each sensor generates its data based on a predefined sampling rate and transmits data at maximum rate of 250Kb/s using transmission power at  $-10$  dBm. Furthermore, we make the following assumptions about the sensors, WBANs and the network.

- Star topology between sensors and the coordinator is employed within each WBAN.
- All sensors within each WBAN as well as the individual WBANs are subject to mobility.

**Table 5.1:** Notation & meaning

Notation	Meaning
$WBAN_k$	$k^{th}$ WBAN
Ack	acknowledgment
TS	time-slot
Pkt	packet
CFP	contention free period
OLR	orthogonal Latin rectangle
$Crd_q$	coordinator of $q^{th}$ WBAN
$S_{i,k}$	$i^{th}$ sensor of $k^{th}$ WBAN
$DFC_k$	a default channel of $k^{th}$ WBAN
$BKC(S_{i,k})$	a backup channel picked by $i^{th}$ sensor of $k^{th}$ WBAN
$BKTS_{i,k}$	a backup time-slot allocated for $i^{th}$ sensor of $k^{th}$ WBAN

- TDMA scheme is employed within each WBAN.
- All sensor and coordinator nodes use the 2.4 GHz international license-free band and have access to all ZigBee channels at any time.
- All coordinators are equipped with significantly richer power supply than sensors, and are not affected by channel hopping.
- No coordination and time synchronization are considered among WBANs.

Table 5.1 shows notations meanings.

## 5.2.2 Latin Squares Overview

In this section, we provide a brief overview of Latin squares that we used to allocate interference mitigation channels. Throughout this chapter, we denote a symbol by the ordered pair  $(i,j)$  referenced at the  $i^{th}$  row and  $j^{th}$  column in the Latin square, which refers to the assignment of  $i^{th}$  interference mitigation channel to the  $j^{th}$  sensor in the dedicated interference mitigation time-slot.

**Definition 5.1.** A Latin square is a  $K \times K$  matrix, filled with  $K$  distinct symbols, each symbol appearing once in each column and once in each row.

**Definition 5.2.** Two distinct  $K \times K$  Latin squares  $E = (e_{i,j})$  and  $F = (f_{i,j})$ , so that  $e_{i,j}$  and  $f_{i,j} \in \{1,2,\dots,K\}$ , are said to be orthogonal, if the  $K^2$  ordered pairs  $(e_{i,j}, f_{i,j})$  are all different from each other. More generally, the set  $O = \{E_1, E_2, E_3, \dots, E_r\}$  of distinct Latin squares  $E$  is said to be orthogonal, if every pair in  $O$  is orthogonal.

**Definition 5.3.** An orthogonal set of Latin squares of order  $K$  is of size  $(K-1)$ , i.e., the number of Latin squares in the orthogonal family is  $(K-1)$ , is called a complete set [107, 110].

**Definition 5.4.** A  $M \times K$  Latin rectangle is a  $M \times K$  matrix  $G$ , filled with symbols  $a_{ij} \in \{1,2,\dots,K\}$ , such that each row and each column contains only distinct symbols.

**Theorem 5.1.** If there is an orthogonal family of  $r$  Latin squares of order  $K$ , then  $r \leq K - 1$  [110]

$E$  and  $F$  are orthogonal Latin squares of order 3, because no two ordered pairs within  $E \bowtie F$  are similar.

$$E = \begin{bmatrix} 1 & 2 & 3 \\ 2 & 3 & 1 \\ 3 & 1 & 2 \end{bmatrix} \quad F = \begin{bmatrix} 1 & 2 & 3 \\ 3 & 1 & 2 \\ 2 & 3 & 1 \end{bmatrix} \quad E \bowtie F = \begin{bmatrix} 1,1 & 2,2 & 3,3 \\ 2,3 & 3,1 & 1,2 \\ 3,2 & 1,3 & 2,1 \end{bmatrix}$$

According to *Theorem 5.1*, the number of WBANs using orthogonal Latin squares is upper bounded by  $K-1$ , thus,  $K$  should be large enough so that, each WBAN can pick an orthogonal Latin square with high probability. The orthogonality property of Latin squares avoids inter-WBAN interference by allowing a WBAN to have its unique channel allocation pattern that does not resemble the pattern of other WBANs, i.e., they do not share the same symbol positions, each in its own Latin square and consequently, no other WBAN in the network would simultaneously share the same pattern with  $WBAN_i$  all the time. Generally, our approach makes it highly improbable for two transmissions to collide. Nonetheless, collision may still occur when (i) two WBANs randomly pick the same Latin square, or (ii) more than 16 WBANs coexist in the same area, which means that, the number of WBANs exceeds the number of ZigBee channels in the Latin square.

Basically, if a WBAN picks one Latin square from an orthogonal set, there will be no shared channel among the coexisting Latins. The Latin size will depend on the largest among the number of channels, denoted by  $M$ , and the number of sensors in each WBAN, denoted by  $K$ . The ZigBee standard [23] limits the number of channels which constitutes the rows in the Latin square to 16, no more than 16 transmissions can be scheduled. To overcome such a limitation, our approach employs Latin rectangles instead, i.e., does not restrict the value of  $K$  and hence supports  $K > M$ .

### 5.3 Interference Mitigation Using Latin Rectangles - DAIL

In this section, we develop a distributed algorithm based on Latin rectangles, namely, *DAIL*, for channel allocation and medium access scheduling to diminish the probability of interference among non-cooperative WBANs through dynamic channel hopping. In essence, *DAIL* assigns channel and time-slot combinations to sensors to reduce the probability of collision. *DAIL* suits the high-density of WBANs, and involves overhead in terms of energy and transmission delay due to frequent channel hopping. We then present an analytical model that derives bounds on the collision probability and the throughput for sensors transmissions. Subsequently, we evaluate the performance of *DAIL* by extensive simulations and compare it with that of other competing schemes.

The results demonstrate the effectiveness and the efficiency of *DAIL* in terms of lowering the probability of collision and the energy consumption as well as improving the throughput significantly at the sensor- and *WBAN*-levels.

### 5.3.1 *DAIL* Algorithm

In *DAIL*, each *WBAN*'s coordinator randomly picks an orthogonal Latin rectangle from the orthogonal set through which it assigns a symbol to each sensor within its *WBAN*. According to its symbol in the Latin rectangle, a sensor determines its transmission schedule which is formed of a sequence of channel and time-slot combinations. That means each sensor determines its hopping channels, i.e., each allocated channel to use in which assigned time-slot within every superframe.

*DAIL* enables different coexisting sensors to hop among distinct channels to avoid the collision among their corresponding transmissions that happen in the same time-slot. Thus, the number of collisions depends on the number of coexisting *WBANs*, i.e., the corresponding interfering sensors, and the number of orthogonal Latin rectangles used by the interfering *WBANs*. Therefore, the collision among the transmissions of different coexisting sensors is completely avoided, iff, the number of orthogonal Latin rectangles is larger than the number of that sensors competing to transmit in the same time-slot. Otherwise, *DAIL* extends the number of columns in the Latin which is directly related to the length of the *WBAN*'s superframe by adding extra time-slots to lower the probability of collisions. For example, if the number of coexisting *WBANs* is  $N$  and the Latin rectangles is  $P$ , each of size  $16 \times K$ , where  $K$  is the number of columns in the Latin rectangle, which also denotes the number of time-slots in the superframe. If  $N > \max(16, K)$ , then each *WBAN* will extend the number of columns in the Latin, i.e., the number of time-slots in the superframe from  $K$  to  $K + XT$ , where  $XT = N - \max(16, K)$ . Doing so, such sensors will have higher probability to not pick the same channel in the same time-slot and hence the number of collisions is minimized. **Algorithm 7** provides a high level summary of *DAIL*.

---

#### **Algorithm 7** *DAIL* Scheme

---

**Require:**  $N$  *WBANs*,  $K$  sensors/*WBAN*, Coordinator  $Crd$ ,  $M$  *ZigBee* channels, Latin rectangle  $R$ , frame length  $FL$

- 1: **BEGIN**
- 2:  $FL = K$  // default setting of the frame length;
- 3: **if**  $N > K$  **then**
- 4:    $FL = N$  //  $Crd$  increases the number of time-slots in the superframe;
- 5: **end if**
- 6: Each *WBAN*'s  $Crd$  randomly picks a Latin rectangle  $R$  of size  $M \times FL$ ;
- 7: **END** =0

---

### 5.3.2 DAIL Superframe

Each WBAN's superframe is delimited by two beacons and composed of two successive frames: (i) active, that is dedicated for sensors, and (ii) inactive, that is designated for coordinators as shown in **Figure 5.1**. While, we consider all  $M = 16$  channels of ZigBee available at each WBAN, we still need to determine the number of time-slots per each row of Latin rectangle, in other words, the length of each superframe. In fact, the superframe size depends on two factors, 1) how big the time-slot, which is based on the protocol in use, and 2) the number of required time-slots, which is determined by the different sampling rates of WBAN sensors. Generally, the superframe size is determined based on the highest sampling rate and the sum of number of samples for all sensors in a time period determines the superframe size. DAIL requires the superframe size for all WBANs to be the same so that collision could be better avoided by picking the right value for  $K$ , where  $K$  is the number of time-slots to be made in the superframe, respectively, in the Latin rectangle. We illustrate our approach through a scenario of 3 coexisting

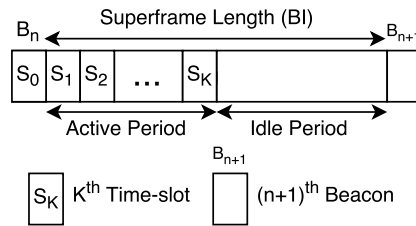


**Figure 5.1:** Superframe structure for DAIL

WBANs, where each circumference represents the interference range as shown in **Figure 5.2**. Furthermore, each WBAN is assigned  $M = 4$  channels and consists of  $L = 4$  sensors, in turn, each sensor is assigned a symbol from the set  $K = \{1,2,3,4\} \iff \{G,B,R,W\}$ . Here, we assume that each sensor requires only one time-slot to transmit its data in each su-

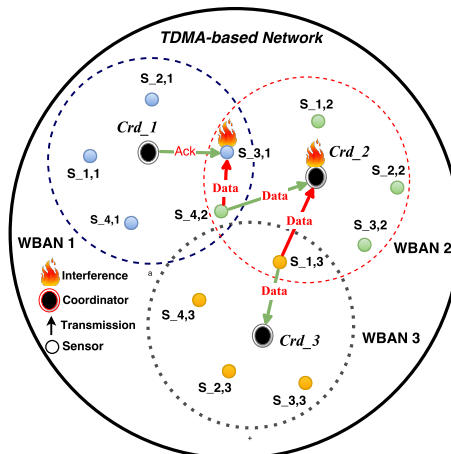


**Figure 5.2:** Collision scenarios at sensor- and coordinator-levels

perframe. Based on this scenario, any pair of sensors are interfering with each other, i.e., they transmit using the same channel at the same time, if both sensors are in the intersection of their corresponding interference ranges. However, as shown in **Figure 5.2**, 4<sup>th</sup> sensor of  $WBAN_1$  denoted by  $S_{1,4}$  and  $S_{2,4}$  are interfering, also,  $S_{3,1}$  and  $S_{2,3}$ . Therefore, in *DAIL*, each  $WBAN$  picks a distinct Latin rectangle from an orthogonal set as follows:  $WBAN_1$  picks E,  $WBAN_2$  picks F and  $WBAN_3$  picks J, where E and F are considered as in section 5.2.2. Assume 3 sensors,  $u$ ,  $v$  and  $w$  of  $WBAN_1$ ,  $WBAN_2$  and  $WBAN_3$  are, respectively, assigned symbols B, R and G in Latin rectangles E, F and J. Thus, the distinct positions of symbol B in E corresponds to the transmission pattern of  $u$  in  $WBAN_1$ 's superframe, similarly for  $v$  and  $w$  in  $WBAN_2$  and  $WBAN_3$ , respectively. However, B=2 in E, R=3 in F and G=1 in J, therefore, the transmission patterns for  $u$ ,  $v$  and  $w$  are, respectively, represented by B, R and G of the matrix shown in **Figure 5.3**. As clearly seen in this figure that  $u$ ,  $v$  and  $w$  neither share the same channel nor the same time-slot, i.e., no collision occurs at all.

		Time-slots			
		1	2	3	4
Channels	1	W	B	G	R
	2	B	G	R	W
	3	G	R	W	B
	4	R	W	B	G

**Figure 5.3:** A  $4 \times 4$  channel to time-slot assignment Latin square

### 5.3.3 *DAIL* Analysis

In this section, we opt to analyze the performance of *DAIL* mathematically. We consider a multichannel TDMA-based network, where superframes are constructed as an  $M \times K$  matrix, where within a superframe, each sensor may be assigned  $M$  time-slots to transmit its data according to a unique channel to time-slot assignment pattern. These patterns are generated from the orthogonal family of  $M \times K$  Latin rectangles. Basically, all sensors of a  $WBAN$  share one common  $M \times K$  Latin rectangle, where, the pattern of each sensor corresponds to a single symbol pattern in the Latin rectangle, as shown in **Figure 5.3**.

#### Interference Bound

In this subsection, we opt to determine the worst-case collision pattern for the individual sensor.

**Definition 5.5.** Let  $E$  and  $F$  be two orthogonal  $M \times K$  Latin rectangles. Symbol  $e$  from  $E$  is assigned to sensor  $u$ , and symbol  $f$  from  $F$  is assigned to sensor  $v$ . Then, there exists a collision at the  $j^{\text{th}}$  slot on  $i^{\text{th}}$  channel for  $u$  and  $v$ , if the ordering  $(e,f)$  of both rectangles appears at  $i^{\text{th}}$  row,  $j^{\text{th}}$  column, which means  $[E_{i,j}] = e$  and  $[F_{i,j}] = f$ .

**Theorem 5.2.** If two sensors are assigned two distinct symbols in the same Latin rectangle, there will be no collision among their transmissions. If they are assigned symbols from two distinct orthogonal Latin rectangles, then, they will face at most one collision in every superframe.

**Proof:** From the definition of Latin rectangles, because every symbol occurs exactly one time in each row and exactly one time in each column, any two time-slot assignment patterns constructed from the same Latin rectangle will not have any overlap in their patterns and so they will not have any collision with each other. Based on **Defintion 5.2**, hence, the ordering  $(e,f)$  for any pair of orthogonal Latin rectangles, where,  $e$  and  $f \in \{1,2,\dots, K\}$ , can only appear one time, which means that these sensors will only have one opportunity of collision.

**Theorem 5.3.** In a network of  $N$  WBANs, each sensor has a channel to time-slot transmission pattern corresponding to a symbol pattern chosen from one of the  $K^{\text{th}}$  set of orthogonal Latin rectangles. Let us consider a sensor denoted by  $S$  surrounded by maximum number of  $O$  WBANs, i.e.,  $O$  sensors from other WBANs, which means,  $O$  sensors may coexist in the communication range of  $S$ . Then,  $S$  may experience at most  $O$  collisions. Additionally, sensor  $S$  may face a minimal number of collisions which equal to  $\max(O-K+1,0)$ .

**Proof:** Based on **Theorem 5.2**, each neighboring sensor can create at most one collision to  $S$ . In the worst case, all  $O$  sensors are within the range of communication of  $S$ . The transmissions patterns of  $O$  sensors are constructed from Latin rectangles that are different from the Latin rectangle utilized by  $S$ . Subsequently, the maximum number of possible collisions experienced by  $S$  is  $O$ . Now, to count the minimal number of collisions for  $S$ , it is required to find the maximum number of sensors that construct their transmission patterns from the same Latin rectangle, which is  $K$ , i.e.,  $K$  sensors will have no collision according to **Theorem 5.2**. Also, **Theorem 5.2** proves that there exists at most one collision for each pair of sensors constructing their transmission patterns from two different orthogonal Latin rectangles. Therefore, each of the remaining sensors  $(O-K+1)$  will cause one collision to  $S$  because they belong to different orthogonal Latin rectangles. As a result, the minimum number of collisions for sensor  $S$  surrounded by  $O$  sensors is equal to  $\max((O-K+1),0)$ .

## Collision Probability

We consider a sensor  $S_i$  of  $WBAN_i$  is surrounded by  $O$  interfering sensors  $v_j$  of different coexisting  $WBAN_j$  in the vicinity, where  $j = 1, 2, \dots, O$  and  $i \neq j$ . For simplicity, we assume, each sensor transmits one data packet in each time-slot. However, sensor  $S_i$  successfully transmits its data packet in time-slot  $t$ , on channel  $h$  to the coordinator, iff, none of the  $O$  neighbors transmits its data packet using the same time-slot on the same channel as sensor  $S_i$ . Let  $X$  denotes the random variable representing the number of sensors that are transmitting their data packets in the same time-slot as sensor  $S_i$ , if  $x$  packets are transmitted in the the same time-slot as  $S_i$ . Then, the probability of event  $X$  is defined by Eq. 5.1 below.

$$Pr(X = x) = C_x^{O+1} \times \omega^x \times (1 - \omega)^{O-x} \times (\min(M, K) / K)^x \quad \forall x \leq O \quad (5.1)$$

Where  $\omega$  is the use factor, defined as the ratio of the time that a sensor is in use to the total time that it could be in use. Now, suppose  $Y$  sensors out of  $X$  sensors schedule their transmissions according to the same Latin rectangle as sensor  $S_i$ , i.e.  $y$  out of  $x$  sensors select symbol patterns from the same Latin rectangle as  $S_i$ .

$$Pr(Y = y | X = x) = \left( C_y^{K+1} \times C_{x-y}^{Z-K} \right) / C_x^{Z-1} \quad \forall x \leq O, \forall y \leq x \quad (5.2)$$

Where  $Z = K \times m$  is the total number of symbol patterns in the orthogonal Latin rectangles family. However, these  $Y$  sensors will not impose any collision with  $S_i$ 's transmission, since they ( $Y$  sensors) use the same Latin rectangle as  $S_i$ . On the other hand,  $X - Y$  sensors may collide with the transmission from sensor  $S_i$  to the coordinator on the same channel, then the conditional probability of transmission collision is denoted by ( $collTx$ ) and defined by Eq. 5.3 below.

$$\begin{aligned} Pr(collTx | Y = y \& X = x) &= 1 - Pr(succTx | Y = y \& X = x) \\ &= 1 - ((\min(M, K) - 1) / \min(M, K))^{x-y} \end{aligned} \quad (5.3)$$

Where  $\min(M, K)$  represents the number of transmission time-slots for each sensor in each superframe. Then, the probability of a successful data packet transmission from

sensor  $S_i$  to the coordinator is denoted by  $\lambda$  as follows:

$$\begin{aligned}
\lambda &= \sum_{x=0}^O \sum_{y=0}^x \Pr(Y = y, X = x) \times \Pr(\text{succTx} \mid Y = y \& X = x) \\
&= \sum_{x=0}^O \sum_{y=0}^x \Pr(Y = y \mid X = x) \times \Pr(X = x) \times \Pr(\text{succTx} \mid Y = y \& X = x) \\
&= \sum_{x=0}^O \sum_{y=0}^x (C_x^O C_y^{K-1} C_{x-y}^{Z-K}) / (C_x^{Z-1}) \times \omega^x \times (1 - \omega)^{O-x} \\
&\quad \times (\min(M, K) / K)^x \times ((\min(M, K) - 1) / \min(M, K))^{x-y}
\end{aligned} \tag{5.4}$$

### Throughput Analysis

Let the size of the orthogonal family of  $K^{\text{th}}$  order Latin squares is  $m = K-1$  and the transmission pattern of each sensor is determined by one of the  $K^2$  distinct symbol patterns in the  $K \times K$  Latin square. When  $K > M$ , each  $K \times K$  Latin square can be cut into  $M \times K$  Latin rectangle. To assure that every sensor has unique transmission pattern according to these Latin rectangles,  $(K \times m \geq N)$  must be satisfied, where  $N$  is the number of WBANs. Furthermore, it has been proven in **Theorem 5.2** that the number of collisions ( $\# \text{ colls}$ ) in each superframe for any two sensors is either one or zero. Assuming the maximum number of neighbors to  $S$  is still  $O$ , then, each sensor will be assigned  $\min(M, K)$  transmission time-slots in each superframe denoted by SF. We denote by TS the number of successful transmissions for each sensor,  $TS_{\min}$  and  $TS_{\max}$  are the lower and the upper bounds of TS, respectively, when **Eq. 5.5** holds, every sensor will have its throughput in **Eq. 5.7** and **Eq. 5.8** as follows:

$$K \geq TS_{\max} \geq TS \geq TS_{\min} > 0 \tag{5.5}$$

$$TS = \min(M, K) - (\# \text{ colls per SF}) \tag{5.6}$$

$$TS_{\max} = \begin{cases} K - \max(O - K + 1, 0) & \text{if } K \leq M \\ M - \max(O - K + 1, 0) & \text{if } K > M \end{cases} \tag{5.7}$$

$$TS_{\min} = \begin{cases} K - O & \text{if } K \leq M \\ M - O & \text{if } K > M \end{cases} \tag{5.8}$$

Therefore, to assure that every sensor has a minimal throughput,  $K$  should be greater than  $O$  when  $K \leq M$ , or  $M$  should be greater than  $O$  when  $K > M$ . In order to evaluate the performance of our approach, the best and the lowest throughput, respectively,

denoted by  $T_{max}$  and  $T_{min}$  are defined in [Eq. 5.9](#) and [Eq. 5.10](#).

**Definition 5.6.**  $T_{max}$  (resp.  $T_{min}$ ) is defined as the ratio of the maximal (resp. minimal) number of successful transmissions in each SF to its length denoted by FL

$$T_{max} = TS_{max}/FL, FL = K \quad (5.9)$$

$$T_{min} = T_{min} = TS_{min}/FL, FL = K \quad (5.10)$$

**Theorem 5.4.** For given  $O$ ,  $N$  and  $M$ , the maximal nonzero upper and lower bounds of throughput  $T$  are as follows:

$$1 \geq T \geq 1 - (O/M), \text{ if } K \leq M \quad (5.11)$$

$$M/\max(M, \lfloor N/m \rfloor) \geq T \geq (M - O)/\max(M, \lfloor N/m \rfloor) \text{ if } K > M \quad (5.12)$$

**Proof:** When  $K \leq M$ , based on [Eq. 5.9](#), the upper and lower bounds of  $T$  are as follows:

$$T_{max} = TS_{max}/FL = (K - \max(O + 1 - K, 0)) / K = 1 - (\max(O - K + 1, 0) / K) \quad (5.13)$$

$$T_{min} = TS_{min}/FL = (K - O) / K = 1 - O/K \quad (5.14)$$

We can deduce from [Eq. 5.13](#) and [Eq. 5.14](#) that the upper and lower bounds of  $T$  will increase with  $K$ . Thus, to ensure that the minimal throughput is greater than zero and every sensor has a unique transmission pattern, then, this inequality;  $O < K < \lfloor N/m \rfloor$  must be satisfied. Also, we can have,  $\max(O + 1 - K, 0) = 0$  and  $\lfloor N/m \rfloor \leq K \leq M$ . Therefore, when  $K = M$ , the maximal upper and lower bounds of the throughput are shown in [Eq. 5.15](#) and [Eq. 5.16](#) below.

$$T_{max} = 1 \text{ and } T_{min} = 1 - O/M \quad (5.15)$$

$$T_{min} = 1 - O/M \quad (5.16)$$

Similarly, if  $K > M$ , the bounds of  $T$  are shown in [Eq. 5.17](#) and [Eq. 5.18](#) below.

$$T_{max} = TS_{max}/FL = (M - \max(O + 1 - K, 0)) / K = M/K \quad (5.17)$$

$$T_{min} = TS_{min}/FL = (M - O) / K \quad (5.18)$$

However, these bounds decrease when  $K$  increases. So, when  $K > \lceil N/m \rceil$  and  $K > M$  are combined, then,  $K > \max(M, \lceil N/m \rceil)$  is true, and so the maximal upper and lower bounds of  $T$  are as in [Eq. 5.19](#) and [Eq. 5.20](#) below.

$$T_{max} = M / \max(M, \lceil N/m \rceil) \quad (5.19)$$

$$T_{min} = (M - O) / \max(M, \lceil N/m \rceil) \quad (5.20)$$

When  $K = \max(M, \lceil N/m \rceil)$ . In [Theorem 5.4](#), when  $M \geq K$  corresponds to the number of available channels is greater than the number of transmission time-slots assigned to a sensor in a WBAN, however, the minimal throughput  $T_{min}$  can be maximized when we choose  $K$  equals to the maximal number of available channels, which is limited to  $M$  in our case, and so,  $M < K$ . Therefore, the bounds of the throughput will be impacted by the size of the Latin rectangles family  $m$ .

### 5.3.4 DAIL Performance Evaluation

This section compares the performance of *DAIL* to that of competing approaches in the literature. In addition, analytical results that derive the collision probability and network throughput are validated by simulations. We have performed simulation experiments through Matlab, where the number of WBANs is varied. The locations of the individual WBANs change to mimic random mobility and consequently, the interference pattern varies. The following performance metrics are considered:

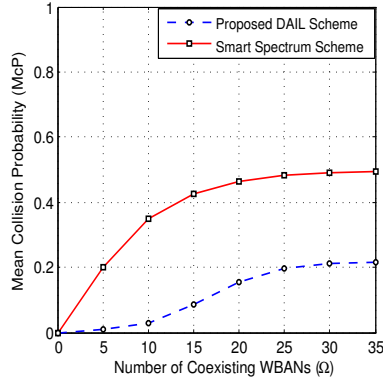
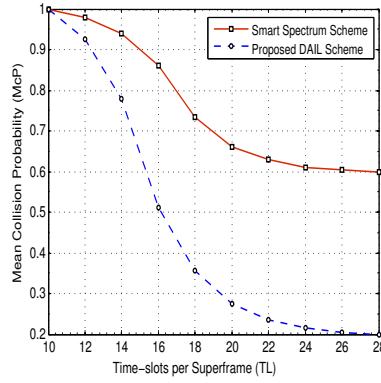
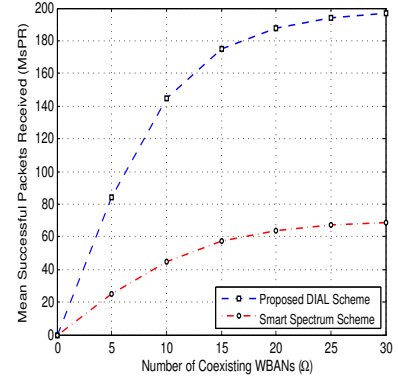
- *Collision probability (McP)* : reflects how often two transmissions of two distinct sensors of different WBANs collide.
- *Mean WBAN power consumption (mPC)* : is defined as the sum of the individual power consumed by the individual nodes due to the data packet collisions within a WBAN's superframe divided by the number of sensors in each WBAN.
- *Mean successful data packets received (MsPR)* : is the total number of packets that are successfully received at the coordinator from all sensors within its WBAN in one superframe divided by the sensor count in that WBAN. This metric is specific for *DAIL*.

We have conducted multiple simulation experiments to evaluate the performance of *DAIL* and compared it with that of the smart spectrum allocation scheme, denoted by *SMS* [39]. *SMS* assigns orthogonal channels to interfering sensors belonging to each pair of coexisting WBANs. The simulation parameters are provided in [Table 5.2](#).

The first experiment is geared for comparing the mean collision probability (*McP*)

**Table 5.2:** Simulation parameters - *DAIL*

	Exp. 1	Exp. 2	Exp. 3	Exp. 4
Sensor TxPower(dBm)	-10	-10	-10	-10
Number of <i>Crds</i> /WBAN	1	1	1	1
Number of Sensors/WBAN	12	12	12	12
Number of WBANs/Network	Var	30	Var	Var
Number of Time-slots/Superframe	12	12	12	12
Latin Rectangle Size	$16 \cdot 12$	$16 \cdot Var$	$16 \cdot 12$	$16 \cdot 12$

**Figure 5.4:** *McP* versus the number of coexisting WBANs ( $\Omega$ )**Figure 5.5:** *McP* versus the number of time-slots per superframe**Figure 5.6:** Mean successful packets received (*MsPR*) versus  $\Omega$ 

versus the number of coexisting WBANs ( $\Omega$ ) for *DAIL* and *SMS*. The results shown in **Figure 5.4** confirm the advantage of *DAIL* by achieving a much lower *McP* because of the combined channel and time-slot hopping. It is observed that *McP* of *DAIL* is very low due to large number of channel and time-slot combinations than WBANs count, and much larger *McP* because of the small number of channel and time-slot combinations than WBANs count. Meanwhile, in *SMS*, *McP* significantly increases because of the number of available channels is smaller than the number of interfering sensors. Whilst, *McP* significantly decreases for as long as the number of channels is larger than WBANs count.

The second experiment studies the effect of the number of time-slots per a superframe denoted by *TL* on *McP* for a network consisting of up to 30 WBANs. As can be clearly seen in **Figure 5.5**, *DAIL* always achieves lower collision probability than *SMS* for all *TL* values. In *DAIL*, *McP* significantly decreases as *TL* increases from 10 to 28, where increasing *TL* is similar to enlarging the size of the Latin rectangle. Therefore, a larger number of channel and time-slot combinations allows distinct sensors to not pick the same channel in the same time-slot, which decreases the chances of collisions among them. However, *SMS* depends only on the 16 available channels to mitigate interference, and the channel assigned to a sensor stays the same at all time. Thus, a high *McP* is expected due to the larger number of interfering sensors than the number of available channels. Moreover, a sensor has 16 choices in *SMS*, while it has  $16 \times framesize$  different

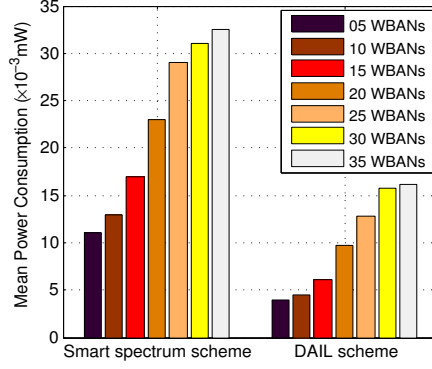


**Figure 5.7:** Mean power consumption ( $mPC$ ) versus  $\Omega$

choices in *DAIL* to mitigate the interference, which explains the large difference in  $M_{cP}$  amongst the two schemes.

In the third experiment, we compare the  $mPC$  of each *WBAN* versus  $\Omega$  for *DAIL* and *SMS*. The results plotted in **Figure 5.7** show that  $mPC$  for *DAIL* is always lower than that of *SMS* for all  $\Omega$  values. Such distinct performance for *DAIL* is mainly due to the reduced collisions that lead to fewer retransmissions and consequently lower power consumption, which is due to the larger number of channel and time-slot combinations than the interfering sensors. Meanwhile, in *SMS*,  $mPC$  is consistently high for large networks due to the collisions resulting from the large number of sensors that compete for the available channels (*16 channels*).

The fourth experiment studies the mean successful data packets received at each *WBAN*, denoted by  $M_{sPR}$ , versus  $\Omega$  for *DAIL* and *SMS*. **Figure 5.6** shows that *DAIL* always achieves higher  $M_{sPR}$  than *SMS* for all values of  $\Omega$ . Such performance improvement is mainly because of the reduced collisions, which boosts the number of data packets that are successfully received in a superframe. However, in *SMS*,  $M_{sPR}$  significantly increases as  $\Omega$  grows for as long as  $\Omega \leq 15$  due to the availability of a larger the number of channels than the number of interfering sensors, and the other way around because none of the channels is available to be assigned for an interfering sensor.

### ***DAIL* Summary**

*DAIL* is a channel allocation scheme that assigns channel and time-slot combinations to *WBAN* sensors in order to diminish the probability of interference among non-cooperative *WBANs*. *DAIL* involves overhead in terms of transmission delay due to the frequent channel hopping, nonetheless, it drains the power resource of the *WBANs* when some of their corresponding sensors do not experience any collision. For example, as an estimate of power cost of a *WBAN* consisting of up to  $L$  sensors,  $L < K$ , is  $L \times HE$ , where  $HE$  is the power consumption resulting from a channel hopping in each superframe.

Therefore, the mean power cost per sensor is defined by Eq. 5.21 below.

$$\text{meanEC} = \frac{L \times HE}{K} \quad (5.21)$$

More specifically, *DAIL* imposes on each *WBAN*'s sensor to hop among the available channels whether that sensor experiences collision or not. Although, interference-free sensors do not need to hop among the channels and hence, the power is wasted at both sensor- and *WBAN*-levels. Another shortcoming in *DAIL* is that no more than 16 transmissions can be scheduled and this limits the number of transmitting sensors, i.e., if more than 16 *WBANs* coexist, then collisions may arise. To overcome such issues in *DAIL*, we propose another distributed scheme, namely, *CHIM*, inspired by *DAIL*, to lower the number of collisions and overhead as well as to save power of the low-density *WBANs*.

## 5.4 Interference Mitigation Using Predictable Channel Hopping - *CHIM*

Like *DAIL*, *CHIM* is completely distributed that enables predictable channel hopping using Latin rectangles in order to avoid interference among non-cooperative *WBANs*. However, *CHIM* adopts exactly the same system model like *DAIL* and does not require any inter-*WBAN* coordination. *CHIM* suits the low-density of *WBANs* to save the power resource at both sensor- and *WBAN*-levels. Basically, *CHIM* enables only sensors that experience collisions to hop among backup channels, each in its allocated backup time-slot. *CHIM* imposes less overhead because only sensors that experience collisions are required to use their pre-computed transmission schedules, i.e., a combination of a backup channel and a time-slot. To mitigate interference, *CHIM* exploits the availability of multiple channels to assign each *WBAN* a distinct default channel and in the case of interference, it allows the individual interfering sensors to hop among the remaining channels in a pattern that is predictable within a *WBAN* and random to the other *WBANs*. To achieve that, *CHIM* extends the size of the superframe through the addition of extra interference mitigation backup time-slots and employs Latin rectangles as the underlying scheme for channel allocation to sensors within each *WBAN*.

### 5.4.1 *CHIM* Superframe

Like *DAIL*, in *CHIM*, each *WBAN*'s superframe is composed of successive active and inactive frames as shown in Figure 5.8. However, the active frame is further divided into

two parts of equal size, the *TDMA* data-collection part and the interference mitigation backup (*IMB*) interference mitigation part, each is of  $K$  time-slots length. In the *TDMA*

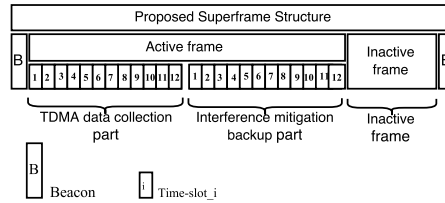


Figure 5.8: Superframe structure for *CHIM*

part, each sensor transmits its data packet in its assigned time-slot to the coordinator through the default channel. However, in the *IMB* interference mitigation part, each interfering sensor retransmits the same data packet in its allocated backup time-slot to the coordinator through a priori-agreed upon the channel. In interference-free conditions, the coordinator stays tuned to the default channel. If communication with a specific sensor  $S_i$  fails during  $S_i$ 's designated time-slot, the coordinator will tune to the  $S_i$ 's backup channel during  $S_i$ 's time-slot in the *IMB* interference mitigation part of the active frame. Whereas, during the inactive frame, all the sensors sleep and hence, the coordinators may transmit all data to a command center.

We still need to determine the length of each frame. Like *DAIL*, the length of *TDMA* data collection part is determined based on the highest sampling rate and the sum of number of samples for all sensors in a time period. However, *CHIM* requires the *TDMA* data collection part for all *WBANs* to be the same length so that collision could be better avoided by unifying the frame size across the various *WBANs* and leveraging the properties of Latin rectangles. Therefore, in *CHIM*, the number of time-slots to be made in the active frame is  $2 \times K$  time-slots, i.e.,  $K$  time-slots are for the *TDMA* data-collection part and  $K$  time-slots are for the *IMB* interference mitigation backup part. Whilst, the inactive frame directly follows the active frame and whose length depends on the underlying duty cycle scheme of the sensors.

### 5.4.2 *CHIM* Algorithm

At the network setup time, each *WBAN*'s coordinator will randomly pick a *default operation channel* and a  $M \times K$  *Latin rectangle* from an orthogonal set. Initially, the coordinator instructs all sensors within its *WBAN* to use the same *default channel* along the whole *TDMA* part. Meantime, the coordinator assigns a *single symbol* from the symbol set  $\{1, 2, \dots, K\}$  to each sensor within its *WBAN*, where the position hopping of each symbol in the Latin rectangle relates a *single interference mitigation channel* and a *unique backup*

*time-slot*. Thereby, each coordinator determines the combination of a *single interference mitigation channel* and a *unique backup time-slot* for each sensor to eventually use in the *IMB* part for interference mitigation. Subsequently, a coordinator informs each sensor within its *WBAN* about its allocated: 1) *interference mitigation channel* and, 2) *backup time-slot* within the *IMB* part of the superframe. Each coordinator reports this information to its sensors through beacon broadcast.

As pointed out, *CHIM* depends on both acknowledgement and time-outs to detect collision/interference at both *sensor-* and *coordinator-* levels. In the *TDMA* active part of a superframe, each sensor transmits a data packet in its assigned time-slot on the default operation channel; it then sets a timer and waits for an acknowledgment packet. If the sensor receives the acknowledgment packet from the corresponding coordinator, it considers the transmission successful, and hence it sleeps until the next superframe. In this case, the transmitting sensor does not need to switch to its allocated interference mitigation channel and use its dedicated backup time-slot in the *IMB* part for interference mitigation.

However, if the transmitting sensor does not successfully receive the acknowledgment within the time-out period, it assumes failed transmission due to interference and subsequently, it applies the interference mitigation procedure. Basically, the sensor waits until the *TDMA* active part completes and then switches its channel to the allocated interference mitigation channel at the beginning of its allocated backup time-slot and retransmits its data packet. In fact, the packet delivery failure is due to data or acknowledgment packets collisions at the *coordinator-* or *sensor-* levels, respectively, i.e., 1) the desired transmitted data packet is lost at the coordinator due to its interference from sensors in other *WBANs* at the same time or, 2) the acknowledgment packet of the desired coordinator is lost at the desired sensor due to the same reason. Therefore, depending on the acknowledgment packets and time-out period, both interfering sensors and coordinator address the collision problem in the same manner, each from its perspective. **Algorithm 8** summarizes the proposed *CHIM* scheme.

### 5.4.3 *CHIM* Analysis

In this section we opt to analytically assess the effectiveness of *CHIM* in terms of reducing the probability of collisions.

#### *TDMA* Collision Probability

In this section, we derive the probability for a designated sensor that experiences collision within the *TDMA* data collection part of the active frame. Let us consider a

sensor  $S_i$  of  $WBAN_i$  that is surrounded by  $P$  different sensors  $S_j$ , where  $i \neq j$ . For

---

**Algorithm 8** CHIM Scheme
 

---

**Require:**  $N$  WBANs,  $K$  Sensors/WBAN, Orthogonal Latin rectangle OLR

```

1: Stage 1: Network Setup
2: for  $i = 1$  to  $N$  do
3:    $Crd_i$  randomly picks a single  $DFC_i$  &  $OLR_i$  for its  $WBAN_i$ ;
4:   for  $k = 1$  to  $K$  do
5:      $Crd_i$  allocates  $BKC_{k,i}$  &  $BKTS_{k,i}$  to  $S_{k,i}$  from  $OLR_i$ ;
6:   end for
7: end for
8: Stage 2: Sensor-level Interference Mitigation
9: for  $i = 1$  to  $N$  do
10:  for  $k = 1$  to  $K$  do
11:     $S_{k,i}$  transmits  $Pkt_{k,i}$  in  $TS_{k,i}$  to  $Crd_i$  on  $DFC_i$  in  $TDMA_i$ ;
12:    if  $Ack_{k,i}$  is successfully received by  $S_{k,i}$  on  $DFC_i$  then
13:       $S_{k,i}$  switches to SLEEP mode until the next superframe;
14:    else
15:       $S_{k,i}$  waits its designated  $BKTS_{k,i}$  within  $IMB_i$  part;
16:       $S_{k,i}$  retransmits  $Pkt_{k,i}$  in  $BKTS_{k,i}$  to  $Crd_i$  on  $BKC_{k,i}$ ;
17:    end if
18:  end for
19: end for
20: Stage 3: Coordinator-level Interference Mitigation
21: for  $i = 1$  to  $N$  do
22:  for  $k = 1$  to  $K$  do
23:    if  $Crd_i$  successfully received  $Pkt_{k,i}$  in  $TS_{k,i}$  on  $DFC_i$  then
24:       $Crd_i$  transmits  $Ack_{k,i}$  in  $TS_{k,i}$  to  $S_{k,i}$  on  $DFC_i$ ;
25:    else
26:       $Crd_i$  will tune to  $BKC_{k,i}$  to receive from  $S_{k,i}$  in  $IMB_i$ ;
27:       $Crd_i$  receives  $Pkt_{k,i}$  in  $S_{k,i}$ 's  $BKTS_{k,i}$  on  $BKC_{k,i}$ ;
28:    end if
29:  end for
30: end for=0

```

---

simplicity, we assume that  $S_i$  transmits one data packet in a single time-slot within the TDMA data collection part.  $S_i$  successfully transmits its data packet on the default channel to the coordinator, *iff*, none of the  $P$  sensors transmits in the same time-slot using  $WBAN_i$  default channel. Now, let  $X$  denote the random variable representing the number of sensors that are transmitting their data packets in the same time-slot as  $S_i$ , if  $x$  sensors transmit in the same time-slot of  $S_i$ , the probability of event  $X=x$  is denoted by  $Pr(X=x)$  and defined by Eq. 5.22 below.

$$Pr(X = x) = C_x^P \alpha^x (1 - \alpha)^{P-x} (\min(M, K) / K)^x, x \leq P \quad (5.22)$$

Where  $\alpha$  denotes the probability for a particular sensor  $S_j$  of  $WBAN_j$  to exist within the communication range of  $WBAN_i$ . Now, suppose  $Y$  out of  $X$  sensors schedule their transmissions according to Latin rectangles that are orthogonal to  $WBAN_i$ 's Latin rectangle,

i.e.,  $y$  out of  $x$  sensors select symbol patterns from other orthogonal Latin rectangles to  $S_i$ 's rectangle. Thus, the probability of  $y$  sensors will not introduce any collision to  $S_i$ 's transmission is defined by Eq. 5.23 below.

$$Pr(Y = y | X = x) = \left( C_y^K C_{x-y}^{Z-K} \right) / C_x^Z, \quad x \leq P \ \& \ y \leq x \quad (5.23)$$

Where  $Z = K \times m$  is the total number of symbol patterns in the orthogonal Latin rectangles family. However,  $X-Y$  is a random variable representing the number of sensors that may collide with  $S_i$ 's transmission on the same channel; thus the probability that  $S_i$ 's transmission experiences collision is denoted by ( $collTx$ ) and defined by Eq. 5.24 below.

$$\begin{aligned} Q &= Pr(collTx | Y = y, X = x) = 1 - Pr(succTx | Y = y, X = x) \\ &= 1 - ((\min(M, K) - 1) / \min(M, K))^{x-y} = 1 - (1 - 1 / \min(M, K))^{x-y} \end{aligned} \quad (5.24)$$

Where  $Q$  represents the probability that a sensor  $S_i$  faces collision in one of its assigned time-slots and  $\min(M, K)$  represents all possible transmission time-slots for each  $S_i$  within the TDMA data collection part of the active frame. Thus, we depend on  $Q$  to determine the whole number of sensors, denoted by  $W$ , that face collisions within the TDMA data collection part, where each sensor  $S_i \in W$  will use its designated backup channel and time-slot within the IMB interference mitigation part. Accordingly, we determine the new set of backup sensors that face collisions in the IMB interference mitigation part in the following subsection .

### IMB Collision Probability

In this subsection, we determine the probability of each backup sensor  $S_i$  that faces collision in the IMB interference mitigation part, when it uses its designated backup channel and time-slot. Let  $T_{imb}$  denote the number of interfering sensors that collide both in the TDMA data collection and the IMB interference mitigation parts, where  $T_{imb}$  follows binomial distribution. If  $t$  sensors of a particular WBAN face collision in the IMB interference mitigation part, then the probability of event  $T_{imb} = t$  is denoted by  $Pr(T_{imb} = t)$  and defined by Eq. 5.25 below.

$$Pr(T_{imb} = t) = C_t^K (Q^2)^t (1 - Q^2)^{K-t}, \quad t \leq K \quad (5.25)$$

And  $Q^2$  is due to the 2-stage collision, i.e., the first collision happens in the TDMA data collection part and the second happens in the IMB interference mitigation part.

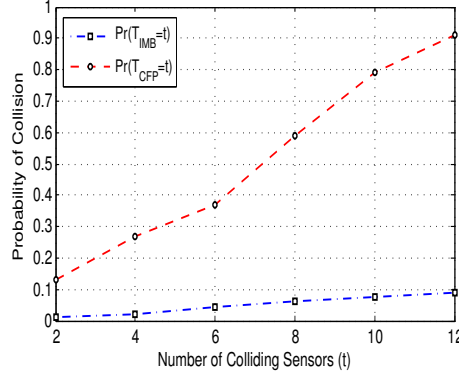


**Figure 5.9:** Mean collision probability versus number (#) of colliding sensors

Substituting  $Q$  of Eq. 5.24 in Eq. 5.26.

$$\Pr(T_{imb} = t) = C_t^K (Q^2)^t (1 - Q^2)^{K-t}, t \leq K \quad (5.26)$$

$$\begin{aligned} \Pr(T_{imb} = t) &= C_t^K \times (Q^2)^t (1 - Q^2)^{K-t}, t \leq K = C_t^K \times (1 - 1/\min(M, K))^{(x-y)(K-t)} \\ &\times (2 - (1 - 1/\min(M, K))^{x-y})^{K-t} \times (1 - (1 - 1/\min(M, K))^{x-y})^{2t} \end{aligned} \quad (5.27)$$

As a baseline for comparison, *ZigBee* standard [23] shows that the active period of the superframe can be divided into two parts, *TDMA ZigBee* part and contention free period part (*CFP*), where some sensors may require additional guaranteed time-slots (*GTSS*) in the *CFP* to avoid collisions have been experienced in the *TDMA ZigBee* part and complete their transmissions. However, these sensors use the same channel to transmit their pending data.

**Lemma 5.1.** *If  $t$  sensors collide in the IMB interference mitigation part, i.e.,  $\Pr(T_{imb} = t)$ , then, the probability of these sensors collide in the CFP is  $\Pr(T_{cfp} = t) = \Pr(T_{imb} = t) \times (\min(M, K))^t$*

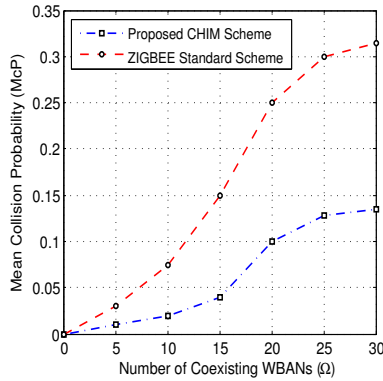
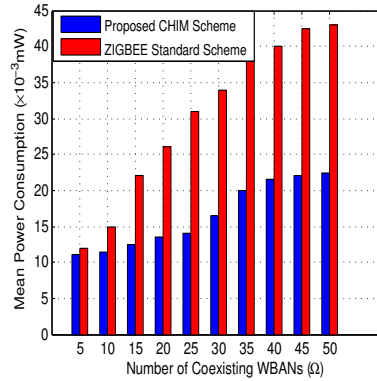
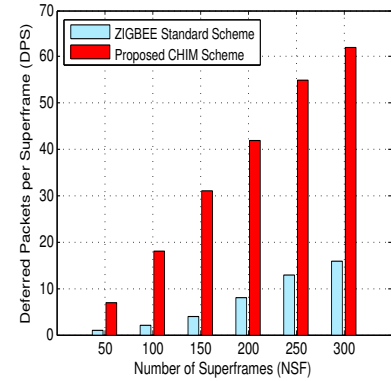
**Proof:** *If each WBAN has a  $M \times K$  Latin rectangle and  $t$  sensors may face collision in the IMB interference mitigation part, then, each sensor may have the chance to pick  $\min(M, K)$  possible backup channel to time-slot combinations for its transmission and hence, for  $t < K$  sensors, there are  $(\min(M, K))^t$  possible combinations. However, in the CFP, there is one and only one channel used by all sensors, therefore each sensor has the same channel for its transmission. Thus, in CHIM, the probability of collisions for  $t$  sensors will be reduced by  $(\min(M, K))^t$  and therefore,  $\Pr(T_{imb} = t) = \frac{\Pr(T_{cfp} = t)}{(\min(M, K))^t}$ . For illustration, see Figure 5.9.*

#### 5.4.4 CHIM Performance Evaluation

This section evaluates the performance of *CHIM* through multiple experiments and compares it to that of other competing approaches in the literature. Unlike *DAIL*, we

**Table 5.3:** Simulation parameters - CHIM

Parameter name	Value
SensorTxPower(dBm)	-10
Sensors/WBAN	20
WBANs/Network	Variable
Time-slots/TDMA CHIM part	20
Time-slots/IMB CHIM part	20
Time-slots/TDMA ZigBee part	20
Time-slots/CFP ZigBee part	20
Latin Rectangle Size	$16 \times 20$

**Figure 5.10:** Mean collision probability ( $McP$ ) versus  $\Omega$  for CHIM & ZIGBEE**Figure 5.11:** Mean power consumption ( $mPC$ ) versus  $\Omega$  for CHIM & ZIGBEE**Figure 5.12:** DPS versus # of TX superframes for CHIM & ZIGBEE

compare the performance of CHIM with ZigBee standard [23] since it resembles CHIM in terms of using one channel for intra-WBAN communication. The ZigBee standard assigns guaranteed time-slots (GTSs) in the contention free period (CFP) to sensors that have experienced interference in the TDMA period of the superframe. In addition, the analytical results are validated by extensive simulations. Like DAIL, the locations of the individual WBANs change to mimic random mobility and consequently, the interference pattern varies. The relevant simulation parameters are provided in Table 5.3, and the following performance metrics are considered:

- *Communication failure probability (CFP)*: is the frequency that two distinct sensors of different WBANs when both sensors are assigned the same channel in the same time, and these sensors are in the communication range of each other.
- *Mean of deferred data packets (DPS)*: This metric is applied for CHIM only since it provisions backup time-slots and reports the average number of transmissions that are made in backup time-slots per superframe.

The effect of the number of coexisting WBANs ( $\Omega$ ) on  $McP$ , which is defined as in Section 5.3.4, for CHIM and ZigBee is reported in Figure 5.10. As can be clearly seen in the figure, CHIM always provides a much lower  $McP$  because of the channel hopping. It is observed from this figure that for CHIM,  $McP$  is very low because of the larger number of channel hopping choices in the IMB frame than the interfering

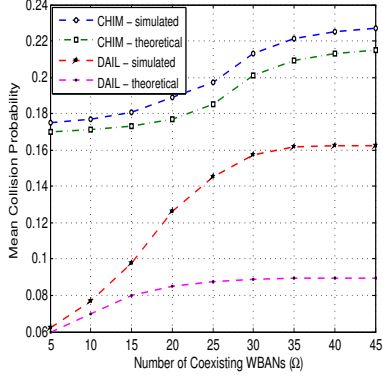
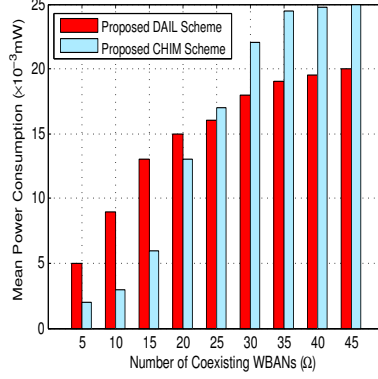
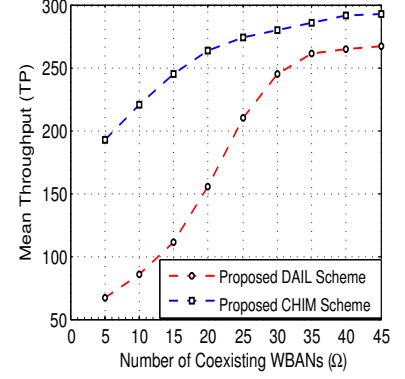
sensors. Whilst,  $McP$  significantly increases because of the larger number of sensors than the number of available channels. When  $\Omega$  exceeds 25,  $McP$  increases and eventually stabilizes, which is due to the fact that all the TDMA and backup time-slots/channels are completely committed, and any competing sensor that has data to transmit will face the collision. In *ZigBee*,  $McP$  slightly increases when the number of interfering sensors and the number of available GTSs are similar. Then,  $McP$  significantly increases due to the growth in the number of interfering sensors, and it stabilizes when the number of interfering sensors exceeds the number of available GTSs.

**Figure 5.11** shows the mean power consumption ( $mPC$ ) of a WBAN versus the number of coexisting WBANs ( $\Omega$ ) for *CHIM* and *ZigBee*. As evident from **Figure 5.11**,  $mPC$  for *CHIM* is always lower than that of *ZigBee* for all values of  $\Omega$ . Such distinct performance for *CHIM* is mainly due to the reduced collisions that lead to fewer retransmissions and consequently lower  $mPC$ . For *CHIM*, the figure shows a trend that is consistent with **Figure 5.10**. Basically,  $mPC$  slightly increases when there is a larger number of channel hopping possibilities than the interfering sensors which lowers the number of collisions among sensors and consequently  $mPC$ . When  $\Omega$  exceeds 40,  $mPC$  increases slightly to stabilize due to the limited availability of the backup channels/time-slots. However, in *ZigBee*,  $mPC$  slightly increases because of the number of interfering sensors approaches the number of available GTSs. When  $\Omega$  grows,  $mPC$  significantly increases due to the growth in the number of interfering sensors, and it stabilizes when  $\Omega$  exceeds 45 due to the larger number of the interfering sensors than the available GTSs.

**Figure 5.12** compares the mean number of deferred data packets ( $DPS$ ) for *CHIM* and *ZigBee* when 20 WBANs coexist, while varying the number of transmitted superframes. The figure shows that  $DPS$  for *CHIM* is always lower than that of *ZigBee* which can be attributed to the reduced medium access contention that leads to fewer number of deferred data packets and consequently lower transmission delay, in consequence, the throughput is increased.  $DPS$  for *ZigBee* is higher than that of *CHIM* due to the usage of one instead of 16 channels and hence the number of competing sensors to the available GTSs is large enough, which leads to higher number of deferred data packets and consequently the throughput is degraded.

**Table 5.4:** Simulation parameters - *DAIL* & *CHIM*

	<i>DAIL</i>	<i>CHIM</i>
Sensor TxPower(dBm)	-10	-10
# Coordinators/WBAN	1	1
# Sensors/WBAN	20	20
# WBANs/Network	Var	Var
# Time-slots/Superframe	40	40
Latin Rectangle Size	$16 \times 20$	$16 \times 20$

**Figure 5.13:** *McP* versus  $\Omega$  for *DAIL* and *CHIM***Figure 5.14:** *mPC* versus  $\Omega$  for *DAIL* and *CHIM***Figure 5.15:** Mean *TP* versus  $\Omega$  for *DAIL* and *CHIM*

## 5.5 Performance Evaluation

### 5.5.1 Comparing *DAIL* & *CHIM*

In this section, we have conducted extensive simulation experiments to compare the performance of *DAIL* and *CHIM*. We have studied the effect of the number of *WBANs* on collision and communication failure probabilities of sensor transmission, *WBAN* power consumption and throughput. The simulation parameters for both *DAIL* and *CHIM* are provided in **Table 5.4**. The theoretical and simulated mean collision probability (*McP*) versus  $\Omega$  for *DAIL* and *CHIM* are compared in **Figure 5.13**. As seen in the figure, for both *DAIL* and *CHIM*, the simulated *McP* is always higher than the theoretical *McP* for all values of  $\Omega$ . This is because  $\Omega$  is made variable in the simulation setup, while a constant in the theoretical study. As seen in the figure, *DAIL* always provides a lower *McP* than that of *CHIM* for all values of  $\Omega$ . Also, *McP* of *DAIL* significantly increases due to the growth in the number of sensors and it slightly increases when  $\Omega$  exceeds 25 until it eventually stabilizes due to the limited availability of orthogonal Latin rectangles. However, *McP* of *CHIM* is low due to the availability of sufficient number of distinct channels, and it significantly increases when  $\Omega$  exceeds 15 until it eventually stabilizes due to the single channel used in the *TDMA* frame and the limited availability of orthogonal Latin rectangles and hence, the number of collisions is larger than the number of available backup time-slots/channels. Therefore, from a design point of view, *DAIL*

is consistently better than *CHIM* in terms of collision probability.

The mean power consumption (*mPC*) versus  $\Omega$  for *DAIL* and *CHIM* are compared. **Figure 5.14** shows that *mPC* for *DAIL* is larger than for *CHIM* when  $\Omega \leq 20$  because all sensors in *DAIL* need to hop among the channels, each within its assigned time-slot regardless of there is interference or not, while, in *CHIM*, a sensor only switches the channel when it experiences an interference. When  $\Omega$  exceeds 20, *mPC* for *CHIM* is higher than that of *DAIL* because of the increased number of collisions (and consequently retransmissions) experienced due to the limited availability of the channels. In *DAIL*, the power consumption is accumulated from the power consumed due to the high frequency of channel switching that results from the frequent channel hopping [23]. Therefore, from power consumption point of view, *CHIM* suits the low-density of *WBANs*, whilst, *DAIL* suits the high-density of *WBANs*.

The throughput (*TP*) for *DAIL* and *CHIM* is reported in **Figure 5.15** as a function of  $\Omega$ . **Figure 5.15** shows that *CHIM* always achieves higher *TP* than *DAIL* for all values of  $\Omega$ . Such high throughput is mainly because of the reduced collisions and availability of backup time-slots, which boosts the number of data packets that are successfully received in a superframe. When  $\Omega$  exceeds 20, *TP* of *CHIM* eventually stabilizes due to the high communication failure probability and the limited availability of orthogonal Latin rectangles, which degrade the effectiveness of the backup time-slots/channels. However, *DAIL* always achieves lower *TP* than *CHIM* for all values of  $\Omega$  due to the absence of backup time-slots/channels and the limited availability of orthogonal Latin rectangles which make the probability of multiple sensors pick the same channel in the same time is low. The mean communication failure probability *CFP* versus  $\Omega$  for *DAIL* and *CHIM* are compared in **Figure 5.16**. As seen in the figure, *CHIM* and *DAIL* yield similar low *CFP* when  $\Omega \leq 15$  due to the availability of channel choices and backup time-slots/channels more than the number of interfering sensors. When  $\Omega$  exceeds 15, the *CFP* of *DAIL* grows significantly until it eventually stabilizes due to the limited availability of orthogonal Latin rectangles. However, when  $\Omega$  exceeds 15, *CFP* of *CHIM* significantly increases until it eventually stabilizes due to the high communication failure probability and the limited availability of orthogonal Latin rectangles.

### 5.5.2 Comparing *CHIM* & *DAIL* & *SMS*

The mean collision probability (*McP*) versus  $\Omega$  for *DAIL*, *CHIM* and *SMS* are compared in **Figure 5.17**. As seen in the figure, for both *DAIL* and *CHIM*, the *McP* is always lower than the *McP* of *SMS* for all values of  $\Omega$  because of the available large number

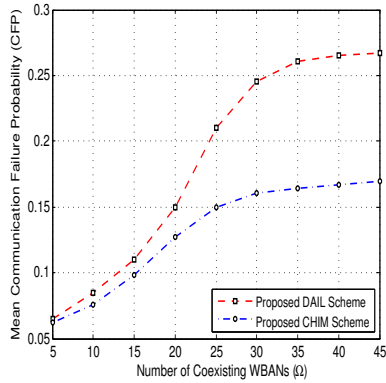


**Figure 5.16:** CFP versus  $\Omega$  for CHIM & DAIL

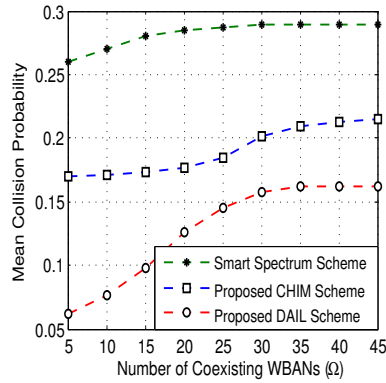


**Figure 5.17:** McP versus  $\Omega$  for CHIM & DAIL & SMS

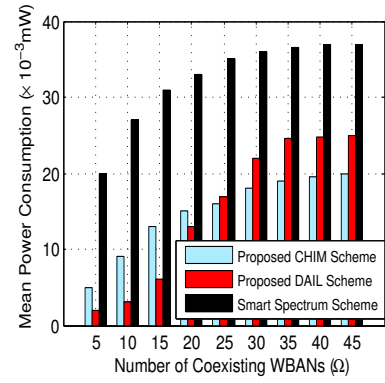


**Figure 5.18:** mPC versus  $\Omega$  for CHIM & DAIL & SMS

of channel and time-slot combinations and the backup time-slots. This large number of combinations reduces the chances of collisions among WBANs. However, SMS depends only on the 16 available channels to mitigate interference, and the channel assigned to a sensor stays the same at all time. Thus, a high  $McP$  is expected due to the larger number of interfering sensors than the number of available channels. Moreover, a sensor has 16 choices in SMS, while it has  $16 \times \text{framesize}$  different choices in our approach to mitigate the interference, which explains the large difference in  $McP$  between our approach and SMS. The mean power consumption ( $mPC$ ) of each WBAN versus  $\Omega$  for DAIL, CHIM and SMS are compared in **Figure 5.18**. As seen in the figure, for both DAIL and CHIM, the  $mPC$  is always lower than that of SMS for all  $\Omega$  values. Both DAIL and CHIM expose such low  $mPC$  because of the reduction in the number of collisions which lead to a fewer number of retransmissions and hence high energy savings. Meanwhile, in SMS,  $mPC$  is consistently high due to the collisions resulting from a large number of sensors that compete for the 16 channels and hence the power consumption is increased accordingly.

# Chapter 6

## Interference Mitigation in WBANs with IoT

### Contents

---

<b>6.1</b>	<b>Introduction</b>	<b>99</b>
6.1.1	<i>IoT</i> Communication Technologies	100
6.1.2	Problem Statement	101
6.1.3	Contribution	102
<b>6.2</b>	<b>Related Work</b>	<b>103</b>
<b>6.3</b>	<b>System Model and Preliminaries</b>	<b>104</b>
6.3.1	Bluetooth Low Energy	104
6.3.2	System Model and Assumptions	104
<b>6.4</b>	<b>Channel Selection Approach for Interference Mitigation - (CSIM)</b>	<b>105</b>
6.4.1	CSIM Algorithm	105
6.4.2	Channel Selection	107
6.4.3	Channel Stability	107
6.4.4	Superframe Structure	109
<b>6.5</b>	<b>Performance Evaluation</b>	<b>110</b>
<b>6.6</b>	<b>Conclusions</b>	<b>113</b>

---

### 6.1 Introduction

The massive growth in wireless devices and the push for interconnecting these devices to form an Internet of Things (*IoT*) can be challenging for *WBANs*. An *IoT* is a



**Figure 6.1:** The overall picture of IoT [13]

short-range wireless network of interconnected devices, e.g., *WiFi*, *ZigBee*, *RFIDs*, *tags*, *sensors*, *PDA*s, *smartphones*, etc, that could sense, process and communicate information. The *IoT* smart devices and objects are expected to reach 212 billion entities deployed globally by the end of 2020 [111]. Within an *IoT*, various types of wireless networks are required to facilitate the exchange of application-dependant data among their heterogeneous wireless devices. However, such diversity could give rise to coexistence issues among these networks, a challenge that limits the large-scale deployment of the *IoT*. Therefore, new protocols are required for robust communication among its heterogeneous devices to deliver high quality low-cost services [13, 111, 112, 113].

Example applications of *IoT* are healthcare, smart city, environment monitoring, transportation and industrial automation, etc., as illustrated in **Figure 6.1**. This figure illustrates the overall concept of the *IoT* in which every domain specific application is interacting with domain independent services, whereas in each domain sensors and actuators communicate directly with each other. The realization of the vision of the *IoT* is a difficult task due to the many challenges that need to be addressed [13, 113, 114]. Such challenges are related to the reliable operation and the desired performance of the *IoT* system, service availability at any time and anywhere, mobility support without service interruption, management of heterogeneous platforms and interoperability among them, scalability without negatively affecting the existing services and the security as well as the privacy of the *IoT* users.

### 6.1.1 *IoT* Communication Technologies

The *IoT* employs heterogeneous communication technologies that interconnect various heterogeneous devices to deliver high-quality services. Basically, the *IoT* devices should properly operate using low power in the presence of lossy and noisy communication links [13, 113, 114]. The communication technologies used for the *IoT* include

IEEE 802.15.6, IEEE 802.15.4 (ZigBee), WiFi, RFID, Bluetooth, Bluetooth Low Energy which are defined in **Chapter 1.1.2 Intra-WBAN Communication**. In addition *Near Field Communication (NFC)*, *Ultra Wide Band (UWB)*, and *Long Term Evolution* are defined as follows:

- **RFID** is a radio technology that provides object's identity. The RFID reader may operate within a range of 10 cm up to 200 m, and at different bands such as 120–150 kHz (10cm), 13.56 MHz (10cm - 1m), 433 MHz (1 - 100m), 865-868 MHz/902-928 MHz (1 - 12m), 2450-5800 MHz (1 - 2m) and 3.1–10 GHz (up to 200m).
- **Near Field Communication (NFC)** is a short-range communication technology that operates at high frequency band at 13.56 MHz with a range that may reach up to 10 cm.
- **Ultra Wide Band (UWB)** is a radio technology that can use a very low energy level for short-range, high-bandwidth communications over a large portion of the radio spectrum (>500 MHz) within a low range coverage area.
- **Long Term Evolution** is a wireless communication standard for high-speed data transfer between mobile phones based on GSM/UMTS network technologies and can cover fast-travelling devices and provide multicasting/broadcasting services. IoT devices based on these standards can communicate over cellular networks and support data rates ranging from 9.6 Kb/s (2G) to 100 Mb/s (4G).
- **Long Term Evolution Advanced (LTA-A)** is an improved version of LTE including bandwidth extension which supports up to 100 MHz with extended coverage, higher throughput and lower latencies.

### 6.1.2 Problem Statement

Basically, the *IEEE 802.15.6 standard* [2], e.g., WBANs utilizes a narrower bandwidth than wireless networks, e.g., *IEEE 802.11* [115]. However, *IEEE 802.11*-based wireless devices may use multiple channels that cover the whole license-free 2.4 GHz ISM band, so there could be overlapping channel covering the *IEEE 802.15.6* based network and thus create collisions between *IEEE 802.15.6* and these devices. In addition, the *IEEE 802.11* based wireless devices may transmit at a high power level and thus relatively distant coexisting *IEEE 802.15.6* devices may still suffer interference. Thus, the pervasive growth in wireless devices and the push for interconnecting them can be challenging for WBANs due to their simple and energy-constrained nature. Basically, a WBAN may suffer interference not only because of the presence of other WBANs but also from wireless devices within the general IoT simultaneously operating on the same channel. Consequently, the co-channel interference may arise due to the collisions amongst the

concurrent transmissions made by sensors in different WBANs collocated in an IoT and hence such potential interference can be detrimental to the operation of WBANs. Therefore, robust communication is necessary among the individual devices of the collocated networks in an IoT.

### 6.1.3 Contribution

In this chapter, we propose a distributed protocol to enable WBAN operation in an IoT and leverage the emerging Bluetooth Low Energy (BLE) technology to facilitate the interference detection and mitigation. The role of BLE is to inform WBANs about the frequency of channels being used in the vicinity. Thus, we integrate a BLE transceiver and a Cognitive Radio (CR) module within each WBAN's coordinator node (Crd). When experiencing high interference, the WBAN Crd will be notified by the BLE device to use the CR module for selecting a different channel. When engaged, the CR selects an Interference Mitigation Channel (IMC) for the WBAN. To mitigate the interference, our approach opts to extend the active period of the superframe to involve not only a TDMA frame, but also a Flexible Channel Selection (FCS) and a Flexible Backup TDMA (FBTDMA) frames. Furthermore, our approach enables WBAN sensors that experience interference on the default channel within the TDMA frame to eventually switch to the IMC that will be used later within the FBTDMA frame for data transmission. In other words, our approach instructs all interfering sensors within the same WBAN to use the same IMC, each in its allocated backup time-slot within the FBTDMA frame of the superframe. The main contributions of this chapter are summarized as follows:

- *Channel Selection algorithm for Interference Mitigation, namely, CSIM, a distributed protocol that enables a WBAN operation within an IoT. CSIM enables the WBAN sensors that experience interference on the default channel within the TDMA frame to eventually switch to another interference mitigation channel that will be used within the FBTDMA frame. Such interfering sensors will eventually switch to the same interference mitigation channel, each in its allocated backup time-slot within the FBTDMA frame to mitigate the interference.*
- *Extensive simulations are conducted to evaluate the performance of CSIM and compare it with that of smart spectrum allocation (SSA) [39]. The results show that our proposed approach can efficiently improve the spectrum utilization and significantly lower the medium access collisions as well as the power consumption among the collocated wireless devices in the general IoT.*

## 6.2 Related Work

Avoidance and mitigation of channel interference have been extensively researched in the wireless communication literature. To the best of our knowledge, the published techniques in the realm of *IoT* are very few. Bakshi et al., [116] proposed an asynchronous and distributed solution, namely, EMIT, for data communication across *IoT*. EMIT avoids the high overhead and coordination costs through employing an interference-averaging strategy that allows users to share their resources simultaneously. Torabi et al., [117] proposed a rapid-response scheme to mitigate the effect of interfering systems (e.g., *IEEE 802.11*) on *WBAN* performance based on frequency allocation method to mitigate interferences that affect the *WBAN* coordinator or the sensors and hence impose them to switch to the same frequency. Shigueta et al., [118] presented a strategy for channel assignment in an *IoT*. They use opportunistic spectrum access via cognitive radio, with a traffic history to guide the channel allocation.

Xiao et al., [119] adopted the approach of power control and considered machine-to-machine (M2M) communication for an *IoT* network. Their proposed framework that enables the energy transfer from the receiver to the transmitter and the data transmission from the transmitter to the receiver to take place at the same time over the same frequency. Meanwhile, Chen et al., [120] introduced a new area packet scheduling technique involving *IEEE 802.15.6* and *IEEE 802.11* devices. The scheduler is based on transmitting a common control signal, which informs *IEEE 802.15.6* devices to not transmit for a certain period of time during which *IEEE 802.11* devices could transmit data packets.

Wang et al., [121] proposed a technique, namely, ACK-ID, that reduces the ACK losses and consequently reduces *ZigBee* packet retransmissions due to the presence of *IEEE 802.11* wireless networks. In ACK-ID, a novel interference detection process is performed before the transmission of each *ZigBee* ACK packet to decide whether the channel is experiencing interference or not. Inoue et al., [122] proposed a novel active channel reservation scheme (DACROS) to solve the problem of *WBAN* and *IEEE 802.11* wireless networks coexistence. DACROS uses the RTS and CTS frames to reserve the channel for a beacon of *WBAN*. Along the beacon, all *IEEE 802.11* devices do not transmit to avoid collisions. Zhang et al., [123] proposed cooperative carrier signaling (CCS) to harmonize the coexistence of *ZigBee* *WBANs* with *IEEE 802.11* wireless networks. CCS allows *ZigBee* *WBANs* to avoid *IEEE 802.11* wireless network-caused collisions and employs a separate *ZigBee* device to emit a busy tone signal concurrently with the *ZigBee*

data transmission.

As pointed out, none of the predominant approaches can be directly applied to *IoT* because they do not consider the heterogeneity of the individual networks forming an *IoT* in their design. Motivated by the emergence of *BLE* technology and compared to the previous predominant approaches for interference mitigation, our approach lowers the power and communication overheads introduced on the coordinator- and sensor-levels within each *WBAN*. In this chapter, we propose a protocol to enable *WBAN* operation and interaction within an existing *IoT*.

## 6.3 System Model and Preliminaries

### 6.3.1 Bluetooth Low Energy

Bluetooth Low Energy (*BLE*) is one of the promising technologies for *IoT* services because of its low energy consumption and cost. *BLE* is a wireless technology used for transmitting data over short distances and broadcasting advertisements at a regular interval via radio waves. The *BLE* advertisement is a one-way communication method. *BLE* devices, e.g., iBeacons, that want to be discovered can periodically broadcast self-contained packets of data. These packets are collected by devices like smartphones, where they can be used for a variety of applications to trigger prompt actions. We envision that each collocated set (cluster) of wireless devices of such *IoT* will have to include a *BLE* transceiver that periodically broadcasts the channel that is being used by the *IoT* devices in the vicinity. In fact, with the increased popularity of *BLE*, it is conceivable that every *IoT* device will be equipped with a *BLE* transceiver to announce its services and frequency channel. Standard *BLE* has a broadcast range of up to 100 meters, which makes *BLE* broadcasts an effective means for mitigating interference between *WBANs* and other *IoT* devices.

### 6.3.2 System Model and Assumptions

The *IoT* environment consists of different wireless networks, each uses some set of common channels in the ISM 2.4 GHz band. In addition, we assume that each network transmits using different levels of transmission power, bandwidth, data rates and modulation schemes. Meanwhile, *WBANs* are getting pervasive and thus form a building block for the ever-evolving future *IoT*. We consider  $N$  TDMA-based *WBANs* that coexist within the general *IoT*. Each *WBAN* consists of a single *Crd* and up to  $K$  sensors, each transmits its data on a channel within the ISM 2.4 GHz band [2]. Basically, we assume all *Crds* are equipped with richer energy supply than sensors and all sensors have access

to all *ZigBee* channels at any time. In addition, each *Crd* is integrated with *BLE* to enable effective coordination in channel assignment and to allow the interaction with the existing *IoT* devices. Furthermore, each *Crd* has a *CR* module to decide the usability and the stability of a channel.

## 6.4 Channel Selection Approach for Interference Mitigation - (CSIM)

In this section, we develop a distributed protocol for channel selection and allocation to sensors, namely, *CSIM*. *CSIM* relies on both the Bluetooth Low Energy and the Cognitive Radio to enable a *WBAN* operation within an *IoT*. *CSIM* allows high interfering sensors within a *WBAN* to later switch to another interference mitigation channel, each in its allocated backup time-slot to mitigate the interference. Subsequently, we evaluate the performance of the proposed *CSIM* protocol and compare it with that of smart spectrum allocation (*SSA*) [39].

### 6.4.1 CSIM Algorithm

A co-channel interference takes place if the simultaneous transmissions of sensors and the *Crd* in a *WBAN* collide with those of other *IoT* coexisting devices. The potential for such a collision problem grows with the increase in the communication range and the density of sensors in the individual *WBANs* as well as the number of collocated *IoT* devices. To address this problem, our approach assigns each *WBAN* a *default channel* and in the case of interference, it allows the individual sensors to switch to a different channel to be picked by the *Crd* in consultation with the *CR* module to mitigate the interference. The use of *BLE* enables the *Crd* to be aware of interference conditions faster and more efficiently. To achieve that, our approach extends the size of the superframe through the addition of a flexible number of backup time-slots to lower the collision probability of transmissions. At the network setup time, each *Crd* randomly picks a *default channel* from the set of *ZigBee* channels and informs all sensors within its *WBAN*, i.e., through a beacon, to use that channel along the *TDMA* frame of the superframe.

*CSIM* depends on acknowledgements (*Ack*) and time-outs to detect the collision at *sensor-* and *coordinator-* levels. In the *TDMA* frame shown in **Figure 6.3**, each sensor transmits its packet in its assigned time-slot to the *Crd* using the *default channel* and then sets a time-out timer. If it successfully receives an *Ack* from its corresponding *Crd*, it considers the transmission successful, and hence it sleeps until the *TDMA* frame of the next superframe. However, if that sensor does not receive an *Ack* during the time-out

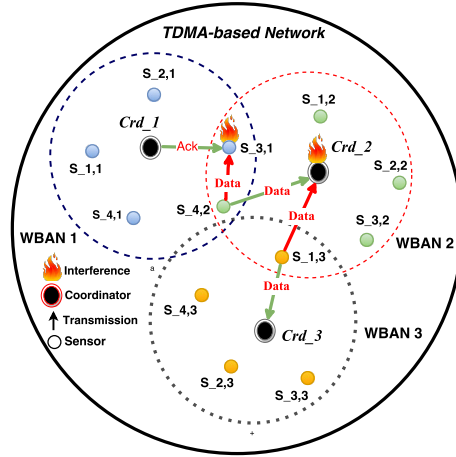


**Figure 6.2:** Collision scenarios at sensor- and coordinator-levels

**Table 6.1:** Notation meaning

Notation	Meaning
$WBAN_i$	$i^{th}$ WBAN
$S_{i,j}$	$j^{th}$ sensor of $i^{th}$ WBAN
$defaultChannel_i$	default channel of $i^{th}$ WBAN
$stableChannel_i$	stable channel of $i^{th}$ WBAN
$Crd_i$	coordinator of $i^{th}$ WBAN
$BLE_i$	bluetooth low power device of $i^{th}$ coordinator
$CR_i$	cognitive radio module of $i^{th}$ coordinator
$Pkt_{i,j}$	$j^{th}$ packet of $i^{th}$ sensor
$Ack_{i,j}$	$i^{th}$ acknowledgement transmitted to $j^{th}$ sensor
$TS_{i,j}$	$j^{th}$ time-slot of $i^{th}$ TDMA frame
$IMTS_{i,j}$	$j^{th}$ time-slot of $i^{th}$ FBTDMA frame
$LCH_i$	$i^{th}$ set of channels used by nearby IoT devices
$LIS_i$	$i^{th}$ list of interfering sensors in $TDMA_i$
$FCS$	Flexible Channel Selection
$FBTDMA$	Flexible Backup TDMA

period, it assumes failed transmission due to interference. Basically, all sensors experienced interference within the TDMA frame wait until the flexible channel selection (FCS) frame completes, and then each switches to the common interference mitigation channel. Afterwards, each sensor retransmits its packet in its allocated time-slot within the flexible backup TDMA (FBTDMA) frame to the  $Crd$ . **Figure 6.2** shows collision scenario at sensor- and coordinator-levels of three coexisting TDMA-based WBANs collocated within the general IoT. A coordinator's acknowledgement packet experiences a collision at the receiving sensor when this latter is in the transmission or radio range of another active sensor or coordinator. As illustrated in **Figure 6.2**, when a sensor  $S_{k,i}$ , e.g.  $S_{3,1}$ , receives from its corresponding coordinator  $Crd_i$ , e.g.,  $Crd_1$ , while at the same time, another sensor  $S_{j,q}$ , e.g.,  $S_{4,2}$ , or  $Crd_q$  transmits using the same channel that  $S_{k,i}$  ( $S_{3,1}$ ) uses, i.e., a collision occurs under the following condition:  $S_{k,i}$  ( $S_{3,1}$ ) is in the transmission range of  $Crd_q$  or  $S_{j,q}$  ( $S_{4,2}$ ); and  $Crd_q$  or  $S_{j,q}$  ( $S_{4,2}$ ) transmits using the same channel used by  $S_{k,i}$  ( $S_{3,1}$ ). **Algorithm 9** provides high level summary of the proposed CSIM. **Table 6.1** shows the notations and their corresponding meanings that we used in our approach.

## 6.4.2 Channel Selection

Along the TDMA frame, each *Crd*'s BLE collects information based on broadcast announcements made by other nearby BLE transceivers about the set of channels being used by wireless devices in the vicinity of a designated WBAN ( $\{LCH\}$ ), and then reports this information to its associated CR. In low or moderate conditions of interference, where there are some available channels, i.e.,  $\{US\}$  is not empty, or the size of the set  $\{LCH\}$  is smaller than the size of the set  $\{G\}$ , the *Crd* will not exploit the service of the CR when notified by the BLE about a channel conflict; instead, the *Crd* selects one available channel from the set  $\{US\}$  for efficient data transmission. CR uses the following sets of channels which are defined as follows:

- $\{G\}$ : is a set of all ZigBee channels.
- $\{LCH\}$ : is a set of all channels that are being used in the vicinity of a designated WBAN.
- $\{defaultChannel\}$ : is a unique set of the default channel that is being used by a WBAN's *Crd*.
- $\{US\}$ : is a set of the remaining ZigBee channels that are not being used in the vicinity, where  $\{US\} = \{G\} - \{\{LCH\} \cup \{defaultChannel\}\}$ .

However, in high interference conditions, the set  $\{US\}$  will be empty. Therefore, once notified by the BLE, the *Crd* can not select one available channel from  $\{US\}$ , and hence the CR should scan the set  $\{LCH\}$  to eventually select the most stable channel to be used within the FBTDMA frame for interference mitigation. Basically, the designated CR looks for a usable channel from the set  $\{LCH\}$ , if the first channel is not, then it starts sequentially sensing channels until a usable channel will be found. If it finds a usable channel and satisfies the stability condition, then it reports its index to the associated *Crd* to be eventually used for interference mitigation [13].

## 6.4.3 Channel Stability

Our approach relies on CR to decide the usability and stability of a channel using the received noise power as an indicator ( $Y_i$ ) [124].  $Y_i$  during time-slot  $i$  is given by Eq. 6.1.

$$Y_i = \frac{1}{2u} \sum_{j=1}^{2u} n_j \times n_j \quad (6.1)$$

**Algorithm 9** CSIM scheme**Require:**  $N$  WBANs,  $K$  Sensors/WBAN,  $G$  ZigBee Channels/WBAN

---

```

1: Stage 1: Network Setup & TDMA Data Collection
2: Sensor-level collision:
3: for  $i = 1$  to  $N$  do
4:    $Crd_i$  randomly picks one  $defaultChannel_i$  from  $G$  for  $WBAN_i$ ;
5:   for  $J = 1$  to  $K$  do
6:      $S_{i,j}$  transmits  $Pkt_{i,j}$  in  $TS_{i,j}$  to  $Crd_i$  using  $defaultChannel_i$ ;
7:     if  $S_{i,j}$  receives  $Ack_{i,j}$  on  $defaultChannel_i$  then
8:        $S_{i,j}$  sleeps until next superframe;
9:     else
10:       $S_{i,j}$  waits its  $IMTS_{i,j}$  within  $FBTDMA_i$  frame;
11:    end if
12:  end for
13: end for
14: Coordinator-level collision:
15: for  $i = 1$  to  $N$  do
16:   for  $j = 1$  to  $K$  do
17:     if  $Crd_i$  receives  $Pkt_{i,j}$  in  $TS_{i,j}$  on  $defaultChannel_i$  then
18:        $Crd_i$  transmits  $Ack_{i,j}$  in  $TS_{i,j}$  to  $S_{i,j}$  on  $defaultChannel_i$ ;
19:     else
20:        $Crd_i$  will tune to  $stableChannel_{i,j}$  within  $FBTDMA_i$  frame;
21:     end if
22:   end for
23: end for
24: Channel Selection Setup:
25:  $BLE_i$  forms set of channels ( $LCH_i$ ) being used in the vicinity to  $Crd_i$ ;
26:  $Crd_i$  forms list of interfering sensors ( $LIS_i$ ) within its  $WBAN_i$ ;
27: Stage 2: Channel Selection
28: for  $i = 1$  to  $N$  do
29:    $Crd_i$  forms  $FBTDMA_i$  frame from  $LIS_i$ ;
30:    $CR_i$  selects  $stableChannel_i$  from  $G - (\{defaultChannel_i\} \cup LCH_i)$ ;
31:    $Crd_i$  informs  $LIS_i$  sensors by  $stableChannel_i$  &  $FBTDMA_i$  frame;
32: end for
33: Stage 3: Interference Mitigation
34: for  $i = 1$  to  $N$  do
35:   for  $s = 1$  to  $size-of(LIS_i)$  do
36:      $S_{i,s}$  retransmits  $Pkt_{i,s}$  in  $IMTS_{i,s}$  on  $stableChannel_i$ ;
37:     if  $Ack_{i,s}$  received by  $S_{i,s}$  on  $stableChannel_i$  then
38:        $S_{i,s}$  sleeps until next superframe;
39:     else
40:        $Crd_i$  receives an earlier  $BLE_i$  alert of interference;
41:     end if
42:   end for
43: end for

```

---

Where,  $u$  is the time-bandwidth product and  $n_j$  is a Gaussian noise signal with zero mean and unit variance. The probability density function (pdf) of  $Y_i$  is given by **Eq. 6.2**.

$$f_{Y_i}(y) = \frac{U}{\Gamma(\cdot)} k e^{-uy} \quad (6.2)$$

Where,  $\Gamma(\cdot)$  is the gamma function,  $k = y^{u-1}$  and  $U = u^u$ . Based on  $Y_i$ , the CR decision criterion can be expressed as follows.

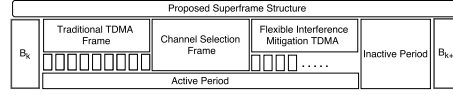


Figure 6.3: superframe structure

1. A channel  $C_i$  is usable, if  $Y_i < \lambda_1$ .
2.  $C_i$  requires power boost (usable), if  $\lambda_1 < Y_i < \lambda_2$ . In this case, we can use the theorem of Shannon (1948) [125] of the maximum transmission capacity ( $P$ ) given in bit/s in Eq. 6.3.
3.  $C_i$  cannot be used in time-slot  $i$  (unusable), if  $Y_i > \lambda_2$ , where  $\lambda_1$  and  $\lambda_2$  are thresholds depend on the receiver sensitivity and the channel model in use.

$$P = B \log_2(1 + SNR) \quad (6.3)$$

Thus, the range of  $Y_i$  is divided into three regions:  $R_j = \{Y_i : \lambda_{j-1} \leq Y_i \leq \lambda_j\}$ ,  $j = 1, 2, 3$ , where  $\lambda_0$  is equal to 0 and  $\lambda_3$  is equal to  $\infty$ . We mean by, a stable channel, if the probability of channel quality can not be decreased before the end of the transmission on that channel. The probability to being in a stable state  $j$  is given by:  $\pi_j = \Pr\{Y_i \in R_j\} = \Pr\{\lambda_{j-1} \leq Y_i < \lambda_j\}$ ,  $j = 1, 2, 3$ . The integration is done between  $\lambda_{j-1}$  and  $\lambda_j$ . When the CR is engaged, it looks for a usable and stable channel which is done in the steps below.

- **Step 1**, the *Crd* looks for  $n$  usable channels. If the first channel is not, then the CR starts sequentially sensing channels until a usable channel is found. If the CR module finds a usable channel, then **step 2** is executed to test the stability of the selected channel. Otherwise, the CR module informs *Crd* that no usable channel is available, *Crd* stays silent during a predetermined time-slot.
- **Step 2**, if the selected usable channel satisfies the stability condition, then CR reports the index of this stable channel back to *Crd*.

#### 6.4.4 Superframe Structure

We consider each WBAN's superframe delimited by two beacons and composed of two successive frames: (i) active, that is dedicated for sensors, and (ii) inactive, that is designated for *Crd*s. The superframe structure is shown in Figure 6.3. During the inactive frame, *Crd*s transmit collected data to a command center. In addition, the inactive frame directly follows the active frame and whose length depends on the underlying duty cycle being used. However, the active frame is further divided into three successive frames, which are explained as follows:

### Traditional TDMA Data Collection Frame - (TDMA)

The traditional *TDMA* frame consists of up to  $K$  time-slots, where each *WBAN*'s sensor transmits its packet to its associated *Crd* in its assigned time-slot using the *default channel*.

### Channel Selection Frame - (FCS)

In *WBANs*, sensors sleep and wake up dynamically and hence, the number of sensors being active during a period of time is unexpected. Therefore, a flexible way of scheduling different transmissions is required to avoid interference. During the *FCS* which is of a fixed size, each *WBAN*'s *Crd* selects a stable interference mitigation channel and instructs all interfering sensors within its *WBAN* to use that channel during the *FBTDMA* frame. Based on the number of interfering sensors, each *Crd* determines the size of the *FBTDMA* frame and reports this information, i.e., through a short beacon broadcast using the *default channel*, to the designated sensors within its *WBAN*. In addition, the *Crd* allocates a time-slot within the *FBTDMA* frame for each interfering sensor to eventually retransmit its packet. Although, the beacon could be lost due to the interference, our approach enables early mitigation. Basically, the *BLE* alert limits the probability of collision on the *default channel* since the *Crd* will get a hint earlier than typical.

### Flexible Backup TDMA frame - (FBTDMA)

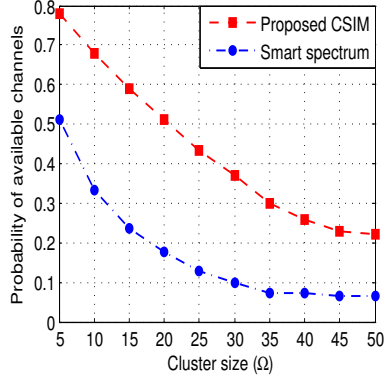
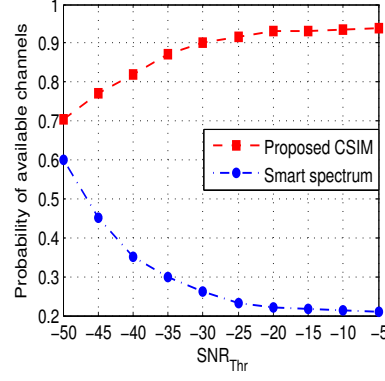
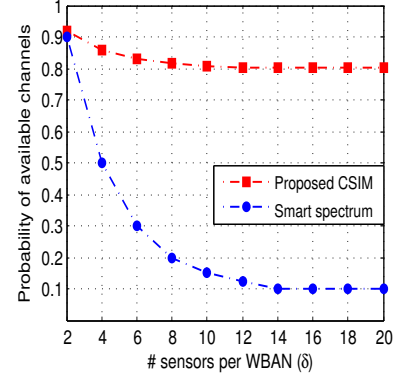
The *FBTDMA* frame consists of a flexible number of backup time-slots that depends on the number of sensors experiencing interference in the *TDMA* frame. Basically, each *Crd* knows about these sensors through using the expected number of *Ack* and data packets received in an allocated time-slot for each sensor. In *FBTDMA* frame, each interfering sensor retransmits in its allocated backup time-slot to the *Crd* using the selected stable channel.

## 6.5 Performance Evaluation

In this section, we have conducted simulation experiments to evaluate the performance of the proposed *CSIM* scheme. We compare the performance of *CSIM* with smart spectrum allocation *SSA*) scheme [39], which assigns orthogonal channels to sensors belonging to the intersection of the communication ranges of each *WBANs* pair. Furthermore, we compare the energy consumption of the *WBAN*'s coordinator with and without switching the *BLE* transceiver on [126].

**Table 6.2:** Simulation parameters

	Exp. 1	Exp. 2	Exp. 3
# Sensors/WBAN	10	10	Var
# WBAN/network	Var	10	10
Sensor txPower (dBm)	-10	-10	-10
SNR threshold (dBm)	-25	Var	-25
# Time-slots/TDMA frame	K	K	K

**Figure 6.4:**  $Pr_{AvChs}$  versus cluster size ( $\Omega$ )**Figure 6.5:**  $Pr_{AvChs}$  versus SNR threshold ( $SNR_{Thr}$ )**Figure 6.6:**  $Pr_{AvChs}$  versus # sensors/WBAN ( $\delta$ )

**Definition 6.1.** the probability of channel's availability, denoted by  $Pr_{AvChs}$ , at each  $Crd$  is defined as the frequency that a channel is not being used by any of the nearby IoT devices.

**Definition 6.2.** an IoT cluster is defined as a collection of WBANs, Wi-Fi devices, Tags and other wireless devices collocated in the same space.

The simulation network is deployed in three dimensional space ( $10 \times 10 \times 4m^3$ ) and the locations of the individual WBANs change to mimic uniform random mobility and consequently, the interference pattern varies. The channel interference between any two wireless devices is evaluated on probabilistic interference thresholds. The simulation parameters are provided in **Table 6.2**.

In *experiment 1*, the probability of channel's availability ( $Pr_{AvChs}$ ) versus the cluster size ( $\Omega$ ) for CSIM and SSA are compared, and results are shown in **Figure 6.4**. As seen in the figure, CSIM always provides a higher  $Pr_{AvChs}$  than SSA because of the channel selection is done at the WBAN- rather than *sensor*-level. For CSIM, the  $Pr_{AvChs}$  significantly decreases, when  $5 \leq \Omega < 40$  because of the larger number of ZigBee channels that are being used by IoT devices than the number of channels available at each  $Crd$ . When  $\Omega \geq 40$ ,  $Pr_{AvChs}$  decreases very slightly and eventually stabilizes because all ZigBee channels are used by the IoT devices. However, for SSA, it is also observed from this figure that  $Pr_{AvChs}$  decreases significantly when  $5 \leq \Omega < 35$  because of the larger number of ZigBee channels that are being assigned to the sensors in the interfering set ( $IS$ ) for any pair of WBANs. When  $\Omega \geq 35$ ,  $Pr_{AvChs}$  decreases very slightly and eventually stabilizes

because of the maximal number of *ZigBee* channels being assigned to sensors coexisting within the interference range of the *WBAN*, i.e., the number of these sensors exceeds the 16 channels.

*Experiment 2* studies the effect of *SNR* threshold, denoted by  $SNR_{Thr}$ , on  $Pr_{AvChs}$ . The results in **Figure 6.5** shows that *CSIM* always achieves higher  $Pr_{AvChs}$  than *SSA* for all  $SNR_{Thr}$  values. In *CSIM*, the  $Pr_{AvChs}$  significantly increases as  $SNR_{Thr}$  increases; similarly increasing  $SNR_{Thr}$  in *CSIM* diminishes the interference range, i.e., lowers the number of interfering *IoT* devices. Therefore, limiting the frequency of channel assignments allows distinct *WBANs* to not pick the same channel, which decreases the probability of collisions among them. When  $SNR_{Thr} \geq -35$ , the  $Pr_{AvChs}$  increases very slightly and eventually stabilizes because of the minimal number of interfering *IoT* devices and hence, a high  $Pr_{AvChs}$  is expected due to the larger number of *ZigBee* channels than the number of those interfering devices. However, *SSA* always achieves lower  $Pr_{AvChs}$  than *CSIM* for all  $SNR_{Thr}$  values. The  $Pr_{AvChs}$  significantly decreases as  $SNR_{Thr}$  increases. Basically, increasing  $SNR_{Thr}$  in *SSA* is similar to increasing the interference range of each *WBAN*, and hence putting more sensors in *IS*. Therefore, more channels are needed to be assigned to those sensors and that  $Pr_{AvChs}$  is reduced. When  $SNR_{Thr} \geq -25$ , the  $Pr_{AvChs}$  eventually stabilizes because of the maximal number of sensors in *IS* is attained.

*Experiment 3* studies the effect of the number of sensors per a *WBAN* denoted by  $\delta$  on  $Pr_{AvChs}$ . As can be seen in **Figure 6.6**, *CSIM* always achieves higher  $Pr_{AvChs}$  than *SSA* for all values of  $\delta$ . It is also observed from this figure that  $Pr_{AvChs}$  decreases very slightly when  $2 \leq \delta \leq 10$  and eventually stabilizes when  $\delta \geq 10$ . In both cases, the  $Pr_{AvChs}$  is high due to two reasons, 1) the number of *WBANs* is fixed to 10 which is smaller than the number of *ZigBee* channels, and, 2) *CSIM* selects a stable channel based on the number of interfering *WBANs* rather than the number of interfering sensors. However, the  $Pr_{AvChs}$  decreases significantly when  $2 \leq \delta \leq 14$  because adding more sensors into *WBANs* increases the probability of interference and consequently requires more channels to be assigned; consequently  $Pr_{AvChs}$  is reduced. Furthermore, *SSA* assigns channels to interfering sensors rather than to interfering *WBANs*, which justifies the decrease of  $Pr_{AvChs}$  when  $\delta$  grows. When  $\delta \geq 14$ , the  $Pr_{AvChs}$  eventually stabilizes because of the maximal number of sensors in *IS* is attained by each *WBAN*.

**Figure 6.7** shows the average reuse factor denoted by  $avgRF$  versus the interference threshold ( $\rho$ ) for all *WBANs*. As seen in this figure, *CSIM* achieves a higher  $avgRF$  for all  $\rho$  values. However, increasing the interference threshold puts more interfering sensors

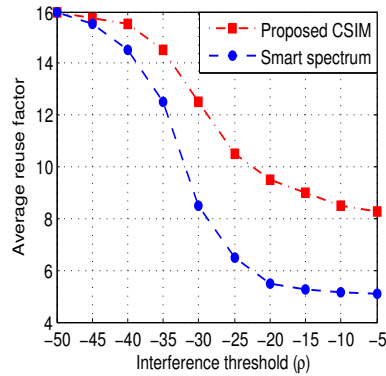


**Figure 6.7:** Average reuse factor ( $avgRF$ ) versus interference threshold ( $\rho$ )

in the interference range of any specific *WBAN* than the corresponding *WBANs* of these sensors, i.e., *SSA* requires more channels to be assigned to sensors than to *WBANs* in *CSIM*.

The average energy consumption of the *WBAN* coordinator denoted by  $avgEC$  versus the interference threshold ( $\rho$ ) for *CSIM* with (*CSIM-W*) and without switching the *BLE* transceiver on (*CSIM-WO*) are compared, and results are shown in **Figure 6.8**. As seen in the figure, *CSIM-W* always provides a lower  $avgEC$  than *CSIM-WO* because of the earlier *BLE* alerts of interference to the coordinator, i.e., the coordinator scans the channels only upon receiving of these alerts. For *CSIM-W*, the  $avgEC$  increases slightly as the interference threshold grows, which increases the number of interfering sensors, hence the frequency of *BLE* alerts of interference increases, and consequently, the energy consumption increases due to the additional scanning. When  $\rho$  exceeds -20, the  $avgEC$  increases very slightly and eventually stabilizes at  $0.46 \times 10^{-3}mW$ ; this reflects the case where all channels are used by nearby *IoT* devices forcing the *Crd* to engage the *CR* for finding a stable channel. For *CSIM-WO*, the  $avgEC$  increases significantly with all values of  $\rho$  because of the continuous scanning of all ZigBee channels all the time, i.e., the coordinator periodically scans all the channels to find out which channels are not noisy. It is worth saying that the *BLE* alerts reduces the frequency of channel scanning and hence saves the coordinator's energy.

## 6.6 Conclusions

In this chapter, we have presented *CSIM*, a distributed protocol to enable *WBAN* operation and interaction within an existing *IoT*. *CSIM* leverages the emerging *BLE* technology to enable channel selection and allocation for interference mitigation. In addition, the superframe's active period is further extended to involve not only a *TDMA* frame, but also a *FCS* and *FBTDMA* frames, for interference mitigation. We integrate

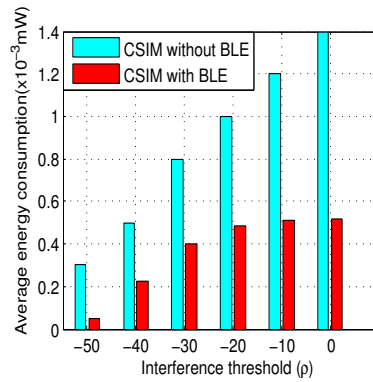


**Figure 6.8:** Coordinator's average energy consumption ( $avgEC$ ) versus interference threshold ( $\rho$ ) a *BLE* transceiver and a *CR* within the *WBAN*'s coordinator, where the role of the *BLE* transceiver is to inform the *WBAN* about the frequency channels that are being used in its vicinity. When experiencing high interference, the *BLE* device notifies the *WBAN*'s *Crd* to call the *CR* which determines a different channel for interfering sensors that will be used later within the *FBTDMA* frame for interference mitigation. The simulation results show that *CSIM* mitigates the co-channel interference, saves the power resource at both the *sensor*- and *coordinator*-levels. *CSIM* outperforms sample competing schemes.

# Chapter 7

## Conclusions

### Contents

---

<a href="#">7.1 Thesis Summary</a>	115
<a href="#">7.2 Future Works and Research directions</a>	117
<a href="#">7.2.1 Mobility</a>	117
<a href="#">7.2.2 Putting Human Bodies Into the Internet of Things</a>	117
<a href="#">7.2.3 Extension to cloud computing</a>	118

---

### 7.1 Thesis Summary

In this thesis, we address the fundamental problem of radio co-channel interference algorithms and protocols in *WBANs* at both the theoretical modeling and analysis. Chapter 3 focuses on addressing intra-*WBAN* co-channel interference through multi-channel and superframe length adjustment. Chapter 4 addresses the problem of co-channel interference among cooperative *WBANs* using multi-code and superframe interleaving. Chapter 5 deals with co-channel interference among non-cooperative *WBANs* and addresses the problem using multi-channel and time-slot hopping based on Latin rectangle. Chapter 6 addresses the problem of *WBANs* coexistence in an *IoT* through multi-channel and time-slot adjustment.

More specifically, in chapter 3 we presented a hybrid contention- and contention-free-based approach for a two-hop-based *WBAN*. The first distributed scheme is called *CFTIM* that allocates time-slots and stable channels to nodes to diminish the intra-*WBAN* interference. The second is an improved version of *CFTIM* called *IAA* that adjusts the length of the superframe and limits the number of channels to only 2 rather than 16. Basically, *IAA* enables the interfering nodes to either adjust their contention window or

use another channel to avoid the intra-WBAN interference. Moreover, we presented a probabilistic model that proves analytically the SINR outage probability is minimized at the individual nodes of the WBAN. Meantime, extensive simulation results demonstrated the effectiveness and efficiency of our hybrid approach in terms of extending the overall network energy lifetime, improving the throughput and lowering the probability of medium access collision.

In Chapter 4, we address the problem of sensor-level co-channel interference among cooperative WBANs based on multi-code and superframe interleaving. Firstly, we presented a DTRC scheme for determining which superframes and their corresponding time-slots overlap with each other. Secondly, we proposed the OCAIM scheme that allocates orthogonal codes to interfering sensors belonging to sensor interference lists. Then, we conducted an analysis of the success and collision probability model for frames transmissions. Extensive simulations and benchmarking are conducted and results demonstrate that OCAIM can significantly diminish the inter-WBAN interference, improves the throughput and saves the power resource at sensor- and WBAN-levels.

Furthermore, in Chapter 5, we address the problem of co-channel interference among non-cooperative WBANs using Latin rectangles. Firstly, we proposed a distributed scheme called DAIL, which enables time-based channel hopping using Latin rectangles in order to minimize the medium access collision and avoid the co-channel interference amongst coexisting WBANs. Secondly, we presented CHIM, which is an improved version of DAIL, that allocates a random channel to each WBAN and provisions backup time-slots for failed transmission. The backup time-slots are scheduled in a way that is similar to DAIL. CHIM enables only a sensor that experiences collisions to hop to an alternative backup channel in its allocated backup time-slot. Moreover, we developed an analytical model that derives bounds on the collision probability and throughput for sensors transmissions. Meanwhile, extensive and intensive simulation results demonstrate the effectiveness and efficiency of DAIL and CHIM in terms of medium access collision probability among the individual transmissions of the WBANs, transmission delay, network energy lifetime, throughput and the reliability compared with other competing solutions.

Finally, in Chapter 6, we address the problem of WBAN coexistence within an existing IoT, and propose a distributed protocol, namely, CSIM, to enable WBAN operation and interaction within the IoT. To mitigate the interference, CSIM extends the active period of the superframe to involve not only a TDMA frame but also a Flexible Channel

Selection and a Flexible Backup frames. Basically, *CSIM* enables *WBAN* sensors that experience interference on the default channel within the *TDMA* frame to eventually switch to the Interference Mitigation Channel (*IMC*) that will be used later within the Flexible Backup frame for data transmission. Ultimately, *CSIM* instructs all interfering sensors within the same *WBAN* to use the same *IMC*, each in its allocated backup time-slot within the Flexible Backup frame.

In the balance of this subsection, we discuss a number of open issues we judge pertinent to our work and outline several important potential directions for future research.

## 7.2 Future Works and Research directions

### 7.2.1 Mobility

Even though lots of researchers addressed the importance of mobility support and proposed new networking technology for *WBAN*, it is still worthwhile to mention points for further study. Currently, *OMNeT++* and *NS-2/3* are general frameworks to conduct simulation for *WBAN*. Therefore, it is demanded to get a free, available *WBAN* mobility model as an add-on for these frameworks. Thus, it is desirable for mobility models to emulate the movement pattern of targeted real-life applications in a feasible way. Even though a few applications are now available and deployable nowadays, current mobility models are not enough to describe the movement of nodes accurately. Therefore, further research for human behavior is required to enhance mobility models. Recently, smartphones have become pervasive so research work for smartphone-based human mobility prediction has been initiated. Thus, it will be a good way to make use of smartphones to predict the movement and develop the mobility models [127].

### 7.2.2 Putting Human Bodies Into the Internet of Things

As our bodies or at least, the clothing that adorn them could become key network nodes in the Internet of things. The sensors and transmitters on our bodies can be used to form cooperative ad-hoc networks that could be used for group indoor navigation, crowd-motion capture, health monitoring on a massive scale, and especially collaborative communications. A distributed wireless network could aggregate data from hundreds, if not thousands, of nearby devices and then find the most efficient link to offload that collective data to the Internet at large. This kind of collaboration is the same principle proposed by mesh-networking as a means of optimizing wireless systems: If everyone shares connections and relays each others' data, everyone benefits. There's an

additional benefit to this kind of collaborative communication: By linking to one another, body area networks could create new useful data about users' surroundings and locations. By measuring the signal strength of nearby connections, the network could determine the precise location of every node, or person, within it [111, 112].

You can imagine some possible applications for such technology. In a busy airport or train station, proximal location-based services could route departing passengers en masse to their proper gates or trains, or send arriving passengers to the proper baggage claim. City planners could use the technology to track and manage the flow of pedestrian traffic. Emergency agencies could use it to coordinate the evacuation of a building. Sociologists could use it to study group behavior, and game designers and movie CGI could use it to digital-map crowd movements. On the flip side, creating such collaborative networks has ominous security implications. Our own notions of individual privacy suffer if we know that every transmitter in a hundred-foot radius is talking to our devices, even helping to carry our personal data back to the cloud.

### 7.2.3 Extension to cloud computing

In this thesis, we mainly focused on energy-efficient, reliable and interference-free protocols design and analysis in *WBANs*. Basically, the sensed data and the corresponding feedback from the medical doctor should be timely processed. The increasing requests from customers and patients consume significantly the network resources such as storage, computation and communication power. However, it is very hard to achieve these goals by only relying on the traditional *WBANs*. Therefore, the cloud computing is introduced to assist *WBANs* to store and process the sensing data in a real time fashion [128, 129].

Taking the advantage of the cloud server to store the large volume of sensing data and process them for doctor's diagnosis, the cloud assists *WBANs* to become more robust and provide the desirable services for patients and users. However, when a large number of users located at the same place upload their data at the same time, the connection between *WBANs* and cloud the servers might be intermittent. The available bandwidths from *WBANs* to cloud servers for each individual user are also limited so that the network performance is considerably degraded. Therefore, the communication between *WBANs* and cloud servers is the bottleneck with the perspective of efficiency and reliability. We plan to design suitable protocols to handle such challenges.

# Bibliography

- [1] G. T. Chen, W. T. Chen, and S. H. Shen. 2l-mac: A mac protocol with two-layer interference mitigation in wireless body area networks for medical applications. pages 3523–3528, June 2014.
- [2] Ieee standard for local and metropolitan area networks - part 15.6: Wireless body area networks.
- [3] M. Ali, H. Moun gla, M. Younis, and A. Mehaoua. Iot-enabled channel selection approach for wbans. In *2017 IEEE International Wireless Communications and Mobile Computing Conference (IWCMC'17)*, pages 1–7, 2017.
- [4] M. Ali, H. Moun gla, M. Younis, and A. Mehaoua. Distributed scheme for interference mitigation of coexisting wbans using latin rectangles. In *The 14th Annual 2017 IEEE Consumer Communications and Networking Conference (CCNC'17), Las Vegas, United States*, pages 1–6, 2017.
- [5] M. Ali, H. Moun gla, M. Younis, and A. Mehaoua. Distributed scheme for interference mitigation of wbans using predictable channel hopping. In *2016 IEEE 18th International Conference on e-Health Networking, Applications and Services (Healthcom)*, pages 1–6, Sept 2016.
- [6] M. Ali, H. Moun gla, M. Younis, and A. Mehaoua. Inter-wbans interference mitigation using orthogonal walsh hadamard codes. In *2016 IEEE 27th Annual International Symposium on Personal, Indoor, and Mobile Radio Communications (PIMRC)*, pages 1–7, Sept 2016.
- [7] M. Ali, H. Moun gla, and A. Mehaoua. Interference avoidance algorithm (iaa) for multi-hop wireless body area network communication. In *2015 17th International Conference on E-health Networking, Application Services (HealthCom)*, pages 540–545, Oct 2015.
- [8] M. Ali, H. Moun gla, and A. Mehaoua. Dynamic channel access scheme for interference mitigation in relay-assisted intra-wbans. In *2015 International Conference*

- on Protocol Engineering (ICPE) and International Conference on New Technologies of Distributed Systems (NTDS), pages 1–6, July 2015.
- [9] M. Ali, H. Moun gla, A. Mehaoua, and Y. Xu. Dynamic channel allocation for interference mitigation in relay-assisted wireless body networks. In *2015 2nd International Symposium on Future Information and Communication Technologies for Ubiquitous HealthCare (Ubi-HealthTech)*, pages 1–6, May 2015.
- [10] M. Ali, H. Moun gla, , M. Younis, and A. Mehaoua. Efficient medium access arbitration among interfering wbans using latin rectangle. In *Elsevier Ad Hoc Networks Journal*, 2017.
- [11] M. Ali, H. Moun gla, M. Younis, and A. Mehaoua. In *Book Chapter (2017)*.
- [12] M. Ali, H. Moun gla, and A. Mehaoua. Energy aware competitiveness power control in relay-assisted interference body networks. 2017.
- [13] A. Al-Fuqaha, M. Guizani, M. Mohammadi, M. Aledhari, and M. Ayyash. Internet of things: A survey on enabling technologies, protocols, and applications. *IEEE Communications Surveys Tutorials*, 17(4):2347–2376, 2015.
- [14] Benoît Latré, Bart Braem, Ingrid Moerman, Chris Blondia, and Piet Demeester. A survey on wireless body area networks. *Wirel. Netw.*, 17(1):1–18, January 2011.
- [15] Samaneh Movassaghi, Mehran Abolhasan, Justin Lipman, David Smith, and Abbas Jamalipour. Wireless body area networks: A survey. *Communications Surveys Tutorials, IEEE*, 16(3):1658–1686, Third 2014.
- [16] M. Sukor, S. Ariffin, N. Fisal, S. K. S. Yusof, and A. Abdallah. Performance study of wireless body area network in medical environment. In *2008 Second Asia International Conference on Modelling x00026; Simulation (AMS)*, pages 202–206, May 2008.
- [17] S. Movassaghi, A. Majidi, A. Jamalipour, D. Smith, and M. Abolhasan. Enabling interference-aware and energy-efficient coexistence of multiple wireless body area networks with unknown dynamics. *IEEE Access*, 4:2935–2951, 2016.
- [18] Ieee standard for information technology– local and metropolitan area networks– specific requirements– part 15.1a: Wireless medium access control (mac) and physical layer (phy) specifications for wireless personal area networks (wpan). *IEEE Std 802.15.1-2005 (Revision of IEEE Std 802.15.1-2002)*, pages 1–700, June 2005.
- [19] S. Bluetooth. Specification of the bluetooth system v4. 2. *Standard, Bluetooth SIG*, 27, 2014.

- [20] Bluetooth low energy technology. <http://www.bluetooth.com/Pages/low-energy-tech-info.aspx>.
- [21] Carles Gomez, Joaquim Oller, and Josep Paradells. Overview and evaluation of bluetooth low energy: An emerging low-power wireless technology. *Sensors*, 12(9):11734–11753, 2012.
- [22] Front-matter. In Shahin Farahani, editor, *ZigBee Wireless Networks and Transceivers*, pages i – iii. Newnes, Burlington, 2008.
- [23] Ieee standard for local and metropolitan area networks–part 15.4: Low-rate wireless personal area networks (lr-wpans). *IEEE Std 802.15.4-2011 (Revision of IEEE Std 802.15.4-2006)*.
- [24] Ieee standard for low-rate wireless networks. *IEEE Std 802.15.4-2015 (Revision of IEEE Std 802.15.4-2011)*, pages 1–709, April 2016.
- [25] Jie Dong and D. Smith. Cooperative body-area-communications: Enhancing co-existence without coordination between networks. In *Personal Indoor and Mobile Radio Communications (PIMRC), 2012 IEEE 23rd International Symposium on*, pages 2269–2274, Sept 2012.
- [26] Abi research: Wearable computing devices, like apple’s iwatch, will exceed 485 million annual shipments by 2018, december 2014. Available online <https://www.abiresearch.com/press/wearable-computing-devices-like-apples-iwatch-will>.
- [27] P. R. Grassi, V. Rana, I. Beretta, and D. Sciuto. *b<sup>2</sup>irs*: A technique to reduce ban-ban interferences in wireless sensor networks. In *2012 Ninth International Conference on Wearable and Implantable Body Sensor Networks*, pages 46–51, May 2012.
- [28] Mohammad Deylami and Emil Jovanov. A distributed and collaborative scheme for mitigating coexistence in ieee 802.15.4 based wbans. In *Proceedings of the 50th Annual Southeast Regional Conference, ACM-SE ’12*, pages 1–6, New York, NY, USA, 2012. ACM.
- [29] Xuan Wang and Lin Cai. Interference analysis of co-existing wireless body area networks. In *Global Telecommunications Conference (GLOBECOM 2011), 2011 IEEE*, pages 1–5, Dec 2011.
- [30] L. Tan, Z. Feng, W. Li, Z. Jing, and T. A. Gulliver. Graph coloring based spectrum allocation for femtocell downlink interference mitigation. In *2011 IEEE Wireless Communications and Networking Conference*, pages 1248–1252, March 2011.
- [31] R. Y. Chang, Z. Tao, J. Zhang, and C. C. Kuo. A graph approach to dynamic fractional frequency reuse (ffr) in multi-cell ofdma networks. In *2009 IEEE International*

- Conference on Communications*, pages 1–6, June 2009.
- [32] E. Pateromichelakis, M. Shariat, A. u. Quddus, and R. Tafazolli. On the evolution of multi-cell scheduling in 3gpp lte / lte-a. *IEEE Communications Surveys Tutorials*, 15(2):701–717, Second 2013.
- [33] P. Fan (eds.) G. Min, Y. Pan. Design fundamentals and interference mitigation for cellular networks. *advances in wireless networks: Performance modelling, analysis and enhancement*. 2008.
- [34] R. Fantacci. Proposal of an interference cancellation receiver with low complexity for ds/cdma mobile communication systems. *IEEE Transactions on Vehicular Technology*, 48(4):1039–1046, Jul 1999.
- [35] D.M. Barakah and M. Ammad-uddin. A survey of challenges and applications of wireless body area network (wban) and role of a virtual doctor server in existing architecture. In *Intelligent Systems, Modelling and Simulation (ISMS), 2012 Third International Conference on*, pages 214–219, Feb 2012.
- [36] Nadeem Javaid, NA Khan, M Shakir, MA Khan, Safdar Hussain Bouk, and ZA Khan. Ubiquitous healthcare in wireless body area networks-a survey. *arXiv preprint arXiv:1303.2062*, 2013.
- [37] N. Thepvilojanapong, S. Motegi, A. Idoue, and H. Horiuchi. Adaptive channel and time allocation for body area networks. *IET Communications*, 5(12):1637–1649, August 2011.
- [38] Shipeng Liang, Yu Ge, Shengming Jiang, and Hwee Pink Tan. A lightweight and robust interference mitigation scheme for wireless body sensor networks in realistic environments. In *Wireless Communications and Networking Conference (WCNC), 2014 IEEE*, pages 1697–1702, April 2014.
- [39] Samaneh Movassaghi, Mehran Abolhasan, and David Smith. Smart spectrum allocation for interference mitigation in wireless body area networks. In *Communications (ICC), 2014 IEEE International Conference on*, pages 5688–5693. IEEE, 2014.
- [40] S. Movassaghi, M. Abolhasan, D. Smith, and A. Jamalipour. Aim: Adaptive inter-network interference mitigation amongst co-existing wireless body area networks. In *Global Communications Conference (GLOBECOM), 2014 IEEE*, pages 2460–2465, Dec 2014.
- [41] S. H. Cheng and C. Y. Huang. Coloring-based inter-wban scheduling for mobile wireless body area networks. *IEEE Transactions on Parallel and Distributed Systems*, 24(2):250–259, Feb 2013.

- [42] S. Movassaghi, M. Abolhasan, and D. Smith. Cooperative scheduling with graph coloring for interference mitigation in wireless body area networks. In *IEEE Int. Conf. on WCNC*, 2014.
- [43] Z. Yan, B. Liu, and C. W. Chen. Qos-driven scheduling approach using optimal slot allocation for wireless body area networks. In *2012 IEEE 14th International Conference on e-Health Networking, Applications and Services (Healthcom)*, pages 267–272, Oct 2012.
- [44] Zhijun Xie, Guangyan Huang, Jing He, and Yanchun Zhang. A clique-based wban scheduling for mobile wireless body area networks. *Procedia Computer Science*, 31:1092 – 1101, 2014.
- [45] Sanghyun Seo, Hakjeon Bang, and Hunjoo Lee. Coloring-based scheduling for interactive game application with wireless body area networks. *The Journal of Supercomputing*, 72(1):185–195, 2016.
- [46] W. Huang and T. Q. S. Quek. On constructing interference free schedule for coexisting wireless body area networks using distributed coloring algorithm. In *IEEE Int. Conf. on BSN*, 2015.
- [47] S. Movassaghi, A. Majidi, D. Smith, M. Abolhasan, and A. Jamalipour. Exploiting unknown dynamics in communications amongst coexisting wireless body area networks. In *2015 IEEE Global Communications Conference (GLOBECOM)*, pages 1–6, Dec 2015.
- [48] Mingbo Xiao, Ness B. Shroff, and Edwin K. P. Chong. A utility-based power-control scheme in wireless cellular systems. *IEEE/ACM Trans. Netw.*, 11(2):210–221, April 2003.
- [49] M. Cagalj, S. Ganeriwal, I. Aad, and J. P. Hubaux. On selfish behavior in csma/ca networks. In *Proceedings IEEE 24th Annual Joint Conference of the IEEE Computer and Communications Societies.*, volume 4, pages 2513–2524 vol. 4, March 2005.
- [50] Dongjin Son, B. Krishnamachari, and J. Heidemann. Experimental study of the effects of transmission power control and blacklisting in wireless sensor networks. In *2004 First Annual IEEE Communications Society Conference on Sensor and Ad Hoc Communications and Networks, 2004. IEEE SECON 2004.*, pages 289–298, Oct 2004.
- [51] Shan Lin, Jingbin Zhang, Gang Zhou, Lin Gu, John A. Stankovic, and Tian He. Atpc: Adaptive transmission power control for wireless sensor networks. In *Proceedings of the 4th International Conference on Embedded Networked Sensor Systems, SenSys '06*, pages 223–236, New York, NY, USA, 2006. ACM.

- [52] N. A. Pantazis and D. D. Vergados. A survey on power control issues in wireless sensor networks. *Commun. Surveys Tuts.*, 9(4):86–107, October 2007.
- [53] T. S. P. See, Yu Ge, Tat Meng Chiam, Jeng Wai Kwan, and Chee Wee Kim. Experimental correlation of path loss with system performance in wban for healthcare applications. In *2011 IEEE 13th International Conference on e-Health Networking, Applications and Services*, pages 221–224, June 2011.
- [54] Yu Ge, Jeng Wai Kwan, J. S. Pathmasuntharam, Zhengye Di, T. S. P. See, Wei Ni, Chee Wee Kim, Tat Meng Chiam, and Maode Ma. Performance benchmarking for wireless body area networks at 2.4 ghz. In *2011 IEEE 22nd International Symposium on Personal, Indoor and Mobile Radio Communications*, pages 2249–2253, Sept 2011.
- [55] M. Quwaider, J. Rao, and S. Biswas. Body-posture-based dynamic link power control in wearable sensor networks. *IEEE Communications Magazine*, 48(7):134–142, July 2010.
- [56] T. Guan, C. Yi, D. Qiao, L. Xu, and Y. Li. Pid-based transmission power control for wireless body area network. In *2014 12th International Conference on Signal Processing (ICSP)*, pages 1643–1648, Oct 2014.
- [57] S. Xiao, A. Dhamdhere, V. Sivaraman, and A. Burdett. Transmission power control in body area sensor networks for healthcare monitoring. *IEEE Journal on Selected Areas in Communications*, 27(1):37–48, January 2009.
- [58] S. Kim and D. S. Eom. Link-state-estimation-based transmission power control in wireless body area networks. *IEEE Journal of Biomedical and Health Informatics*, 18(4):1294–1302, July 2014.
- [59] Samaneh Movassaghi, Mehran Abolhasan, David Smith, and Abbas Jamalipour. Joint energy harvesting and internetwork interference mitigation amongst coexisting wireless body area networks. ICST, 11 2014.
- [60] Q. Chen, C. Su, H. Zhang, and R. Chai. User service oriented power allocation algorithm for wireless body area sensor networks. In *5th IET International Conference on Wireless, Mobile and Multimedia Networks (ICWMMN 2013)*, pages 37–40, Nov 2013.
- [61] Eui-Jik Kim, Sungkwan Youm, Taeshik Shon, and Chul-Hee Kang. Asynchronous inter-network interference avoidance for wireless body area networks. *The Journal of Supercomputing*, 65(2):562–579, 2013.
- [62] L. Wang, C. Goursaud, N. Nikaein, L. Cottatellucci, and J. M. Gorce. Cooperative scheduling for coexisting body area networks. *IEEE Transactions on Wireless*

- Communications*, 12(1):123–133, January 2013.
- [63] G. Fang, E. Dutkiewicz, K. Yu, R. Vesilo, and Y. Yu. Distributed inter-network interference coordination for wireless body area networks. In *2010 IEEE Global Telecommunications Conference GLOBECOM 2010*, pages 1–5, Dec 2010.
- [64] D. Du, F. Hu, F. Wang, Z. Wang, Y. Du, and L. Wang. A game theoretic approach for inter-network interference mitigation in wireless body area networks. *China Communications*, 12(9):150–161, 2015.
- [65] R. Kazemi, R. Vesilo, E. Dutkiewicz, and G. Fang. Inter-network interference mitigation in wireless body area networks using power control games. In *2010 10th International Symposium on Communications and Information Technologies*, pages 81–86, Oct 2010.
- [66] R. Kazemi, R. Vesilo, E. Dutkiewicz, and Ren Ping Liu. Reinforcement learning in power control games for internetwork interference mitigation in wireless body area networks. In *2012 International Symposium on Communications and Information Technologies (ISCIT)*, pages 256–262, Oct 2012.
- [67] R. Kazemi, R. Vesilo, and E. Dutkiewicz. A novel genetic-fuzzy power controller with feedback for interference mitigation in wireless body area networks. In *2011 IEEE 73rd Vehicular Technology Conference (VTC Spring)*, pages 1–5, May 2011.
- [68] H. Moosavi and F. M. Bui. Optimal relay selection and power control with quality-of-service provisioning in wireless body area networks. *IEEE Transactions on Wireless Communications*, 15(8):5497–5510, Aug 2016.
- [69] Z. Zhang, H. Wang, C. Wang, and H. Fang. Interference mitigation for cyber-physical wireless body area network system using social networks. *IEEE Transactions on Emerging Topics in Computing*, 1(1):121–132, June 2013.
- [70] Jie Dong, David B. Smith, and Leif W. Hanlen. Socially optimal coexistence of wireless body area networks enabled by a non-cooperative game. *ACM Trans. Sen. Netw.*, 12(4):26:1–26:18, September 2016.
- [71] X. Zhao, B. Liu, C. Chen, and C. W. Chen. Qos-driven power control for inter-wban interference mitigation. In *2015 IEEE Global Communications Conference (GLOBECOM)*, pages 1–6, Dec 2015.
- [72] Jing Zhou, Aihuang Guo, Juan Xu, Hung Nguyen, and S. Su. A game theory control scheme in medium access for wireless body area network. In *10th International Conference on Wireless Communications, Networking and Mobile Computing (WiCOM 2014)*, pages 404–409, Sept 2014.

- [73] L. Zou, B. Liu, C. Chen, and C. W. Chen. Bayesian game based power control scheme for inter-wban interference mitigation. In *Global Communications Conference (GLOBECOM), 2014 IEEE*, pages 240–245, Dec 2014.
- [74] S. Movassaghi, A. Majidi, A. Jamalipour, D. Smith, and M. Abolhasan. Enabling interference-aware and energy-efficient coexistence of multiple wireless body area networks with unknown dynamics. *IEEE Access*, 4:2935–2951, 2016.
- [75] M. N. Deylami and E. Jovanov. A distributed scheme to manage the dynamic coexistence of ieee 802.15.4-based health-monitoring wbans. *IEEE Journal of Biomedical and Health Informatics*, 18(1):327–334, Jan 2014.
- [76] K. Y. Yazdandoost and K. Sayrafian-Pour. Channel model for body area network (ban). *Networks*, p. 91, 2009.
- [77] P. S. Hall, Y. Hao, Y. I. Nechayev, A. Alomainy, C. C. Constantinou, C. Parini, M. R. Kamarudin, T. Z. Salim, D. T. M. Hee, R. Dubrovka, A. S. Owadally, W. Song, A. Serra, P. Nepa, M. Gallo, and M. Bozzetti. Antennas and propagation for on-body communication systems. *IEEE Antennas and Propagation Magazine*, 49(3):41–58, June 2007.
- [78] W. Huang and T. Q. S. Quek. Adaptive csma/ca mac protocol to reduce inter-wban interference for wireless body area networks. In *2015 IEEE 12th International Conference on Wearable and Implantable Body Sensor Networks (BSN)*, pages 1–6, June 2015.
- [79] Y. Zhou, Z. Sheng, V. C. M. Leung, and P. Servati. Beacon-based opportunistic scheduling in wireless body area network. In *2016 38th Annual International Conference of the IEEE Engineering in Medicine and Biology Society (EMBC)*, pages 4995–4998, Aug 2016.
- [80] B. Yuan, J. Liu, W. Liu, and S. Zheng. Dim: A novel decentralized interference mitigation scheme in wban. In *Wireless Communications Signal Processing (WCSP), 2015 International Conference on*, pages 1–5, Oct 2015.
- [81] S. Rezvani and S. A. Ghorashi. Context aware and channel-based resource allocation for wireless body area networks. *IET Wireless Sensor Systems*, 3(1):16–25, March 2013.
- [82] B. Liu, Z. Yan, and C. W. Chen. Medium access control for wireless body area networks with qos provisioning and energy efficient design. *IEEE Transactions on Mobile Computing*, PP(99):1–1, 2016.

- [83] J. Mahapatro, S. Misra, M. Manjunatha, and N. Islam. Interference mitigation between wban equipped patients. In *Wireless and Optical Communications Networks (WOCN), 2012 Ninth International Conference on*, pages 1–5, Sept 2012.
- [84] S. Kim, J. Kim, and D. Eom. A beacon interval shifting scheme for interference mitigation in body area networks. *Sensors*, 12(8):10930–10946, 2012.
- [85] S. Kim, S. Kim, J. W. Kim, and D. S. Eom. Flexible beacon scheduling scheme for interference mitigation in body sensor networks. In *2012 9th Annual IEEE Communications Society Conference on Sensor, Mesh and Ad Hoc Communications and Networks (SECON)*, pages 157–164, June 2012.
- [86] Ernesto Ibarra, Angelos Antonopoulos, Elli Kartsakli, and Christos Verikoukis. Heh-bmac: Hybrid polling mac protocol for wbans operated by human energy harvesting. *Telecommunication Systems*, 58(2):111–124, 2015.
- [87] Anagha Jamthe, Amitabh Mishra, and Dharma P Agrawal. Scheduling schemes for interference suppression in healthcare sensor networks. In *Communications (ICC), 2014 IEEE International Conference on*, pages 391–396. IEEE, 2014.
- [88] Ismail Kirbas, Alper Karahan, Abdullah Sevin, and Cuneyt Bayilmis. ismac: An adaptive and energy-efficient mac protocol based on multi-channel communication for wireless body area networks. *TIIS*, 7(8):1805–1824, 2013.
- [89] W. B. Yang and K. Sayrafian-Pour. Interference mitigation for body area networks. In *2011 IEEE 22nd International Symposium on Personal, Indoor and Mobile Radio Communications*, pages 2193–2197, Sept 2011.
- [90] O. Omeni, A. C. W. Wong, A. J. Burdett, and C. Toumazou. Energy efficient medium access protocol for wireless medical body area sensor networks. *IEEE Transactions on Biomedical Circuits and Systems*, 2(4):251–259, Dec 2008.
- [91] H. W. Tseng, S. T. Sheu, and Y. Y. Shih. Rotational listening strategy for ieee 802.15.4 wireless body networks. *IEEE Sensors Journal*, 11(9):1841–1855, Sept 2011.
- [92] Wen-Bin Yang and Kamran Sayrafian-Pour. Interference mitigation using adaptive schemes in body area networks. *International Journal of Wireless Information Networks*, 19(3):193–200, 2012.
- [93] F. Martelli, R. Verdone, and C. Buratti. Link adaptation in ieee 802.15.4-based wireless body area networks. In *Personal, Indoor and Mobile Radio Communications Workshops (PIMRC Workshops), 2010 IEEE 21st International Symposium on*, pages 117–121, Sept 2010.

- [94] H. Moun gla, A. Jarray, A. Karmouch, and A. Mehaoua. Cost-effective reliability- and energy-based intra-wban interference mitigation. In *2014 IEEE Global Communications Conference*, pages 2399–2404, Dec 2014.
- [95] Paul Ferrand, Mickael Maman, Claire Goursaud, Jean-Marie Gorce, and Laurent Ouvry. Performance evaluation of direct and cooperative transmissions in body area networks. *Annals of Telecommunications - annales des télécommunications*, 66(3):213–228, 2011.
- [96] Jie Dong, Yu Ge, and David B. Smith. Two-hop relay-assisted cooperative communication in wireless body area networks: An empirical study. *ACM Trans. Sen. Netw.*, 12(4):32:1–32:13, September 2016.
- [97] Hui Feng, Bin Liu, Zhisheng Yan, Chi Zhang, and Chang Wen Chen. Prediction-based dynamic relay transmission scheme for wireless body area networks. In *Personal Indoor and Mobile Radio Communications (PIMRC), 2013 IEEE 24th International Symposium on*, pages 2539–2544, Sept 2013.
- [98] A. Manirabona, L. C. Fourati, and S. Boudjit. Decode and merge cooperative mac protocol for intra wban communication. In *e-Health Networking, Applications and Services (Healthcom), 2014 IEEE 16th International Conference on*, pages 146–151, Oct 2014.
- [99] Jie Dong and David Smith. Opportunistic relaying in wireless body area networks: Coexistence performance. In *Communications (ICC), 2013 IEEE International Conference on*, pages 5613–5618. IEEE, 2013.
- [100] J. Dong and D. Smith. Joint relay selection and transmit power control for wireless body area networks coexistence. In *2014 IEEE International Conference on Communications (ICC)*, pages 5676–5681, June 2014.
- [101] Wen-Bin Yang and Kamran Sayrafian-Pour. Interference mitigation using adaptive schemes in body area networks. *International Journal of Wireless Information Networks*, 19(3):193–200, 2012.
- [102] E. H. Dinan and B. Jabbari. Spreading codes for direct sequence cdma and wide-band cdma cellular networks. *IEEE Communications Magazine*, 36(9):48–54, Sep 1998.
- [103] A. Salmasi and K. S. Gilhousen. On the system design aspects of code division multiple access (cdma) applied to digital cellular and personal communications networks. In *[1991 Proceedings] 41st IEEE Vehicular Technology Conference*, pages 57–62, May 1991.

- [104] J. G. Andrews. Interference cancellation for cellular systems: a contemporary overview. *IEEE Wireless Communications*, 12(2):19–29, April 2005.
- [105] F. Adachi, M. Sawahashi, and H. Suda. Wideband ds-cdma for next-generation mobile communications systems. *IEEE Communications Magazine*, 36(9):56–69, Sep 1998.
- [106] A. Tawfiq, J. Abouei, and K. N. Plataniotis. Cyclic orthogonal codes in cdma-based asynchronous wireless body area networks. In *2012 IEEE International Conference on Acoustics, Speech and Signal Processing (ICASSP)*, pages 1593–1596, March 2012.
- [107] J. Ju and V. O. K. Li. Tdma scheduling design of multihop packet radio networks based on latin squares. In *IEEE Journal on Selected Areas in Communications*, vol. 17, no. 8, pp. 1345-1352, Aug 1999.
- [108] Zhijun Cai, Mi Lu, and C. N. Georghiades. Topology-transparent time division multiple access broadcast scheduling in multihop packet radio networks. *IEEE Transactions on Vehicular Technology*, 52(4):970–984, July 2003.
- [109] David Tse and Pramod Viswanath. *Fundamentals of Wireless Communication*. Cambridge University Press, New York, NY, USA, 2005.
- [110] Latin squares and their applications. new york: Academic. volume 52, pages 970–984, July 1974.
- [111] J. Gantz and D. Reinsel. "the digital universe in 2020: Big data, bigger digital shadows, and biggest growth in the far east. *IDC iView: IDC Analyze the Future*, vol. 2007, pp. 1-16, 2012.
- [112] Charith Perera, Chi Harold Liu, Srimal Jayawardena, and Min Chen. Context-aware computing in the internet of things: A survey on internet of things from industrial market perspective. *CoRR*, abs/1502.00164, 2015.
- [113] S. M. R. Islam, D. Kwak, M. H. Kabir, M. Hossain, and K. S. Kwak. The internet of things for health care: A comprehensive survey. *IEEE Access*, 3:678–708, 2015.
- [114] P.P. Ray. A survey on internet of things architectures. *Journal of King Saud University - Computer and Information Sciences*, pages –, 2016.
- [115] Ieee standard for information technology–telecommunications and information exchange between systems local and metropolitan area networks–specific requirements - part 11: Wireless lan medium access control (mac) and physical layer (phy) specifications. *IEEE Std 802.11-2016 (Revision of IEEE Std 802.11-2012)*, pages 1–3534, Dec 2016.

- [116] A. Bakshi, L. Chen, K. Srinivasan, C. E. Koksal, and A. Eryilmaz. Emit: An efficient mac paradigm for the internet of things. In *IEEE INFOCOM - The 35th Annual IEEE Int. Conf. on Computer Communications*, 2016.
- [117] N. Torabi, W. K. Wong, and V. C. M. Leung. A robust coexistence scheme for iee 802.15.4 wireless personal area networks. In *IEEE Consumer Communications and Networking Conference (CCNC)*, 2011.
- [118] R. F. Shigueta, M. Fonseca, A. C. Viana, A. Ziviani, and A. Munaretto. A strategy for opportunistic cognitive channel allocation in wireless internet of things. In *IFIP Wireless Days (WD)*, 2014.
- [119] Y. Xiao, Z. Xiong, D. Niyato, Z. Han, and L. A. DaSilva. Full-duplex machine-to-machine communication for wireless-powered internet-of-things. In *IEEE Int. Conf. on Communications (ICC)*, 2016.
- [120] D. Chen, J. Y. Khan, and J. Brown. An area packet scheduler to mitigate coexistence issues in a wpan/wlan based heterogeneous network. In *Telecommunications (ICT), 22nd Int. Conf. on*, 2015.
- [121] Z. Wang, T. Du, Y. Tang, D. Makrakis, and H. T. Mouftah. Ack with interference detection technique for zigbee network under wi-fi interference. In *Broadband and Wireless Computing, Communication and Applications (BWCCA), 8th Int. Conf. on*, 2013.
- [122] F. Inoue, M. Morikura, T. Nishio, K. Yamamoto, F. Nuno, and T. Sugiyama. Novel coexistence scheme between wireless sensor network and wireless lan for hems. In *Smart Grid Communications (SmartGridComm), IEEE Int. Conf. on*, 2013.
- [123] X. Zhang and K. G. Shin. Cooperative carrier signaling: Harmonizing coexisting wpan and wlan devices. *IEEE/ACM Transactions on Networking*, 21(2):426–439, 2013.
- [124] H. Mounгла, K. Haddadi, and S. Boudjit. Distributed interference management in medical wireless sensor networks. In *13th IEEE Annual Consumer Communications Networking Conference (CCNC)*, 2016.
- [125] Martial Coulon ENSEIHT. Systemes de telecommunications. 2007-2008.
- [126] S. Kamath J. Lindhh. Measuring bluetooth low energy power consumption. In *Application Note AN092; Texas Instruments: Dallas, TX, USA*, 2010.
- [127] Benoît Latré, Bart Braem, Ingrid Moerman, Chris Blondia, and Piet Demeester. A survey on wireless body area networks. *Wirel. Netw.*, 17(1):1–18, January 2011.

- 
- [128] Chun-Ta Li, Cheng-Chi Lee, and Chi-Yao Weng. A secure cloud-assisted wireless body area network in mobile emergency medical care system. *J. Med. Syst.*, 40(5):1–15, May 2016.
- [129] S. Moulik, S. Misra, and A. Gaurav. Cost-effective mapping between wireless body area networks and cloud service providers based on multi-stage bargaining. *IEEE Transactions on Mobile Computing*, 16(6):1573–1586, June 2017.



# Nomenclature

## *B :*

BER Bit Error Rate

BI Superframe Length

BLE Bluetooth Low Energy

## *C :*

CDF Cumulative Distribution Function

CO<sub>2</sub> Carbon dioxide

COWHC Cyclic Orthogonal Walsh Hadamard Code

Crd WBAN Coordinator

CSMA/CA Carrier Sense Multiple Access with Collision Avoidance

## *D :*

DC Duty Cycle

DR Data Rate

## *E :*

ECG Electrocardiogram

Exp Experiment

## *G :*

3G Third Generation of Wireless Mobile Telecommunications Technology

GSM Global System for Mobile Communications

GTS Guaranteed Time-slot

**H :**

HBC Human Body Communication

**I :**

IEEE Institute of Electrical and Electronics Engineers

ISM Industrial, Scientific and Medical

**L :**

LDC Low Duty Cycle

LOS Line of Sight

LTE Long-Term Evolution

**M :**

M2M Machine to Machine

MAC Medium Access Control

MANET Mobile Ad-hoc Network

MICS Medical Device Radio Communications Service

**N :**

NB Narrow Band

NE Nash Equilibrium

NFC Near Field Communication

NLOS Non Line of Sight

**P :**

PC Power Consumption

PD Personal Device

PDA Personal Digital Assistant

PDR Packet Delivery Ratio

PER Packet Error Rate

PHY Physical

PRR Packet Reception Rate

PV Privacy

**Q :**

QoS Quality of Service

**R :**

RFID Radio Frequency IDentification

RSSI Received Signal Strength Indicator

**S :**

SIFS Short Inter-Frame Spacing

SINR Signal to Interference plus Noise Ratio

SNR Signal to Noise Ratio

SOA Service Oriented Architecture

SpO<sub>2</sub> Peripheral Capillary Oxygen Saturation

**T :**

TDMA Time Division Multiple Access

TPC Transmission Power Control

TxPower Transmission Power

**U :**

UMTS Universal Mobile Telecommunications System

UWB Ultra Wide Band

**W :**

WBAN Wireless Body Area Network

WiFi Wireless Fidelity

WSN Wireless Sensor Network